A CONTROL SYSTEM FRAMEWORK FOR BUILDING ENERGY RETROFITTING AND MAINTENANCE PLANNING

by

Bo Wang

Submitted in partial fulfillment of the requirements for the degree
Philosophiae Doctor (Electronic Engineering)

in the

Department of Electrical, Electronic and Computer Engineering
Faculty of Engineering, Built Environment and Information Technology

UNIVERSITY OF PRETORIA

February 2017

SUMMARY

A CONTROL SYSTEM FRAMEWORK FOR BUILDING ENERGY RETROFITTING AND MAINTENANCE PLANNING

by

Bo Wang

Supervisor(s):	Prof. Xiaohua Xia
Department:	Electrical, Electronic and Computer Engineering
University:	University of Pretoria
Degree:	Philosophiae Doctor (Electronic Engineering)
Keywords:	Building energy efficiency, retrofitting planning, maintenance planning, optimal control, model predictive control, interacting energy effects, multi-state system, maintenance intensities, maintenance time schedule, grouping, differential evolution algorithm

The building energy efficiency has received massive attention from the government, industry and academia, due to the mismatch between the shortage of energy resources and the growing energy demands. The building is a complex system with a variety of components. One or several components can comprise a subsystem that provides additional or enhanced functionality to the building. These subsystems reveal enormous energy efficiency opportunities in buildings, including the power quality control, smart appliance operation, energy flow balance and energy efficiency project planning. Accordingly, a hierarchical building energy efficiency framework can be identified by categorising these energy efficiency opportunities into four layers: the power electronics layer, smart appliance layer, energy flow layer and planning layer. The four layers are distinguished by different functionalities and control intervals. While the first three layers involve excessively studied engineering fields, the energy efficiency planning is nevertheless less well understood, due to the lack of a systematic approach to model, evaluate and optimize the planning of building energy efficiency projects. As a result, the energy efficiency project planning has received increasing attentions from the researchers in the recent years.

The retrofitting of existing buildings is one of the most important types of building energy efficiency projects, as the existing buildings account for a large portion of final energy consumptions in the world. The retrofitting planning aims at maximizing the energy and economy performances with limited budget and manpower. Therefore, the retrofitting planning is a kind of investment decision to make best use of the investment. However, such an investment decision is difficult due to the interactions of the multiple layers in building energy efficiency framework. Furthermore, the retrofitting investment decisions suffer significant risks from the failures of retrofitted items during operation. According to measurement and verification principles, failures of retrofitted items result in the decrease of the energy savings, which are the major concern of a retrofitting project. Although the deteriorated energy savings can be restored by applying maintenance actions, the economy performances receive further impacts from the maintenance costs. In summary, the investment decision of a retrofitting project can be very complex, manifesting multiple time scales and significant dynamics when simultaneously taking into account the retrofitting and maintenance planning.

In order to address the investment decision complexity, a control system framework is proposed, where the dynamics of aggregated performances can be addressed and optimized. A necessary simplification is adopted where the retrofitted items are categorised into several groups. Each group consists of items that are considered to be homogeneous ones, i.e., with the same inherent energy and reliability performances, the same operating schedules and similar operational environment. Thereafter, the aggregate energy savings can be computed by the individual item savings and the item group populations. In this way, the control system modelling at management level can be obtained. The state variables are the item group populations, and the control inputs are the maintenance intensities, i.e., the count of the restored items from one group at a specific instant. Such instant is called maintenance instant, i.e., a time point at which the maintenance actions are scheduled to take place. The statistical laws of the item group population decay comprise the system dynamics. The measured outputs are the aggregate energy and economy performances. Thereafter, the retrofitting and maintenance planning are cast into an optimal control problem. A finite decision horizon, namely the sustainability period is defined, based on which the control objectives are obtained, i.e., maximising the aggregate energy savings and financial benefits. A series of constraints are accordingly introduced, e.g., the targeted energy saving limit, budget limit and payback period limit, etc. The influences of uncertainty factors are taken into account to be random noises on the state variables and measured outputs. Consequently, the control approaches can be introduced to address the retrofitting and maintenance planning. A model predictive control approach with a differential evolution algorithm based numerical solver is employed for the controller design in most of the illustrative studies.

The control system framework allows development and expansion by selecting different state variables and control inputs. Given that the selective control inputs involve a broad field of maintenance engineering, a number of maintenance categories comprise the alternatives of control inputs. The introduction of different maintenance categories provides more options to decision makers. Thereafter, the complexity of performance dynamics can be addressed, and the utility of limited capitals and manpower can be improved. Following this idea, a series of extensive studies are conducted and illustrated after the elaboration of the control system framework. Firstly, a control system modelling with coupled state variables is proposed to address the interacting energy effects between different categories of retrofitted item groups. Secondly, the energy saving deterioration of retrofitted items before malfunctions is modelled by a multi-state system approach, which incorporates two different maintenance categories into the planning. Thirdly, the collaborative optimisation of the maintenance intensities and instants is proposed, where additional energy efficiency opportunities are identified. Finally, the robustness of control system performances when different grouping methods are applied is investigated. These extensive studies will be introduced in respective chapters in this dissertation.

The highlighted main contributions of the work is listed as following:

- Introducing the life-cycle cost analysis and corresponding dynamics modelling into building energy retrofitting planning.

- The thesis's works contribute to the investment decision at management level. Different with the conventional control topics, the thesis focuses on managing item groups via a management level modelling. Such a modelling is connected with both the planning and operation interests.

- It is identified in this thesis that the maintenance problems at management level can be modelled as an optimal control problem, thus allows the employment of control system approaches.

- Many different maintenance options from reliability engineering are introduced into the control system framework to better reflect the practical maintenance strategies. The control approaches are accordingly developed.

ACKNOWLEDGMENT

I would like to deliver my deepest gratitude to my supervisor, Prof. Xiaohua Xia, who inspires me to pursuit the career of research. Prof. Xia has been a perfect demonstration of the life of a good researcher. The training and supervision that I received from Prof. Xia stimulate my passions to devote myself to studying and exploring. He not only teaches me to work as a researcher, but also encourages me to keep fighting with my weaknesses. It is no exaggeration to say that Prof. Xia incurred my biggest change in my life. Thanks to him, I am able to write this acknowledgement with great satisfaction.

I would also like to thank my colleagues in South Africa, including Dr. Donghui Wei and his family, Mr. Nan Wang and his family, Dr. Lijun Zhang and his wife, Mrs. Yuling Fan, Dr. Xianming Ye and his family, Dr. Zhou Wu, Dr. Bing Zhu, Dr. Fei Yang, Mr. Shi Wang, Mr. Jun Mei, etc. They are all excellent researchers and wonderful friends. I learned a lot from them. More importantly, they are the best friends that give me the feeling of home at South Africa.

Finally, I want to thank my parents. No words can express my gratitude. They are the strongest support in my life. I had, in the past years, made them worried, but I never received any stress from them, only comforts and encouragements. I hope I can bring them more joy in their future life.

Bo Wang
University of Pretoria, South Africa
February 2017

PUBLICATIONS

JOURNAL PAPERS

[J1] B. Wang, X. Xia, and J. Zhang, "A multi-objective optimization model for the life-cycle cost analysis and retrofitting planning of buildings," *Energy and Buildings*, vol. 77, pp. 227–235, 2014.

[J2] B. Wang and X. Xia, "Optimal maintenance planning for building energy efficiency retrofitting from optimization and control system perspectives," *Energy and Buildings*, vol. 96, pp. 299–308, 2015.

[J3] B. Wang and X. Xia, "A multistate-based control system approach toward optimal maintenance planning," *IEEE Transactions on Control Systems Technology*, vol. 25, no. 1, pp. 374–381, 2017.

[J4] B. Wang and X. Xia, "Optimal maintenance planning in building retrofitting with interacting energy effects," *IEEE Transactions on Control Systems Technology, submitted*, 2016.

[J5] B. Wang and X. Xia, "Optimal Control of Maintenance Instants and Intensities in Building Energy Efficiency Retrofitting Project," *Applied Energy, submitted*, 2017.

[J6] Z. Wu, X. Xia, and B. Wang, "Improving building energy efficiency by multiobjective neighborhood field optimization," *Energy and Buildings*, vol. 87, pp. 45–56, 2015.

[J7] Z. Wu, B. Wang, and X. Xia, "Large-scale building energy efficiency retrofit: Concept, model and control," *Energy*, vol. 109, pp. 456–465, 2016.

CONFERENCE CONTRIBUTIONS

[C1] B. Wang and X. Xia, "A control system approach to corrective maintenance planning of building retrofitted facilities," in *The 19th World Congress of the International Federation of Automatic Control (IFAC 2014)*, Capetown, South Africa, 24-28 August, 2014.

[C2] B. Wang and X. Xia, "A control system approach to optimal maintenance planning for building retrofitting project," *2014 Maintenance Performance Measurement and Management Conference (MPMM 2014)*, Coimbra, Portugal, 4-5 September, 2014.

[C3] B. Wang and X. Xia, "Maintenance plan optimization in building retrofitting with interacting energy efficiency effects," in *2015 Chinese Automation Congress (CAC 2015)*, Wuhan, China, 27-29 November, 2015.

[C4] B. Wang, Z. Wu, B. Zhu, and X. Xia, "Optimal control of maintenance instants and intensities in building energy efficiency retrofitting project," in *The 54th IEEE Conference on Decision and Control (CDC 2015)*, Osaka, Japan, 15-18 December, 2015.

[C5] B. Wang and X. Xia, "A preliminary study on the robustness of grouping based maintenance plan optimization in building retrofitting," in *2016 International Conference on Applied Energy (ICAE 2016)*, Beijing, China, 08-11 October, 2016.

TABLE OF CONTENTS

LIST OF TABLES

LIST OF FIGURES

CHAPTER 1 INTRODUCTION AND LITERATURE REVIEW

1.1 BACKGROUND

The energy crisis has been a serious issue to the worldwide dwellers, manufacturers, builders and traders since 1970s, resulted from the mismatch between the growing energy demands and the limited petroleum and coal supply. The energy crises never really goes far. After 2000, there have been several energy crisis all over the world, including the global energy crisis in 2003, California electricity crisis in 2001, Argentine energy crisis in 2004, central Asia energy crisis in 2008, etc. South Africa suffers serious electricity shortage as well. Since 2007, the major power supplier Eskom [1] has faced deficiency in the electricity generation. At the same time, the energy demands from the industry and consumers kept growing. This incurred several months of load shedding in 2008 and 2015, during which the South African dwellers had to suffer periodical blackouts.

In response to the energy shortage, the energy efficiency studies are encouraged by worldwide governments, industries and research facilities. Among the massive relevant topics, building energy efficiency has drawn significant attentions. This is due to the important role of building energy consumptions. Generally, the building sector accounts for 32% of the final energy consumption in the world [1]. The U.S. Energy Information Administration (EIA) announced that in 2015, the residential and commercial buildings consumed about 40% of total U.S. energy consumption [2]. The proportion of the building energy consumption keeps growing as the energy demands increase with the development of technologies. Therefore, the building energy efficiency projects can achieve significant effects. For example, in 2009, in South Africa, 7.5 millon South Africa Rand annual savings had been delivered

[1] http://www.eskom.co.za
[2] http://www.eia.gov/tools/faqs/faq.cfm?id=86&t=1

from nearly 900 building energy efficiency projects [2]. The South African Department of Minerals and Energy have been rewarding such efforts to improve the building energy efficiency against the growing energy demands over the country.

The study in this dissertation is motivated by the considerable energy efficiency potentials in the building sector. Given that the building is a complicated system that assembles the topics pertaining to the architect, material, environment engineering, electrical engineering, psychology, social science. etc., the building energy efficiency is also a very broad field involving multiple layers and focuses, from the operation of very specific equipment to the investment decision of a large scale project. The following section introduces a scope of the residential and commercial building energy efficiency, from which the main topic of this study, i.e., a control system framework for building energy retrofitting and maintenance planning, can be deduced.

1.2 BUILDING ENERGY EFFICIENCY FRAMEWORK

1.2.1 Building energy efficiency scope

The building is a complicated system with massive different components. The building energy efficiency potentials can be identified from many of the building components. Taking residential building as an example. A set of building components pertaining to different functionalities and manifesting energy efficiency potentials are illustrated in Fig. 1.1.

Some components pertain to the power generation. Apart from the main grid power supply, several supplementary power supply or renewable energy resources can be incorporated into the building system, e.g., the diesel generator, fuel cell, photovoltaic (PV) system, wind generator, biomass, etc. The supplementary power supplies improve the cost effectiveness and reliability subject to the occupant energy demands and energy prices. For example, in South Africa, the time-of-use (TOU) tariffs are applied by Eskom. Consequently, the scheduling of alternative power sources result in the improvement of cost effectiveness [3]. Furthermore, in South Africa, off-grid applications are required in the rural sites, where the combination of several supplementary power supplies including the battery system are implemented [4]. Although the battery storage system is too expensive to provide full supply back up at the current stage, it is however the most effective and promising solution at present to improve

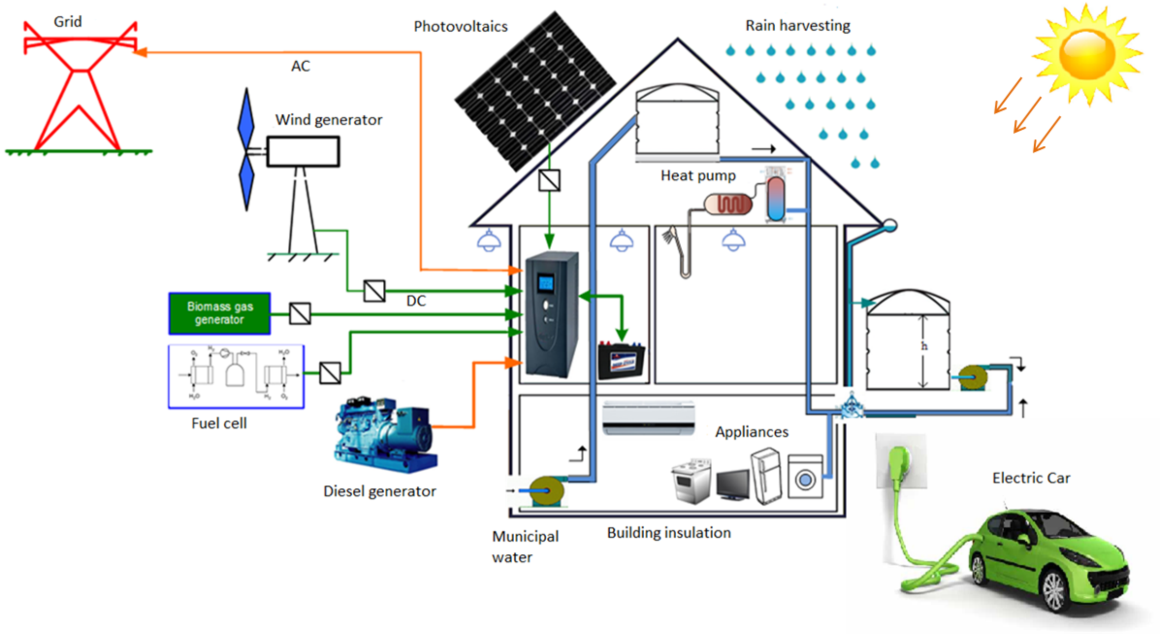

Figure 1.1. The scope of residential building energy efficiency

the supply reliability against the risk of main grid failures and intermittent renewable energy sources. A recent article [5] introduces a trend of rapidly falling costs of battery packs for electric vehicles. There is a reason to believe that the battery systems can become affordable component for domestic buildings.

The building materials and envelope comprise another important category of components. The building envelope delivers a significant impact to the energy consumptions of building heating ventilation and air conditioning (HVAC) system. A large proportion of the HVAC system workload comes from the heat transmission between the interior and exterior of the building. The transmission rate is greatly influenced by the building materials and envelope, e.g., the insulations and windows. Improving building materials and envelope can reduce the building HVAC system workload and corresponding energy consumptions [6]. In this way, the materials and envelope also influence the occupant thermal comfort [7, 8, 9]. Some building envelop studies also take into account the building orientation [10, 11, 12] and corporate with the geographic information system (GIS) platform [13, 14]. The orientation of the building can be taken into account to maximise the effectiveness of heating and PV generation. The GIS platform provides further energy efficiency opportunities via the 'geospatial awareness', i.e., the integration of energy and GIS modelling. The geographic information is incorporated into the building modelling and data analysis and energy optimisation. Thereafter, the building envelop design can be assisted by the GIS platform to better identify the impacts to building energy efficiency. In summary, although the building materials and envelope do not consume any energy, they still manifest significant energy efficiency potentials.

The appliances are energy-consuming components pertaining to various functionalities and energy efficiency opportunities. Generally, we categorise the appliances into four classes according to the functionalities: the lighting, HVAC, water heating and plug devices. The existing studies reveal that appliance energy efficiency can be improved from developing more energy-efficient equipment. For example, with the development of lighting technologies, new efficient lamps have been developed, e.g., the compact fluorescent lamps (CFLs) and light-emitting diodes (LEDs). Significant energy savings can be achieved by replacing inefficient lamps with efficient ones [15, 16]. Similar strategies can be applied to the water heaters. The inefficient resistive element water heaters can be replaced with the heat pump water heaters, which are identified to have approximately two thirds less consumption [17]. The plug devices, e.g., the TV, refrigerator and microwave oven can be replaced with efficient ones with high energy rating as well. Apart from developing efficient equipment, employing advanced control strategies can also improve the appliance energy efficiency. A series of studies where energy efficiency control strategies are employed to facilitate the air conditioner energy efficiency can be found from [18, 19, 20].

Further building energy efficiency can be achieved by incorporating the water energy nexus, which is receiving increasing attentions [21]. The water-energy nexus brings a series of direct and indirect benefits to the domestic dwellers, including the water savings, energy savings from water purification, utility pumping and carbon emission reduction [22]. Given that South Africa is a water-scarce country, the energy efficiency impact from water-energy nexus deserves more attention.

One or several aforementioned components can comprise a subsystem in buildings, which provides additional and enhanced functionality to the building. Many such subsystems can be identified in the building context, each brings in a number of energy efficiency opportunities. For example, an air conditioning system comprises a subsystem in the building that adjusts the indoor thermal comfort, where the control of the air conditioner components bring in energy efficiency potentials; several supplementary power sources can also comprise a subsystem that increases the reliability and cost-effectiveness of the power supply, where the energy balancing offers additional energy efficiency opportunities; the supplementary power sources and appliances, e.g., the heat pump water heater, can be combined to simultaneously take into account the supply side and demand side energy efficiency. These subsystems define the scope of building energy efficiency, and the subsystem modelling is the foundation of building energy efficiency studies. Various studies have been conducted with focuses on different subsystems, where massive energy efficiency issues have been identified. These energy efficiency issues involve different time scales, from μs level to year level, due to different focused subsystems. According to the multiple time scales, we categorise the energy efficiency opportunities into four levels. A hierarchical building energy efficiency framework is thereby proposed.

1.2.2 Hierarchical building energy efficiency framework

There are four layers in the building energy efficiency framework, including the *power electronics layer*, *smart appliance layer*, *energy flow layer* and *planning layer*. Each layer corresponds to a different subsystem category and energy efficiency perspective. Generally, the four layers are distinguished by the following criteria. The *power electronics layer* involves energy optimisations that focus on maintaining and improving the power quality where the control intervals can be very small, e.g., several μs . The *smart appliance layer* involves bringing energy efficiency intelligence to the appliances, where the control intervals range from a few minutes to half an hour. The *energy flow layer* involves energy balances for grid-connected or off-grid systems that aim at different objectives, where the control intervals are often several hours. The *planning layer* involves organising and managing an energy efficiency project with limited capital investment and manpower. The decisions are made via evaluating performances over a long time period, e.g., 5-10 years. More detailed explanations are introduced as following:

The *power electronics layer* pays attention to maintain the power quality, i.e., the electricity quality in buildings. Specifically, a satisfying power quality can be characterised as a power supply with 1) steady voltage within a predefined range; 2) steady alternating current (A.C) frequency and 3) smooth voltage curve waveform [23]. The power quality is a traditional topic for the power system, as low quality power supply, e.g., unstable voltage or A.C frequency can damage the equipment, including the power generator, power consumer and power line. According to the definition, the major concerns of maintaining power quality is the voltage, frequency and AC phase [24]. From the energy efficiency viewpoint, the power quality also plays an important role. This is because the damaged equipment results in deterioration of energy efficiency. For example, the lighting, air conditioner and refrigerator are the most common appliances in domestic environment. If the power quality cannot sustain, these equipment can either consume more energy or become malfunctioning, i.e., the energy performances deteriorate due to the worse working state. In this way, the power quality is essential to building energy efficiency. In South Africa, the power quality is generally well maintained, however the capacity of the main grid is not very satisfying comparing with the growing demands. In 2014 and 2015, a major coal supply incident in South Africa resulted in continuous load shedding: Eskom shed load for the first time in six years for 14 hours on 6 March 2014, and three more load shedding events occurred during June 2014 due to multiple unit trips, as well as a constrained power system in meeting demand [25]. The shortage of supply capacity encouraged the deployment of supplementary power supplies such as renewable energy facilities, especially in the rural sites [4]. As a result, new power quality challenges are brought in. Firstly, the electricity generated from supplementary power supplies, especially from the renewable energy sources, must be processed to meet the service level power quality requirement. Secondly, for grid-tied systems, the generated electricity must further meet the power quality standard from the grid. Given the distributed nature of the renewable energy system, additional building energy efficiency opportunities are revealed at the power electronics layer. In domestic context, the inverter is the main method to adjust the power quality. A number of studies have been conducted with the focus on inverter control. Abo-Al-Ez *et al.* [26] proposes the design of a dual-loop model predictive controller for voltage source inverter operation in smart microgrids. Liu *et al.* [27] proposes a control strategy for microgrid inverters based on adaptive three-order sliding mode and optimised droop controls. Wilson *et al.* [28] proposes a non-linear power flow control design that regulates renewable energy sources, loads and identifies energy storage requirements for an AC inverter based microgrid system. Mokgonyana et al. [29] investigates daily volt/var control in distributed networks, where the proposed approach determines the most suitable substation secondary bus reference voltage and dispatch sequences to minimise daily voltage deviations and total loss over 24h. There are many other studies contributing to similar topics [30, 31, 32, 33]. The switch interval of inverters can be as small as μs level and control actions usually take place every hundreds of *ms*. Such intervals are much smaller than the control problems at the other layers.

The *smart appliance layer* aims at bringing in energy efficiency intelligence to the appliances in addition to the built-in control logic. In practice, additional energy efficiency opportunities can be identified to allow the appliance to coordinate with the ambient and user behavior. For example, Wang *et al.* [34] proposes a quantitative model to estimate the the energy performances of an air conditioning system under different set point conditions. Such a knowledge provides better understanding of the energy efficiency potentials with an air conditioning system apart from improving the control logic of a chiller system itself. In fact, many further energy efficiency opportunities lie within the interactions between the equipment and the working environment. Similarly, Catherine *et al.* [35] investigates the energy efficiency impacts from the collaboration of an intelligent geyser usage profiling system and geyser timer. Arens *et al.* [36] emphasises the energy efficiency opportunities from ambient intelligence in buildings, and a number of relevant studies have been conducted on implementing ambient intelligence to improve the building energy efficiency [37, 38, 39]. The appliances can also be organised and managed as one subsystem to achieve the energy savings and load balancing. Setlhaolo *et al.* [40, 41, 42] propose a series of relevant studies, where household appliances are scheduled in accordance with a battery energy storage system. The purpose of the scheduling is cost minimisation and load balance under the circumstance of TOU tariffs, where the battery energy storage system is utilized to provide peak shaving and valley filling of the load profile. In this way, the appliance energy efficiency intelligence also provide financial benefits to the occupants. Given that the main purpose of the appliances is satisfying the occupant demands, the corresponding control interval is often 10-20 minutes, so that the occupant intentions can be rapidly responded to.

The *energy flow layer* focuses on the energy efficiency opportunities from balancing different energy sources. In practice, the supplementary power sources manifest different problems. The diesel generator has been the most popular solution for off-grid applications due to the low initial capital cost and reliable performances. However the operation and maintenance costs of diesel generator is very high, in addition, the diesel generator increases the carbon emission. The photovoltaic system and wind generator are renewable and clean energy sources, with advantages such as little maintenance, absence of fuel costs and flexibility of expansion. However, their ability of continuous and reliable power supply is limited by the intermittent nature. Incorporating battery storage systems or hydrogen fuel cells into the renewable energy system can improve the reliability. However, the oversizing of the storage and renewable energy system capacity is inevitable, which results in high capital costs and inefficient use of the system. In order to address the above issues, the hybrid energy system is proposed, where the aforementioned power sources are combined and scheduled to achieve an environmentally friendly, reliable and cost-effective power supply system. Great energy efficiency opportunities are identified from such hybrid systems. Tazvinga *et al.* [43, 4, 44, 45, 46] conducted a series of studies to investigate the energy efficiency opportunities of hybrid system in off-grid applications. The usage of diesel generator is minimised and usage of renewable energy is encouraged in these studies. In this way, the advantages of the renewable energy system are amplified while the supply reliability is guaranteed. Such a hybrid system can be extended by incorporating demand side management into the energy balancing. Sichilalu *et al.* [3, 47, 48] investigated such a scenario that the hybrid system is connected with a thermal heat pump load. Both the supply side and demand side performances are optimised to minimise the energy costs and maximise the fuel cell outputs subject to TOU tariffs. In this way, the supply reliability of the hybrid system is verified. Nwulu and Xia [49, 50, 51] investigated the energy balance with demand response in a grid-connected microgrid scenario. The energy balance is implemented via optimising an economic dispatch of the microgrid, where the conventional generators fuel cost and transaction costs of the transferable power are minimised while the microgrid operator's demand response benefit is maximised, subject to a series of constraints including the load demand constraint. The control interval at the energy flow layer is approximately 1-2 hours, due to the daily basis of the energy balance.

The *planning layer* energy efficiency issues are actually management level issues. As introduced in preceding paragraphs, the evaluation period are usually 5-10 years, which are less than the building life cycle. This is often defined by the measurement and verification projects. It is not necessarily the whole building life cycle, but a prescribed time period, during which the savings are identified and confirmed. The identified savings are the basis of a series of energy footprints, national level analysis and financial incentives. Therefore, the performances during the evaluation period are extremely important. The term 'management level' implies a fact that an individual equipment or subsystem is not the focus of the planning layer. Instead, organising, planning and managing an energy efficiency project becomes the major concern. The cost effectiveness is the most important objective at planning layer, i.e., the decisions are made to make best use of the capital investment. Take building energy retrofitting as an example. In a retrofitting project, due to the limitation of capital and manpower, the retrofit options must be carefully evaluated and selected to maximise the overall energy savings. Different budget limits can result in different retrofitting plans [52, 53, 54]. From this viewpoint, the planning layer energy optimisations are actually a kind of investment decisions and budget competitions. Such investment decisions are extremely important to achieve energy efficiency, as limited capitals and manpower are common situations in practice. Accordingly, massive studies have been conducted on energy efficiency project planning. However, when comparing with the preceding three layers, less studies have been conducted on organising the methodologies in a systematic framework to model, evaluate and optimise the energy efficiency projects at planning layer. A control system framework to the building retrofitting and maintenance planning is thereby proposed in this dissertation to fill this research gap. The control system context and details are attentively introduced in the following sections and chapters.

1.3 ENERGY RETROFITTING IN BUILDINGS: STATE OF THE ART

Before introducing the control system framework, the state of the art studies on building retrofitting are hereby investigated. The retrofitting is an important part of the green building studies. Zuo and Zhao [55] concludes that the green building studies cover three main topics: the definition and scope of green buildings, the quantification of the benefits of green buildings against conventional buildings and the technologies to achieve green buildings. Over the last twenty years, a number of green building assessment tools have been developed among many countries, e.g., the Leadership in Energy and Environmental Design (LEED, United States), BRE Environmental Assessment Method (BREEAM, United Kingdom), Hong Kong Building Environmental Assessment Method (HK BEAM), Green Building Council of Australia Green Star (GBCA, Australia), Green Star South Africa rating system (Green Star SA, South Africa), etc. Most assessment tools allow a credit based evaluation that covers various aspects of the green building sustainability, from the energy efficiency, environmental impact to the human aspect. These assessment tools provide a thorough guideline to the design of green buildings and facilitate the development of green building projects. For example, the LEED v2.2 has accredited over 5000 projects globally since its first launch in 2005 [56].

There are different types of building energy efficiency projects, where retrofitting is the most common one. Although the newly erected green buildings are energy efficient and environmental friendly, removing most of the existing inefficient buildings and erecting brand new green buildings can be too expensive, even infeasible in the near future. The growing energy demands in existing buildings remain an unaddressed issue. Therefore, retrofitting is the main solution to improve the energy efficiency in existing buildings.

1.3.1 Building retrofitting: a difficult problem

The retrofitting of existing buildings is never an isolated topic from the green building design. Many technologies aims at achieving green buildings also facilitate the energy retrofitting in existing buildings. A very common part of the building energy efficiency technologies is the utilisation of the renewable energy. The utilisation of renewable energy includes but is not limited to: photovoltaic and wind turbine driven electricity, the solar water heating, the geothermal heat pump, the biomass energy [57, 58, 59]. The renewable energy resources cause less emission than the conventional energy resources, e.g., coal and petrol. Furthermore, utilising the renewable energy resources reduces the power demand from the main grid. This is essential to achieve net zero energy buildings [60, 61]. There have been many studies pertaining to renewable energy retrofitting projects [62, 63, 64]. Another aspect of technologies in common is the energy conservation interventions that aims at reducing the energy consumption and improve the resource utilisation efficiency [65, 66]. The term 'energy conservation intervention' is 'used to mean measures to improve efficiency or conserve energy or water, or manage demand' as defined in [67]. The utilisation of the energy conservation interventions involves many of the studies introduced in the previous section. The control strategies implemented to the appliances for energy efficiency purpose can be a type of energy conservation interventions. Apart from the improvement on the appliance itself, applying the management policy or disseminate the knowledge can also be a form of energy conservation interventions. Some relevant studies can be found from [68, 69, 70, 71, 72].

However, the building energy retrofitting remains a holistic planning problem while involving so many energy efficiency technologies. The retrofitting is a systematic process including five phases [73]: 1) the project setup phase, where the scope of the work is defined and the project target is set; 2) the energy auditing phase, where a thorough understanding of the retrofitted building is established by energy auditing at different level; 3) retrofit option identification phase, where a number of energy conservation interventions can be assessed and selected; 4) implementation phase, where selected interventions will be applied to the retrofitted building; 5) measurement and verification (M&V) phase, where the impact of the retrofitting is quantitatively assessed following a series of standardised methodologies, i.e., the M&V method. Ma *et al.* [73] interprets the retrofitting planning as 'to determine, implement and apply the most cost effective retrofit technologies to achieve enhanced energy performance while maintaining satisfactory service levels and acceptable indoor thermal comfort, under a given set of operating constraints'. During the planning, a large number of the alternative interventions are often involved in a project. The project target usually needs to take into account the energy performances, the economy and the human aspects. Furthermore, building is a complicated system including several interacting subsystems. All these factors make the retrofitting planning difficult to address.

1.3.2 State of the art methodologies

During the last decade, the retrofitting plan optimisation problem has been extensively studied. As aforementioned, a retrofitting plan takes into account multiple considerations that are often contradictory. Consequently, the multi-criteria model is widely employed to select proper retrofit options. The criteria usually involves the energy performances, the economy and human aspects. The energy performance in a retrofitting project is evaluated by the amount of reduced energy consumptions [74, 75, 76, 77, 78]. Malatji *et al.* [52] further introduces the M&V methodology to evaluate the energy performances by the energy savings obtained against an adjusted baseline. In some early studies [79, 80], the economy criterion is the amount of capital investment. Actually, some common economic analysis methods can be introduced to evaluate the cost effectiveness of the retrofit options, e.g., Net Present Value (NPV), Internal Rate of Return (IRR), Overall Rate of Return (ORR), Benefit-Cost Ratio (BCR), Discounted Payback Period (DPP) and SPP [81, 82, 83]. Some of the aforementioned methods have already been employed in the life cycle analysis and the economic evaluation in green building designs [84, 85, 86, 87]. The human aspects can involve the thermal comfort, indoor environmental quality, occupants health and productivity, etc [55]. The human aspects can pertain to some criticisms against green buildings. Thermal comfort issues, e.g., high level of humidity or higher temperature during summer, have incurred some negative experience with green buildings [88, 89, 90]. These issues draw the attention from the building retrofitting researchers. A number of studies take into account the human aspects in their retrofitting projects [91, 92, 93, 94, 95, 96].

The reliable estimation and quantification of the energy conservation intervention benefits is essential to the building retrofitting plan optimisation. The popular method to quantitatively evaluate the intervention benefits is implementing the building energy simulation. There are a number of simulation tools, including EnergyPlus, eQUEST, DOE-2, ESP-r, BLAST, TRNSYS, etc [73]. Generally, these simulation tools include a variety of building component models, ranging from the detailed physical models to the data driven models, which allows the decision maker to simulate the performances of the interventions in a virtual environment considering as many details as possible. A number of building retrofitting and green building design studies have been conducted by taking advantage of the building simulation tools [97, 98, 99, 100, 101, 102].

However, even with the simulation support at highest accuracy, risks are inevitable to the retrofitting planning. This is because of the many uncertainty factors all over the retrofitting process. The possible uncertainty factors can come from the uncertainty in parameters such as savings estimation or weather, the random nature of occupant behavior, the measurement uncertainty such as sampling error, the system performance degradations, etc. Consequently, the overall energy and economy performances in building retrofitting involve significant uncertainty. One important research topic pertaining to this issue is the risk assessment. Risk assessment allows the decision maker to estimate the deviation that the uncertainty factors can deliver to the retrofitting plan [82]. The methodologies include expected value analysis, mean-variance criterion and coefficient of variation, risk-adjusted discount rate technique, certainty equivalent technique, Monte Carlo simulation, decision analysis, real options and sensitivity analysis [73]. A number of studies take into account or focus on the risk assessment in building retrofitting. Gustafsson [103] introduces the sensitivity analysis approach to facilitate the decision making in building retrofitting to choose optimal strategies that are relatively robust against parameter changes. Heo [104] proposes a systematic approach to support large scale analysis and risk conscious decision making in building retrofitting. Menassa [105] proposes an augmented net present value method to estimate the investment that takes into account different uncertainties associated with the life cycle costs and perceived benefits of the investment. Ye et al. [106, 107, 108, 109, 110] propose a series of methodologies to overcome the risks in measurement and verification from sampling uncertainties and minimise the sampling costs.

Although the existing studies have taken into account the life cycle cost analysis and risk assessment, most of the state of the art methodologies only take into account the intervention performances at an early stage. Some life cycle cost analysis studies include the operation cost. The performance degradations and the possibility of equipment malfunctions are hardly mentioned in existing studies. Furthermore, the risk assessment studies mainly address the retrofitting planning as a static optimisation problem. The opportunity of introducing control approaches to address the investment decisions remains an open question.

1.3.3 Optimisation technologies

As aforementioned, the building retrofitting plan optimisation problems are difficult as multiple considerations are involved. The decision maker must take into account several contradictory considerations that leads to conflicting objectives [111], i.e., the retrofitting planning is often a multi-objective optimisation. While the single objective optimisation is relatively straightforward to solve, multi-objective optimisation involves the trade-off between the conflicting objectives, which makes multi-objective optimisation more complicated. There are mainly two kinds of approaches to obtain the solution: the weighted sum approach and the Pareto optimisation. In a weighed sum approach, the objectives are combined into one single objective function with a set of specific weighting factors. This allows the employment of the normal solver for single objective optimisation. The Pareto optimisation is more complicated. It is built on the concept of *dominance* [112]: if solution *a* outperforms solution *b* on each objective, then *a* dominates *b*. Contrarily, if there is no feasible solution that dominates *a*, then *a* is *non-dominated*. The mathematical definition of *dominance* can be found in [112]. The Pareto optimisation finds the collection of non-dominated feasible solutions. Usually, the result of Pareto optimisation, namely Pareto front, is illustrated by a range of non-dominated solutions that are sorted to illustrated the trade off between each objective. Both approaches can be employed to solve the building retrofitting plan optimisation. Malatji *et al.* [52] employs a weighted sum of two objectives with a non-stationary penalty function to solve a retrofitting planning problem involving large amount of retrofit options. Wu *et al.* [113] investigates a similar problem and employs a multi-objective neighborhood field optimisation (MONFO) algorithm to obtain the Pareto front. Generally, the weighted sum approach provides the decision maker a clear answer to the optimisation problem while the Pareto approach offers a concrete understanding of the conflicting nature of the objectives. Both approaches are valuable to the decision maker.

Once the formulation of the objective function is confirmed, there are a variety of solvers to be employed. The evolutionary computing approaches are easy to implement and verified to be effective against non-linear optimisation problems [114]. Evins [111] illustrates the popularity of the evolutionary computing with the retrofitting optimisation studies. The review did a broad search among the relevant studies from 1990 to 2012. According to the statistics, the Genetic Algorithm has been the most popular solver that is employed by over half of the investigated studies. Some other commonly employed evolutionary computing approaches include the Simulated Annealing, Particle Swarm Optimisation and Differential Evolution. For high dimensional optimisation problems, the conventional evolutionary computing approaches result in great computational burden. This is resulted from the stochastic nature of the evolutionary computing. During the last decade, improved algorithms have been investigated to address such a issue. Wu et al. [115, 116] propose a neighborhood field optimisation method to improve the convergence accuracy and speed of the evolutionary computing approaches in high dimensional optimisation problems. This method has been utilised in different building energy optimisation problems [113, 117].

1.4 A CONTROL SYSTEM FRAMEWORK

1.4.1 Complexity of retrofitting and maintenance planning

The time scale of retrofitting planning is much larger than the smart appliance operation or power energy flow balance. However, retrofitting planning is not an isolated issue within the scope of building energy efficiency. There are strong connections between different layers of the building energy efficiency framework: the power quality is essential to guarantee the performances of the appliances; the smart appliance operation and energy flow balance are the basis to evaluate the performances of retrofit options. On the other hand, the investment decisions introduce a series of objectives to the energy flow balance, smart appliance operation and power quality control. If the energy efficiency at the other three layers cannot sustain during operation, further risks are introduced into the investment decisions due to the deviations of evaluation.

Actually, the investment decisions suffer significant risks from the failures of retrofitted items during operation. In practice, failures and malfunctions are inevitable as most subsystems in buildings are subject to deterioration with usage and age [118]. In the retrofitting planning, the most concerned performance is the energy savings. The energy savings cannot be directly measured, since they represent the absence of energy use. Instead, savings are determined by comparing measured use before and after implementation of a project, making appropriate adjustments for changes in conditions. According to the measurement and verification (M&V) principles [67, 119], a failed item no longer contributes energy savings to the retrofitting project. The results comes from the fact that in M&V, savings are computed by the difference between the actual performance and an estimated (adjusted) baseline performance, as Fig. 1.2 indicates [119]. According to M&V principles, when a failed item appears, the energy consumption baseline is adjusted accordingly. More, specifically, the baseline consumption and the actual consumption of the failed item are both absent, resulting in the absence of the desired energy saving from the item. Thereafter, such an absence of energy savings from individual items result in the decrease of overall energy savings. The clean development mechanism (CDM)[120] guideline for energy efficiency lighting project already notices the negative impacts of failures. An additional constraint is added to the project: if 50% of the initial installed lamps are lost during the evaluation period, project is considered to be a failure [121]. In practice, maintenance actions are periodically applied over the item life cycle to restore the failed item to normal working state, and the

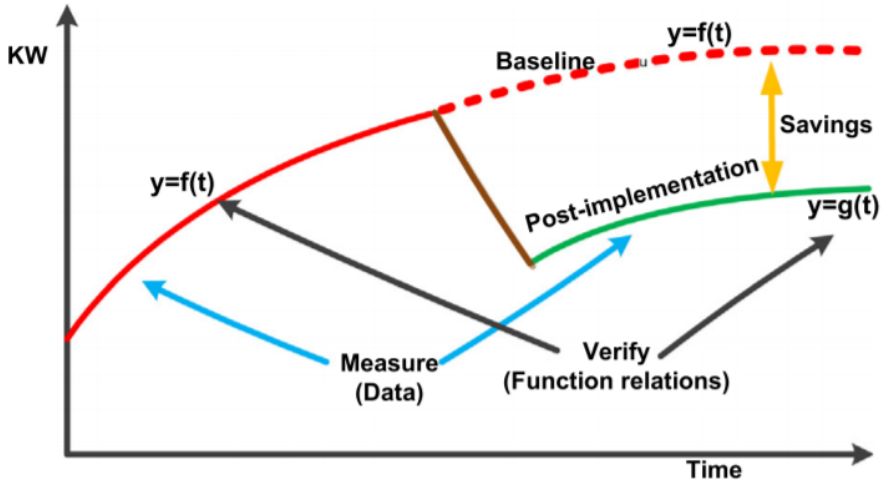

Figure 1.2. Concept of measurement and verification (M&V)

energy savings are accordingly restored. However, maintenance actions result in additional capital and manpower investment. Under the joint impacts of failures and maintenance, the aggregate energy and economy performances manifest strong dynamics during operation.

However, the impacts of maintenance are unique. Different with the stochastic nature of the item failures, maintenance is a kind of activities that can be planned and scheduled. While maintenance contributes to the dynamics of energy and economy performances in a retrofitting project, it also implies that the performances can be 'controlled' by maintenance planning. More specifically, in a retrofitting project, the aggregate energy and economy performances can be further improved against the impacts of failures by incorporating maintenance planning into the investment decision. Consequently, such investment decisions become even more complicated: the time interval of maintenance planning ranges from several months to one or two years, which is very different with the aforementioned energy efficiency issues; the maintenance planning involves both management level performances and actions on individual retrofitted items; the costs of applying maintenance actions must be taken into account to be a part of the investment. Furthermore, maintenance engineering is also a broad research field. The diverse maintenance actions can bring in more complicated interacting effects, e.g., some maintenance actions can influence the possibilities of items becoming failure.

In summary, the investment decision of a retrofitting project can be very complex, manifesting multiple time scales and significant dynamics when simultaneously taking into account the retrofitting and maintenance planning. Such a novel investment decision is promising to overcome the risks from inevitable retrofitted item failures. However, the aggregate performances are dynamical during operation due to the joint effects of failures and maintenance. The inevitable uncertainties, the interplay between different item groups and the item performance degradation before malfunctions result in additional complexity to the performance dynamics. The state of the art optimisation methodologies cannot address investment decisions with such complexity. There lacks a systematic approach to allow the modelling, optimisation and development of investment decisions in retrofitting projects. Therefore, we propose a control system framework to address the above issues.

1.4.2 Control system framework

The conventional building automation has already brought in a large number of relevant studies that employ control approaches. Although the control system perspective remains novel to the planning layer decision makings, the control approaches are specialised to address problems with dynamic natures. In the above discussion, we already mention that the aggregate performances can be ‘controlled’ by maintenance planning. Ideally, the dynamic nature of the aggregate performances can be described to be the system dynamics under the influence of the control inputs, i.e., the maintenance actions. Thereafter, the investment decision can be cast into an optimal control problem. However, there are two gaps to fill to implement control approaches in such a way: 1) the gap between the management level concerns and the individual item characteristics; 2) the gap between the conventional optimal control modelling and the investment decision modelling.

On the one hand, the major concerns of retrofitting planning are the aggregate energy and economy performances rather than individual item or subsystem performances. On the other hand, the computation of aggregate performances requires information regarding each individual item. In practice, it is very expensive (from both capital and manpower viewpoints) to inspect each item. Therefore, modelling each retrofitted item is infeasible for the investment decision. In the CDM energy efficiency lighting projects, sampling strategies are introduced to address similar issues [107]. The performances of a large scale lighting group are estimated by monitoring a small group of lamps. The metering data are processed to represent the whole lighting group, at the cost of additional uncertainties. Following the idea of sampling strategies, a grouping method is introduced to allow the system dynamics modelling at the management level. The retrofitted items are categorised into several groups. Each group consists of items that are considered to be homogeneous ones, i.e., with the same inherent energy and reliability performances, the same operating schedules and similar operational environment. Thereafter, the aggregate energy savings can be computed by the individual item savings and the item group populations. The term 'population' hereby refers to the count of retrofitted items. The term 'population' is frequently used in this dissertation, and the above explanation applies to most contexts. The retrofitted item failures are represented by the population decay of the item groups. The population decay modelling is another interesting and difficult research topic. Nevertheless, it is not the major concern in this dissertation. Generally, the statistical laws are employed to be our population decay models. Accordingly, the impacts of maintenance actions to the item group population are the main focus in the control system modelling. A term 'maintenance intensity' is hereby introduced to describe the count of the restored items from one item group at a specific instant. Such instant is referred to as the 'maintenance instant', i.e., a time point at which the maintenance actions are scheduled to take place. The maintenance intensities and instants are selected to represent the maintenance plan, instead of individual item maintenance strategies. Similarly, economy performances, e.g., the cash inflow and outflow of the project can be obtained from the item group populations and maintenance intensities.

Taking advantage of the grouping method, the control system modelling is revealed already. Given that the state variables are a set of variables that meet the minimal requirement to describe the future state of a dynamical system, the item group populations are selected to be the state variables. The maintenance intensities are selected to be the control inputs. The population decay of the item groups comprise the system dynamics. The aggregate performances are selected to be the measured output. In this way, a control system framework is obtained, where the retrofitting and maintenance planning is cast into an optimal control problem. A finite decision horizon, namely the sustainability period is defined. Generally, the control objectives are maximising the aggregate energy savings and a certain economy performance indicator, e.g., the internal rate of return (IRR), over the sustainability period. A series of constraints are accordingly introduced, e.g., the targeted energy saving limit, budget limit and payback period limit, etc. The uncertainty factors are inevitable in practice. The impacts of uncertainties are taken into account to be random noises on the state variables and measured outputs.

There are many promising control approaches to address the investment decision with uncertainties, e.g., the model predictive control (MPC). However, the investment decision optimal control problem is different with the conventional optimal control formulation. Firstly, multiple objectives are involved in the investment decision, and the objective formulations are very different with the conventional quadratic performance index. The IRR formulation is even more complicated, as it is non-analytic. Secondly, the constraints involve a series of long-term performances, e.g., the budget limits. Such constraints are unusual to the optimal control problems with uncertainties. To overcome these difficulties, a weighted sum approach is employed to combine the two control objectives. Thereafter, an alternative MPC based approach with an improved differential evolution (DE) algorithm based numerical solver is employed. This controller design is frequently employed in most chapters of the dissertation. The technical details are attentively introduced there.

1.4.3 Control inputs: maintenance

The control system framework allows further development and extensions. Different selections of state variables, control inputs and measured outputs are possible given different situations and purposes. For example, the control inputs, i.e., the maintenance actions, involve a broad field of the maintenance engineering. In practice, there are many maintenance types corresponding to different functionalities. The combinations of different maintenance types can be introduced into the control system framework to achieve the control objectives in different scenarios.

In reliability engineering, the maintenance actions are defined to be the activities required to operate and maintain the facilities and their supporting infrastructures in a condition to be used to meet their intended function over the operating period [3]. The maintenance categories are enormous: there is emergency maintenance, corrective maintenance, preventive maintenance, predictive maintenance and proactive maintenance [122]. The most common maintenance categories are the corrective maintenance (CM) and preventive maintenance (PM). CM involves the repairs and replacements against failures and PM refers to all actions performed in an attempt to retain an item in a specified condition, according to MIL-STD-721C[4]. In reliability engineering, the maintenance actions are implemented subject to the maintenance policy. The objective of the maintenance policy is usually to reduce the failure rate of a specific type of facility during operation. The common maintenance policies include the age-dependent PM policy, periodic PM policy, failure limit policy, repair limit policy, etc [123]. These maintenance policies are similar to a large extent: The PM actions are implemented when a certain

[3] Comprehensive Facility Operation & Maintenance Manual, 2013, http://www.wbdg.org/om/om_manual.php

[4] MILITARY STANDARD: DEFINITIONS OF TERMS FOR RELIABILITY AND MAINTAINABILITY, 1981, http://www.everyspec.com/MIL-STD/MIL-STD-0700-0799/MIL-STD-721C_1040

condition is satisfied. This condition can be the age, failure times or repair times, depending on the policy. This condition is usually the decision variable of the maintenance policy optimisation. The early stage studies take into account the minor failures that can be repaired and catastrophic failures that requires replacement. However, the performance degradation without a failure is not included. The multi-state system (MSS) approach is developed to address this issue. The MSS characterises the multiple performance levels in a system by defining a set of multi-working and failure states [124, 125, 126]. In an MSS, the current working state can degrade to a worse one upon time. CM represents the actions that restore the system from a failure state and the PM actions are carried out before failures, restoring the system to a better state. Such state-transition of the MSS has described to be a Markov process in relevant studies [125, 126, 127, 128, 129, 130]. The decision variables in MSS are more complicated, including the types of maintenance to be implemented under each state, the frequency of inspection and the number of PM actions, etc.

In our studies, the selective control inputs involve PM and CM. The scope of the corresponding maintenance actions is illustrated in Fig. 1.3. The meanings of some terms in Fig. 1.3 can be slightly different with the conventional maintenance engineering definitions. The planned maintenance suggests the existance of the maintenance plan (our decision variables), as opposed to the unplanned maintenance, where maintenance actions take place when the need arises. The scheduled preventive maintenance and deferred corrective maintenance are the selective control inputs, where the deferred corrective maintenance refers that the maintenance action can be delayed until the scheduled instant when maintenance can take place. The immediate corrective maintenance refers to the emergency maintenance, which take place to repair the failed items where downtime cannot be tolerated, e.g., the power supply. The immediate corrective maintenance is excluded from our control inputs. Instead, it is taken into account as part of the uncertainty factors. The condition based maintenance is excluded at the current stage as well. It mainly refers to the routine maintenance that is indicated by the manufacturer. In the future, the condition based maintenance can be designed/optimised as an open-loop control scheduling problem.

The selection of control inputs fulfills different requirements in practice, where decision makers are facing different options while the capitals and manpower are limited. For example, preventive maintenance can reduce the possibility of failures, however, additional manpower is required to apply preventive maintenance. Therefore, the impact of preventive maintenance must be carefully evaluated to decide whether preventive maintenance should be introduced into a retrofitting project. This is the

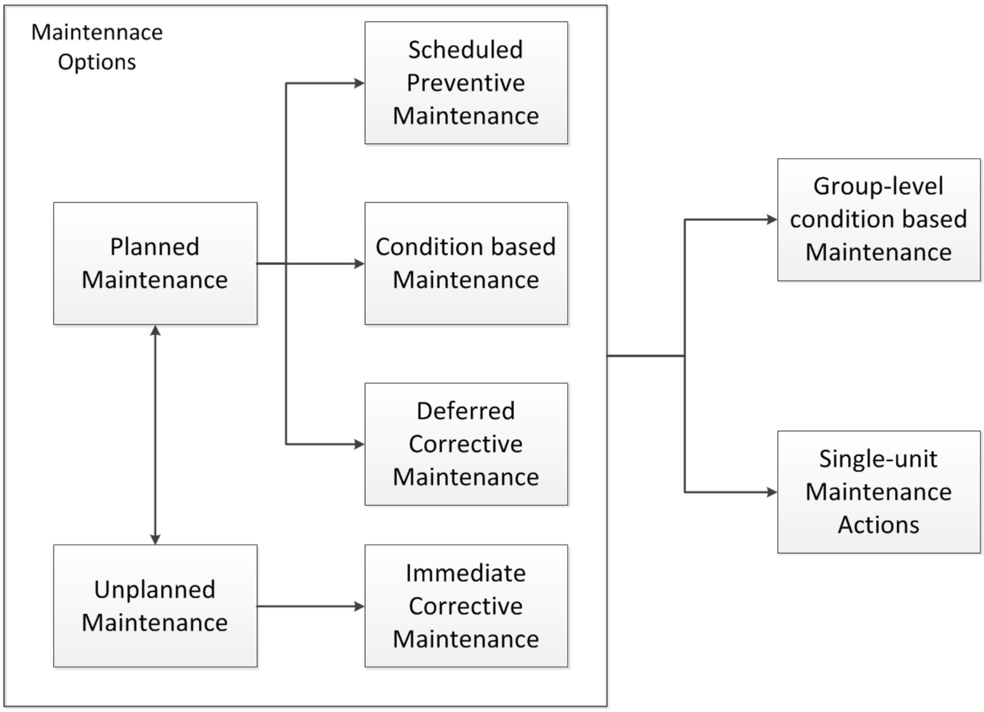

Figure 1.3. The scope of maintenance actions involved in the control system modelling

reason that investment decision optimisation is required. Our studies investigate the impacts of different combinations of control inputs, i.e., the maintenance categories. This dissertation is a precursor study that aims at developing a systematic approach for investment decisions, where expansion is possible via selecting different state variables and control inputs. Furthermore, the new control system perspective to the investment decision for retrofitting and maintenance planning can facilitate the development of control science by investigating the dynamical system modelling and controller design for investment decisions.

1.4.4 The selection of numerical solver

The thesis's works bring in a kind of optimisation problems that includes mixed integer decision variables, non-linear items and non-analytic items. Furthermore, given the complexity of the input (a series of maintenance intensities and even instants), the optimisation problems can be considered as non-convex. Such items make the optimisation problems difficult to solve. A DE based numerical solver is employed for the mixed integer, nonlinear, non-analytic and non convex optimisation problems. DE algorithm is a more recent evolution algorithm that is very easy to implement with computers.

Vesterstrom *et al.* [131] conduct a comparative study to investigate the performances of DE algorithm on a set of 23 numerical benchmark problems and conclude that DE is the best performing algorithm in the study. During recent decade, the number of studies that employ DE algorithm for non convex optimisation problems. In the recent decade, the number of studies that employ DE algorithm for non convex optimisation problems keeps growing. A few literatures that employ DE algorithm to solve non smooth, non convex problems and with over 200 citations are hereby listed [132, 133, 134].

In the thesis, DE algorithm is the selective numerical solver due to its simplicity and rapid searching ability. It however does not guarantee the global optimum. Instead, after sufficient iterations, the DE algorithm can hopefully find a satisfying solution. On the one hand, the DE algorithm is less reliable than conventional gradient based numerical solvers, e.g., sequential quadratic programming (SQP). this is the main drawback of DE and other evolutionary algorithms. On the other hand, DE can be applied to all kind of numerical problems, which allows it to be employed in complicated practical optimisation problems as mentioned in literatures [135, 136]. The comparison of DE solver and other numerical solvers is however excluded from the contributions of the thesis. The thesis will focus on establishing the control system framework rather than investigating numerical solvers.

1.5 RESEARCH CONTRIBUTIONS AND LAYOUT OF THE DISSERTATION

The main contributions of this dissertation have been published in five journal articles and another one has been submitted for publication. Some conference contributions have also been published or accepted. These contributions are listed in the section of publications.

The major topic of the thesis is to develop a control system framework to address the building energy retrofitting and maintenance problems at the planning layer by a control system approach. Although the building retrofitting and maintenance planning has been studies from the perspectives of optimisation, the inherent dynamics of the planning problems are not well addressed. As a result, the control system remains an unexplored perspective for the building energy efficiency project management level planning. The energy performance evaluation is given by the M&V principles. The main contributions are highlighted as following:

- Introducing the life-cycle cost analysis and corresponding dynamics modelling into building energy retrofitting planning.

- The thesis's works contribute to the investment decision at management level. Different with the conventional control topics, the thesis focuses on managing item groups via a management level modelling. Such a modelling is connected with both the planning and operation interests.

- It is identified in this thesis that the maintenance problems at management level can be modelled as an optimal control problem, thus allows the employment of control system approaches.

- Many different maintenance options from reliability engineering are introduced into the control system framework to better reflect the practical maintenance strategies. The control approaches are accordingly developed.

Given the limitations of models and corresponding knowledge, a series of limitations of the current stage work are listed as following to allow the establishment of control system framework.

- The statistical law is employed to characterize the population decay of items. Currently, the stochastic model remains uninvestigated and can be a major challenge of the following researches.

- Many of the engineering facts are simplified, e.g., the multi-state transition models and the MTBF dynamics of air conditioning system. Polishing, improving and removing the simplified engineering facts are another research challenge in the future.

- The numerical solver is limited to evolutionary algorithm. The evaluation of the performances of the numerical solver is not one of the contributions of the thesis, therefore it is not listed in this work.

A layout description of the dissertation are described below.

- The building energy retrofitting planning taking into account the life cycle analysis is investigated.

- The corrective maintenance planning for building energy retrofitting is investigated from the dynamic programming and optimal control perspective.

- The corrective maintenance planning is extended by taking into account the interacting energy effects.

- A multi-state system based maintenance plan optimisation problem is modelled.

- The maintenance time schedule is incorporated into the maintenance plan optimisation.

- The robustness of the grouping method is investigated.

Chapter 2 introduces an improved retrofitting plan optimisation model. The dynamic performances due to the failures and maintenance are incorporated into the optimisation problem by the life cycle cost analysis approach. The life cycle costs mainly come from the maintenance costs. The maintenance plan is pre-decided, based on which the long-term performances are computed. Chapter 2 preliminarily investigates the performance dynamics within the investment decision of the retrofitting planning. Taking advantage of the results in chapter 2, the necessity of the control system framework is revealed.

Chapter 3 further investigates the investment decision with maintenance planning. A corrective maintenance plan optimisation problem is cast into an optimal control problem where the performances dynamics can be addressed. Thereafter, an MPC based control approach is introduced to solve the maintenance plan optimisation. The control inputs are the corrective maintenance intensities subject to pre-decided maintenance time schedule. In this way, the control system framework is established with a lot of opportunities to develop and extend to fulfill different project requirements. The ability of the control approach to reduce the negative impacts of uncertainties is also manifested in Chapter 3.

Chapters 4, 5 and 6 are the extension of the control system framework by selecting different state variables and control inputs. In Chapter 4, the main topic is to address the interplay between different retrofitted item groups. The control system framework is extended by introducing coupled state variables, where the interacting energy and reliability effects are modelled. The new modelling is verified to be able to achieve better energy and economy performances against the interacting effects.

In Chapter 5, the item performance degradation before malfunctions is addressed by introducing preventive maintenance into the control system framework. Accordingly, the control system modelling is improved by employing a multi-state system approach, where the performance degradations and effects of preventive maintenance are modelled. The control inputs are thereby extended to include the preventive maintenance intensities. The case study verifies the energy efficiency contributions from preventive maintenance. Chapter 6 introduces a collaborative optimisation of the maintenance intensities and instants based on the multi-state control system obtained in Chapter 5. By investigating the collaborative optimisation, further energy efficiency opportunities have been identified within maintenance planning.

In the above chapters, the system dynamics are modelled based on a grouping method. The retrofitted items are categorised into several groups of homogeneous items, each consists of items that are considered to have same energy and reliability performances. Thereafter, the performances can be computed from the item group populations. Such a grouping method is inherently subjective, depending on the knowledge of the decision maker. An interesting question is thereby brought in: will the control system performances sustain with different grouping methods? Such robustness of different grouping methods is essential to our control system framework. Therefore, Chapter 7 investigates the grouping robustness. A preliminary theoretical analysis is proposed.

Finally, some general conclusions and ideas of future research topics are drawn in Chapter 8.

CHAPTER 2 OPTIMAL RETROFITTING PLANNING WITH LIFE-CYCLE COST ANALYSIS

2.1 INTRODUCTION

The retrofitting plan optimisation hereby involves selecting the energy conservation interventions on the equipment, e.g., the lights, HVAC devices, water heaters, office appliances, etc. The trade off between the energy performance and cost-effectiveness is taken into account. The objective of the optimisation is to find the best trade off between the two considerations to strike the balance between the interests of the stakeholders.

The energy performances are evaluated by the energy savings of each intervention. The energy savings are obtained following the M&V methodology. As we introduced in Chapter 1, the failures and malfunctions result in the absence of the energy savings. The energy savings during operation can vary over time. Thereafter, the impacts and costs of the maintenance should be taken into account as well. The maintenance actions can restore the failed equipment from absence. From the energy efficiency perspective, this restores the absent energy savings of the failed interventions. The maintenance delivers a significant impact to the energy efficiency of the retrofitting project in this way. Thereafter, the maintenance costs pertaining to the restoration of energy savings should be taken into account as part of the operation cost.

As a result of such dynamics of the energy savings and maintenance costs during operation, the decision maker has to take into account the long-term performances of the interventions. When evaluating alternative interventions, one can appear to be cost-effective at the installation stage but actually more expensive over the long term. Therefore, the life cycle cost analysis (LCCA) is employed to figure out the long term cost-effectiveness of the alternatives. The LCCA is an advanced technique especially for assessing the total cost of facility ownership. The life-cycle cost (LCC) is defined to be *the total cost throughout its life including planning, design, acquisition, support and any other costs directly attributable to owning or using the asset* [1]. In this study, The LCC pertains to the estimation of future cash flows. The cash inflow mainly comes from the energy savings, and the cash outflow comes from the retrofitting investments and maintenance costs. Thereafter, the LCCA can be applied to estimate the overall costs of the alternatives during the life-cycle of the building and evaluate the long term cost-effectiveness. Actually, the LCCA has been employed in relevant studies for the building retrofitting investments. Verbeeck and Hens [84] firstly introduces the concept of LCC to assess the economically feasibility of the retrofit options. Kaynakli [137] uses LCCA to determine the optimal thickness of the insulation material in a building envelope for best cost-effectiveness. Menassa [105] presents a method to determine the retrofitting investment by taking into account different uncertainties within the LCC.

This study hereby proposes a multi-objective optimisation model with life-cycle cost analysis for building retrofitting planning. The objectives including maximising the long term energy savings over a specific period of time, namely the sustainability period, and maximising the internal rate of return (IRR) of the project during the sustainability period. The reason of selecting the sustainability period instead of the whole life cycle of the building is that the uncertainties keep growing until the end of the building life cycle. The IRR is the indicator of the economy performance, i.e., the cost effectiveness. The optimisation model involves both selecting proper energy conservation interventions from a range of available alternatives and determining the quantities of equipment to apply the intervention. The weighted sum approach is employed, i.e., the objective function is a polynomial of the quantitative objectives. The general target is to find the retrofitting plan that achieves the maximum possible energy savings with highest possible IRR subject to the targeted saving, payback period and retrofitting budget constraints. The targeted saving is the minimal saving amount that must be achieved by the retrofitting. The payback period is defined to be the latest possible time that the project NPV remains non-negative. The retrofitting budget constraint indicates how much investment is allowed to implement the retrofitting plan.

[1] NSW Treasury, Life Cycle Costing Guideline, http://www.treasury.nsw.gov.au/__data/assets/pdf_file/0005/5099/life_cycle_costings.pdf

A number of alternatives involved in the optimisation. There are many possible combinations of the alternatives, and the evaluation often involves non-linear performance indicators. The possible interventions and combinations must be taken into account and evaluated simultaneously. With the development of computational powers and algorithms, it is possible to address problems with such complexity. The evolutionary algorithm (EA), a kind of generic population-based meta-heuristic optimisation algorithm, is hereby introduced for the building energy optimisation problems. The Genetic Algorithms (GAs) are a type of very famous EA that are widely employed by the decision makers [138, 52]. However, GAs are difficult to encode and the convergence speed is relatively slow. Storn and Price [139] proposes a simple and efficient meta-heuristic method, namely the differential evolution (DE) algorithm, to improve the conventional GAs. According to [139] and [131], DE generally outperforms GAs and many other algorithms on many numerical benchmark problems, including unimodal and multimodal functions, functions with correlated and uncorrelated variables, and a single problem with plateaus. More importantly, the DE algorithm is very easy to implement compared to the GAs. A DE algorithm based numerical solver is employed for the optimisation model in this study. The employed DE algorithm is an improved one with a binary neighbourhood field optimisation (BNFO) method [116]. An actual building retrofitting project is selected to be the case study. The simulation results illustrates the feasibility and effectiveness of the proposed approach.

2.2 MULTI-OBJECTIVE OPTIMISATION MODELLING

2.2.1 Decision variables

In a retrofitting project, a set of energy conservation interventions and corresponding retrofitting actions constitute the retrofitting plan. The retrofitting actions include the existing equipment to be retrofitted, the alternatives of the new technological interventions and the quantities of equipment corresponding to the selected alternative. Table 2.1 illustrates a sample of the retrofitting plan.

Assuming that I types of retrofitted equipment are involved in the project, and there are J_i types of alternative interventions corresponding to each equipment type. Let x_i^j denote the number of selected items from the *i-th* equipment with *j-th* alternative intervention, namely alternative intervention (i, j). For $i = 1, 2, ..., I$, let $X_i = (x_i^1, x_i^2, ..., x_i^{J_i})$, and $\mathbf{X} = (X_1, X_2, ..., X_I)$. $\mathbf{X}$ is thus the decision variable in

Table 2.1. A sample retrofitting plan

Equipment	Alternatives	Quantities
Lighting	Lighting Intervention 1	20
	Lighting Intervention 2	0
	Lighting Intervention 3	35
Geyser	Geyser Intervention 1	25
Air-Con	Air-Con Intervention 1	0
	Air-Con Intervention 2	30

this retrofitting plan optimisation problem. Given that the decision variables are quantities of selected items, the nature of the investigated problem is an integer programming problem.

2.2.2 Multi-objectives formulation

Let $t_k = kS$, $k = 0, 1, 2, ..., T$ denote the sampling instants over the *sustainability period* $[0, TS)$, where $t_0 = 0$ and S indicates the sampling interval. As aforementioned, there are two objectives, the energy savings and IRR. Let (2.1) and (2.2) indicate the two objectives respectively:

$$f_1(X) = \frac{ES|_{all}}{\alpha}, \tag{2.1}$$

$$f_2(X) = IRR, \tag{2.2}$$

where (2.1) indicates the energy efficiency objective and (2.2) indicates the cost-effectiveness objective. ES_{all} denotes the overall energy savings during the sustainability period $[0, TS)$ and α denotes the targeted energy savings, which is usually a percentage of the energy consumption of the retrofitted building. ES_{all} is computed by (2.3):

$$ES|_{all} = \sum_{k=1}^{T} \sum_{i=1}^{I} \sum_{j=1}^{J_i} a_i^j(t_k) x_i^j(t_k), \tag{2.3}$$

where $a_i^j(t_k)$ denotes the energy savings contributed by a retrofitted item corresponding to alternative (i, j) over the interval $[t_{k-1}, t_k)$. $x_i^j(t_k)$ denotes the number of working items corresponding to alternative (i, j). As a result of the possible failures and malfunctions, $x_i^j(t_k)$ can vary during operation. Generally, ES_{all} is the summation of the energy savings from each retrofitted item over the sustainability period. The IRR is developed based on NPV: it is the discount rate that makes $NPV = 0$ over the sustainability period. The NPV is formulated by (2.4):

$$NPV = \sum_{k=1}^{T} \frac{B(t_k) - h(t_k)}{(1+d)^{n(t_k)-1}} - h_0, \tag{2.4}$$

where d is the selected discount rate. $n(t_k)$ denotes the year where the sampling interval $[t_{k-1}, t_k)$ lies within after t_0. It is an integer that selects value from $1, 2, ...$ $n(t_k)$ is adopted because that the NPV is computed on a yearly basis. h_0 indicates the initial investment of the retrofitting project, i.e., the capital cost to implement the retrofitting. $B(t_k)$ denotes the cash inflow over $[t_{k-1}, t_k)$. In this case, the cash inflow comes from the cost savings corresponding to the energy savings. $h_(t_k)$ denotes the cash outflow that comes from the maintenance actions. h_0, $B(t_k)$ and $h_(t_k)$ are formulated by the following equations:

$$h_0 = \sum_{i=1}^{I} \sum_{j=1}^{J_i} c_i^j x_i^j, \tag{2.5}$$

$$B(t_k) = \sum_{i=1}^{I} \sum_{j=1}^{J_i} b_i^j(t_k) x_i^j(t_k), \tag{2.6}$$

$$h(t_k) = \sum_{i=1}^{I} \sum_{j=1}^{J_i} u_i^j(t_{k-1}) m_i^j(t_k), \tag{2.7}$$

where $b_i^j(t_k)$ indicates the cost savings subject to the energy savings from the items and the energy price. c_i^j is the cost of applying single intervention (i, j). x_i^j, as aforementioned, indicates the number of items corresponding to alternative intervention (i, j). $x_i^j = x_i^j(t_k)$. The estimation of such prices can takes into account the inflation. $m_i^j(t_k)$ indicates the maintenance cost for one item from (i, j) and $u_i^j(t_k)$ denotes the count of items that are restored over $[t_{k-1}, t_k$ from (i, j). The IRR thus is obtained by solving d out of the equation $NPV = 0$.

The objectives are subject to a series of constraints as (2.8) illustrates:

$$\begin{cases} \sum_{j=1}^{J_i} x_i^j \leq x_i, \\ ES|_{all} \geq \alpha, \\ NPV|_0^{T_p} \geq 0, \\ h_0 \leq \beta. \end{cases} \tag{2.8}$$

where x_i denotes the maximum possible number of the items subject to the i-th equipment. T_p denotes the computed payback period and T' the maximum acceptable payback period. T_p is obtained by solving the NPV sequence. Assuming that k' is the last index that makes NPV negative, i.e., $\sum_{k=1}^{k'} \frac{B(t_k)-h(t_k)}{(1+d)^{n-1}} - h_0 < 0$, then $T_p = k' + 1$. T' is the expected payback period. β denotes the budget limit that covers the implementation costs of the retrofitting project. There is an alternative form of the budget limit:

$$h_{all} \leq \beta'. \tag{2.9}$$

where

$$h_{all} = h_0 + \sum_{k=1}^{T} \sum_{i=1}^{I} \sum_{j=1}^{J_i} u_i^j(t_k) m_i^j(t_k). \tag{2.10}$$

β' hereby denotes the budget limit for overall cost, including the implementation costs and maintenance costs, during the sustainability period.

The objectives of this model are maximising objective function $f_1(X)$ and $f_2(X)$ subject to constraints (2.8) or (2.9).

2.2.3 Population decay formulation

$x_i^j(t_k)$ represents the number of working items corresponding to intervention (i,j) over the interval $[t_{k-1},t_k)$. $x_i^j(t_k)$ can be different with x_i^j due to the population decay resulting from the failures and malfunctions. Such population decay delivers a series of impacts to the optimisation model (2.1)-(2.7). The term 'failure' hereby refers to the all the possible problems that prevent the equipment from working, i.e., the malfunctions. A malfunctioning item is considered to be unavailable to the occupants of the building. For example, a faulty, flickering light bulb or an air conditioner having mechanical problems with its condenser or compressor are considered malfunctioning, which no longer contribute energy savings. There could also be some electrical and mechanical problems which do not stop the items from working, for example, the fatigue of a bulb or the refrigerant in an air conditioner needs to be recharged. The equipment performances can deteriorate due to such problems. Such deterioration will be taken into account in Chapter 6. At the current stage, only the the malfunctions are included to clearly illustrate the idea.

$x_i^j(t_k)$ is estimated by the following equation:

$$x_i^j(t_{k+1}) = G_i^j(x_i^j(t_k)) + x_i^j(t_k) + u_i^j(t_k), \tag{2.11}$$

where $x_i^j(t_0) = x_i^j$. $G_i^j(\cdot)$ represents the population decay of the items corresponding to intervention (i,j). Succeeding the decision variables definition, $\forall i,j$ and t_k, $x_i^j(t_k) \in \mathbb{Z}^+$ as x represents the quantity of items, therefore, x is an integer by nature. Carstens *et al.* [109] monitors and formulates the population decay of a lighting group in a Clean Development Mechanism (CDM) lighting retrofitting project. According to the study, such population decay can be considered as a first-order Markov process, which means that the population size after decay only relates to the population size prior to the decay. An assumption is made here: the retrofitted items subject to intervention (i,j) constitute a group of homogeneous items with the same failure rate, namely homogeneous group. This assumption will be discussed in Chapter 7.

According to the existing studies, two population decay models are hereby employed:

$$G_i^j(x_i^j(t_k)) = \mu_i^j \nu_i^j x_i^j(t_k)^2/x_i^j \triangle t - \mu_i^j x_i^j(t_k)\triangle t, \tag{2.12}$$

$$G_i^j(x_i^j(t_k)) = -\frac{\triangle t}{\eta_i^j} x_i^j(t_k), \tag{2.13}$$

where $\triangle t = t_{k+1} - t_k$. The coefficients μ, ν, η are estimated by the mean time to failure (MTTF) for the non-repairable product and mean time between failures (MTBF) for repairable product. (2.12) and (2.13) are discrete time representations of a set of continuous form survival rate models. (2.12) is taken from [109], which describes the population decay for the non-repairable items, e.g., the lamps, showerheads, motion sensors, etc. According to [109], the original continuous time survival rate statistical law is given as (2.14):

$$x_i^j(t) = \frac{x_i^j}{\nu_i^j + e^{\mu_i^j t - L_i^j}}. \tag{2.14}$$

A mathematical transformation is applied to (2.14) to obtain (2.12). The L_i^j denotes the rated lifetime, i.e., the MTTF for the non-repairable items. The coefficients in (2.14) can be identified from the experimental data fitting or solved out from the following equation:

$$\begin{cases} x_i^j(t_0) = x_i^j, \\ x_i^j(L_i^j - t_0) = 0.5 x_i^j. \end{cases} \tag{2.15}$$

$x_i^j(t_0) = x_i^j$ is the initial condition and $x_i^j(L_i^j - t_0) = 0.5x_i^j$ is resulted from the definition of rated life time of light bulbs.

(2.13) describes the population decay of repairable items, e.g., the air conditioners, chillers, heat pumps, etc. These equipment usually have a very long lifespan, several times longer than the MTBF. According to the reliability bathtub curve [140], the failure rate of the equipment is an approximately low constant before the end of the lifetime. Therefore a constant failure rate decay model is adopted from [140], implying the following continuous time survival rate statistical law:

$$x_i^j(t) = e^{-\frac{t}{\eta_i^j}} x_i^j, \tag{2.16}$$

where η_i^j denotes the MTBF of the equipment.

The selections of the scale of L, η and $\triangle t$ are tricky. In case that L and η are much larger than $\triangle t$, (2.12) and (2.13) manifest sufficient accuracy to approximate the continuous time model. However, this is not always the case. In buildings, the sampling interval can be quite large comparing with the rated life time of some equipment. In that case, a iterative differential approximation of (2.12) and (2.13) applies. Furthermore, given the integer nature of x, the continuous variables $x_i^j(t_{k+1})$ in (2.12) and (2.13) are forced to be integers at the end of the differential approximation.

(2.11) describes such a population dynamics: each homogeneous group subject to intervention (i, j) consists of the remained population and the maintained population, after the maintenance actions that take place at t_k, the remain population is estimated by (2.12) or (2.13), depending on the type of the equipment, and the maintained population is given by $u_i^j(t_k)$. $u_i^j(t)$ and the maintenance instant t_k can vary according to different maintenance plan. The maintenance plan optimisation will be introduced in the following chapter. For the non-repairable items, the maintenance action is usually the replacement, therefore the maintenance cost $m_i^j(t)$ is the cost of replacing the malfunctioning item by a new one. For the repairable items, maintenance actions can be the repairs, and $m_i^j(t)$ is often a lower cost than the replacement [141].

2.2.4 The weighted sum objective function

Marler and Arora [142] suggests that, the weighted sum method provides a basic and easy-to-use approach that gives an acceptable approximation of one's preference function when the preference information is not too complex. By employing the weighted sum approach, the optimisation model (2.1)-(2.7) is translated into a minimisation problem. The objective function is formulated to be the weighted sum of two objectives associated with a non-stationary penalty functions:

$$J(x) = -\lambda_1 f_1(X) - \lambda_2 f_2(X) + \omega \sum_{k=1}^{3} max(0, P_k), \tag{2.17}$$

where λ_1, λ_2 are a pair of positive constants, i.e., the weighting factors. ω is a large positive constant associated with the penalties. P_k with $k = 1, 2, 3$ are the penalty functions pertaining to the constraints (2.9). The formulations of P_k are:

$$P_k = \begin{cases} \alpha - ES, & k = 1, \\ T_p - T', & k = 2, \\ h_0 - \beta, & k = 3. \end{cases} \tag{2.18}$$

An alternative form of the penalty function P_3 subject to constraint (2.9) is formulated:

$$h_{all} - \beta', \;\; k = 3. \tag{2.19}$$

A differential evolution (DE) based numerical solver can be adopted for the minimisation problem (2.17)-(2.18). The adopted DE algorithm is an improved one where the binary neighborhood field optimisation (BNFO) method is incorporated. The BNFO method is a mechanism that introduces the binary coding and neighbourhood field optimisation (NFO) mechanism to DE algorithm. The binary coding allows the DE algorithm to be an integer decision variable solver, and the NFO method improves the convergence of the algorithm comparing with the conventional DE. The technical details of the numerical solver can be found in Addendum A. The DE algorithm with BNFO method is employed by most chapters of the thesis as the mixed integer nonlinear programming (MINLP) solver. The comparison of the DE algorithm and conventional MINLP solvers is not the focus of the thesis; for more detailed discussions, please refer to Addendum A.

One important reason to employ the weighted sum approach is that such objective formulation can be extended to the maintenance plan optimisation as an optimal control problem. The weighted sum approach will be our major modelling method. An additional study has been conducted by the author, where a Pareto approach is employed to the multi-objective retrofitting planning taking into account the LCCA [113].

2.3 RESULTS AND ANALYSIS

2.3.1 Case study

An actual building retrofitting project is adopted to be our case study, where 12 types of interventions are taken into account subject to a series of equipment, including lighting facilities, heat pumps, chillers, control systems and other devices. Each intervention type has 2-5 alternatives. The content of the input data is shown in Table 2.2, including information on the existing equipment and specifications of the alternative interventions. 2.2. The *Maximum Possible Quantity* column regulates the count of items from a specific type of intervention that can be retrofitted. The aggregation of the retrofitted items from one intervention type cannot exceed its maximum possible quantity. The *Unit Cost* with unit US dollar $ indicating the cost of purchasing and installing one such item, i.e., the cost of implementing this alternative; *Energy Savings* with unit kWh is the estimation of the average annual energy savings from implementing the selected alternative; *Unit Cost Saving* is the estimation of the cost savings subject to the energy saving. The maintenance cost and the MTTF(MTBF) are illustrated by the *Maintenance Cost* and *MTTF(MTBF)* columns. In reliability engineering area, the units of MTTF and MTBF are usually hours. For the convenience of computation, the unit of MTTF(MTBF) is translated into years, according to respective operating schedules of items. The coefficients of the population decay models for each intervention are shown in Table 2.3. As mentioned in the previous section, there are non-repairable items that apply the decay model (2.12), and repairable items that apply the decay model (2.13). The coefficients η_i^j, μ_i^j and ν_i^j for different alternatives are illustrated in the three columns.

Some parameters in the optimisation model are selected according to the specifics of the project. In this case study, the service provider of the retrofitting is contracted to guarantee the energy performances in 10 years, i.e., the sustainability period is 10 years. The targeted energy savings are 10% of the energy baseline, which is 58,709,110 kWh over the sustainability period. Baseline adjustment is not considered here, as this baseline mainly provides a targeted saving amount. The budget limits and payback period limits are shown in Table 2.4, where 8 scenarios are introduced. The first 4 scenarios A, B, C, D adopt budget constraint from equation (2.18) while the rest scenarios E, F, G, H adopt the budget constraint from equation (2.19). Thus the range of the budget amounts is much larger in the last 4 scenarios. The discount rate for the NPV computation is 9%.

The maintenance plan is decided by the owner of the building. A full maintenance strategy is adopted here, i.e., every time a maintenance takes place, it will restore all the failed items back to working within the scope of the project. The maintenance plan in this case study is scheduled in such a way: at the end of every two years, the maintenance can take place and all failed items are repaired or replaced. (2.20) indicates the values of $u_i^j(t_k)$ under the adopted maintenance plan:

$$u_i^j(t_k) = \begin{cases} 0, & k = 1,3,5... \\ x_i^j - x_i^j(t_k), & k = 2,4,6... \end{cases} \tag{2.20}$$

which means maintenances take place at the end of the year 2,4,6... During each maintenance, all the failed items are fixed, so that the population size is increased to x_i^j. For the 8 scenarios, $\lambda_1 = 0.5$, and $\lambda_2 = 0.5$. Such weights are employed to represent the equal importance of the two objectives: energy savings and IRR.

2.3.2 Illustrative results and analysis

Fig. 2.1 compares the performances from the DE algorithms with the BNFO method and the conventional DE. The solid curve is the BNFO method result and the dashed curve is the conventional DE result. The logarithmic coordinate is applied to the y-axis to better illustrate the iterations. The mean result over 10 runs with the standard errors are illustrated. Given that the global optima of our minimisation problem is an unknown one, the local minima is reached to be a satisfying solution. In

Table 2.2. Detailed information on existing and proposed alternative facilities

Existing equipment	Maximum possible quantity	Proposed alternatives	Unit Cost ($)	Energy Savings (kWh)	Unit Cost Savings ($)	Main-tenance Cost($)	MTTF (MTBF) (years)
No sensors installed	202	Motion sensor type1	196	1141	155.02	196	3
		Motion sensor type2	150.28	1240	168.47	150.28	3.42
50W downlight I	537	energy saver globe type1	16.36	208	10.65	16.36	3.33
		energy saver globe type2	16.93	223	11.42	16.93	2.92
		energy saver globe type3	20.19	195	9.98	20.19	3.5
		energy saver globe type4	18.95	220	11.26	18.95	3.33
50W downlight II	145	35 W new lamp ECG type1	14.19	102	5.2	14.19	3.33
		35 W new lamp ECG type2	15.17	116	5.91	15.17	3.75
		35 W new lamp ECG type3	14.25	107	5.45	14.25	3.58
18W recessed fitting I	270	18 W retrofit ECG type1	11.72	21	1.07	11.72	3.17
		18 W retrofit ECG type2	11.11	20	1.02	11.11	2.58
		18 W retrofit ECG type3	9.47	25	1.27	9.47	2.75
54W recessed fitting II	1271	36 W triphosphor tubes type1	65.67	232	11.88	65.67	3.25
		36 W triphosphor tubes type2	78.09	186	9.52	78.09	3.08
		36 W triphosphor tubes type3	61.54	262	13.42	61.54	3.17
		36 W triphosphor tubes type4	60.77	260	13.31	60.77	2.83
		36 W triphosphor tubes type5	65.29	199	10.19	65.29	3.17
Old chillers	4	New chillers type1	147125	25392	13775.88	14712.5	2
		New chillers type2	170590.31	23539	12770.57	17059.03	2.25
Electric geyser	9	3 kW heat-pumps type1	1250	10989	794.44	125	2
		3 kW heat-pumps type2	1299.22	11166	807.24	129.92	2.25
		3 kW heat-pumps type3	1544.88	12074	872.88	154.49	1.83
Electric geyser	3	22 kW heat-pumps type1	13750	1006	1854.13	1375	2
		22 kW heat-pumps type2	13757.97	875	1612.69	1375.79	1.92
		22 kW heat-pumps type3	12600.01	1152	2123.22	1260.01	2.25
Electric geyser	94	9 kW heat-pumps type1	1250	10989	72.74	125	2
		9 kW heat-pumps type2	1355.36	12447	82.39	135.54	2.17
		9 kW heat-pumps type3	954.95	9019	59.7	95.5	2.17
High-flow showerheads	360	Low-flow showerheads type1	11.25	278	18.61	11.25	5.42
		Low-flow showerheads type2	10.54	254	17	10.54	4.83
No heater wraps	107	Heater wraps type1	21	273	21	21	4.25
		Heater wraps type2	24.32	326	25.08	24.32	4
		Heater wraps type3	22.36	243	18.69	22.36	5
No thermal traps	107	Thermal traps type1	8	380	8	8	5.58
		Thermal traps type2	9.13	350	7.37	9.13	4.08

Table 2.3. Coefficients of the decay models

Existing Facilities	Proposed alternatives	$\frac{1}{\eta_i^j}$	μ_i^j	ν_i^j
No sensors installed	Motion sensor type1		1.2895	0.9502
	Motion sensor type2		1.2521	0.9672
50W downlight I	energy saver globe type1		1.2587	0.9643
	energy saver globe type2		1.2984	0.9459
	energy saver globe type3		1.2458	0.9698
	energy saver globe type4		1.2587	0.9643
50W downlight II	35 W new lamp ECG type1		1.2587	0.9643
	35 W new lamp ECG type2		1.2286	0.9765
	35 W new lamp ECG type3		1.2398	0.9722
18W recessed fitting I	18 W retrofitting ECG type1		1.2732	0.9579
	18 W retrofitting ECG type2		1.3403	0.9245
	18 W retrofitting ECG type3		1.3179	0.9361
54W recessed fitting II	36 W triphosphor tubes type1		1.2658	0.9612
	36 W triphosphor tubes type2		1.2811	0.9542
	36 W triphosphor tubes type3		1.2732	0.9579
	36 W triphosphor tubes type4		1.3078	0.9412
	36 W triphosphor tubes type5		1.2732	0.9579
Old chillers	New chillers type1	0.5		
	New chillers type2	0.4444		
Electric geyser	3 kW heat-pumps type1	0.5		
	3 kW heat-pumps type2	0.4444		
	3 kW heat-pumps type3	0.5455		
Electric geyser	22 kW heat-pumps type1	0.5		
	22 kW heat-pumps type2	0.5217		
	22 kW heat-pumps type3	0.4444		
Electric geyser	9 kW heat-pumps type1	0.5		
	9 kW heat-pumps type2	0.4615		
	9 kW heat-pumps type3	0.4615		
High-flow showerheads	Low-flow showerheads type1		1.1568	0.9956
	Low-flow showerheads type2		1.176	0.992
No heater wraps	Heater wraps type1	0.2353		
	Heater wraps type2	0.25		
	Heater wraps type3	0.2		
No thermal traps	Thermal traps type1	0.1791		
	Thermal traps type2	0.2449		

Table 2.4. Eight scenarios with different budget limits and payback period limits

Scenarios	Description
Scenario A	The initial investment budget limit is \$60,000. The payback period limit is 3 years. The targeted energy saving is 10% of the energy baseline.
Scenario B	The initial investment budget limit is \$95,000. The payback period limit is 3 years. The targeted energy saving is 10% of the energy baseline.
Scenario C	The initial investment budget limit is \$125,000. The payback period limit is 3 years. The targeted energy saving is 10% of the energy baseline.
Scenario D	The initial investment budget limit is \$195,000. The payback period limit is 3 years. The targeted energy saving is 10% of the energy baseline.
Scenario E	The overall investment budget limit is \$100,000. The payback period limit is 3 years. The targeted energy saving is 10% of the energy baseline.
Scenario F	The overall investment budget limit is \$125,000. The payback period limit is 3 years. The targeted energy saving is 10% of the energy baseline.
Scenario G	The overall investment budget limit is \$175,000. The payback period limit is 3 years. The targeted energy saving is 10% of the energy baseline.
Scenario H	The overall investment budget limit is \$250,000. The payback period limit is 3 years. The targeted energy saving is 10% of the energy baseline.

Fig. 2.1, the solid curve decreases faster than the dashed curve and the reached fitness value is a smaller one. The convergence of the dashed curve cannot be reached even after 1500 iterations, manifesting unsatisfying convergence speed. The better convergence and accuracy of the BNFO method is thereby illustrated.

Table 2.5 illustrates the corresponding performances from the optimisation results, where *Energy Saving*, *Overall Profit* and *Overall Investment* are the aggregate performances over the sustainability period. *Percentage saved* indicates the proportion of energy savings against the energy baseline. *IRR* indicate the internal rate of return. *Initial Investment* are the implementation costs of the retrofitting plan and *Overall Investment* are the investment including maintenance costs over the sustainability period.

In Table 2.5, scenarios A, B, C, D are cases with the initial investment budget limit, scenarios E, F, G, H are cases with overall budget limit. In all 8 scenarios, the investments are very close to

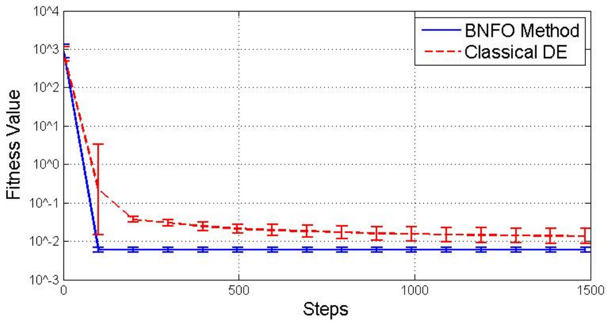

Figure 2.1. The comparison of the convergence of from the BNFO method and classical DE

Table 2.5. Performances of the optimal solutions

	Payback period (months)	Energy savings (kWh)	Percentage Saved	IRR	Investment($) Initial	Investment($) Overall	NPV($)
Scenario A	13	6180190	10.53%	91.23%	59554.26	80579.36	311974.7
Scenario B	21	8906045	15.17%	59.18%	94954.27	121881.5	293950.3
Scenario C	28	11220535	19.11%	44.85%	124975.2	157469.1	270064.1
Scenario D	36	14288310	24.34%	33.27%	170248.5	213768.4	243709.4
Scenario E	17	7532570	12.83%	72.23%	77200.32	99918.37	306113.4
Scenario F	22	9163590	15.61%	56.88%	98492.25	124971.8	290213.4
Scenario G	32	12486805	21.27%	38.52%	141428.2	174989.1	249235.7
Scenario H	36	14259005	24.29%	33.31%	170135	211481.4	244192.1

the budget limits, indicating that as many cost-effective alternatives are selected as possible. With increased budget, the optimal solution take into account more items which are less cost-effective than the prior selected ones. The economy performances degrade with the growing budget limit, however, more energy savings are achieved by increasing the investment. The trade-off between the energy and economy objective are thereby illustrated. The radar charts in Fig. 2.2 illustrate the comparative shapes of the performances in all 8 scenarios. The scales of the values of each performance characteristics are normalised to the similar range for the sake of clear illustration. It can be observed that the shapes of the optimal performances in the radar charts are similar with each other. Table 2.5 and Fig. 2.2 manifest the ability of our optimisation model to find satisfying solutions.

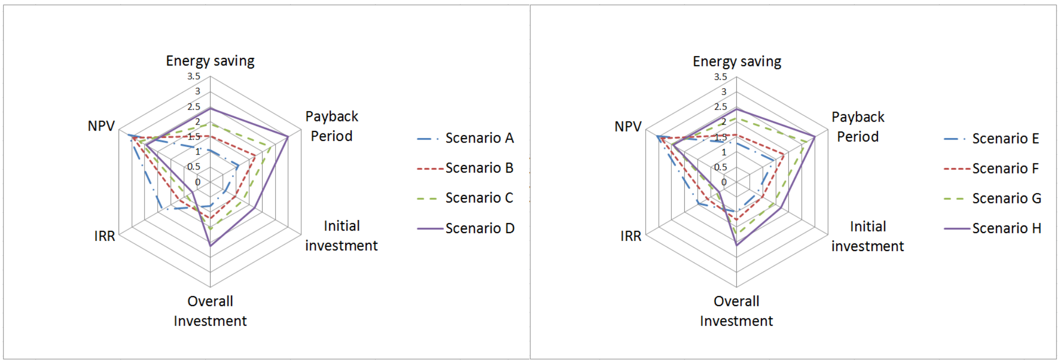

Figure 2.2. Comparative performances (normalized) in 8 Scenarios

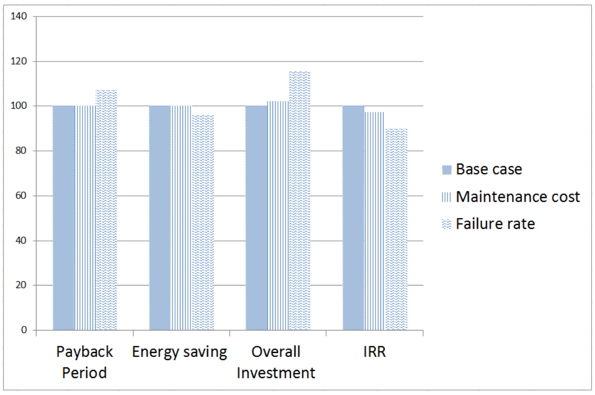

Figure 2.3. Sensitivity analysis of the impacts from maintenance cost and failure rate

2.3.3 Sensitivity analysis

In practice, the confidential level of the parameters cannot reach 100% due to the inevitable uncertainty factors. The actual performances of the project thereby manifest deviations from the estimations. A set of sensitivity analysis is given for several parameters, e.g., the auditing error, electricity prices, wrongly specified energy savings and initial investments. The uncertainties on the maintenance cost and failure rate are selected. The maintenance cost of the interventions can be different due to the fluctuation in economy. The stochastic nature of the equipment failure rates must be taken into account as well. Consequently, the bias on the performance due to the uncertainty factors must be checked.

Fig. 2.3 illustrates the performance bias when the failure rates and the maintenance costs of all interventions are increased by 10%. The performances of Scenario C are selected to be the baseline demonstrate the influences on payback period, energy savings, overall investment and IRR. Given the baseline performances to be 100%, the biased performances against the baseline are illustrated. According to Fig. 2.3, the impacts of the failure rate uncertainties appear to be more significant. When the maintenance costs are increased, the payback period is 28 months and the energy savings are 11220535 kWh. The overall investment increases to \$160718.5 and the IRR decreases to 43.59%. When failure rate is increased, the payback period becomes 30 months and the energy savings are 10768095 kWh. The overall investment increases to \$181463.6 and the IRR decreases to 40.27%.

2.4 CONCLUSION

An optimisation model for building retrofitting planning is introduced in this chapter. The optimisation objectives are maximising the overall energy savings 7and internal rate of return over the sustainability period. A life-cycle cost analysis method is incorporated into the optimisation model, where the population dynamics due to the equipment failures and maintenance is taken into account. In this way, multiple alternative interventions are simultaneously evaluated to select the proper combinations of intervention types and number of retrofitted items, under a series of constraints.

The energy savings are subject to the population dynamics, which can be adjusted by the maintenance. Furthermore, the life cycle costs are highly related to the selective maintenance plan. There are further energy efficiency potentials within the maintenance planning for a retrofitting project.

CHAPTER 3 MAINTENANCE PLAN OPTIMISATION

3.1 INTRODUCTION

In the previous chapters, the necessity and complexity of maintenance for the sustainability of energy efficiency in a building retrofitting project is already mentioned. The maintenance actions, from the building retrofitting perspective, delivers a very different impact from the conventional reliability engineering perspective. In a retrofitting project, absence and restoration of the energy savings are the major concern, instead of the equipment reliability. The aggregate population and the performances manifest significant dynamics under the impacts of the failures and maintenance. However, the maintenance planning in the building energy efficiency context is not a straightforward issue. On the one hand, the decision variables in retrofitting planning can influence several long term performances that are also influenced by the maintenance planning; on the other hand, the operation of the retrofitted items, which usually subjects to short intervals such as days and hours, can also influence the maintenance planning from the reliability and energy perspectives. Furthermore, the budget limits must be taken into account as well. Generally, the building energy optimisation problems becomes complicated due to the complexity and interplay of the retrofitting, maintenance and operation.

To investigate how to incorporate the maintenance plan optimisation into the building energy efficiency framework, the maintenance planning problem from chapter 2 is extended, namely the Building Retrofit Corrective Maintenance Planning (BRCMP) problem. The term ‘retrofit’ hereby refers to the totality of the retrofitted items in the retrofitting project. The BRCMP problem is a simplified subproblem from the broad field of maintenance planning: it only takes into account the planning of the corrective maintenance, and subject to fixed time schedule. The corrective maintenance actions are planned at the aggregate population level, instead of focusing on individual items. In order to allow the retrofit to be planned at the management level, the items are categorised into several groups subject to the interventions. Each group consists of items that are considered to be homogeneous ones, i.e., with the same inherent energy and reliability performances, the same operating schedules and similar operational environment. Such grouping is subjective as different decision makers can have different opinions on the grouping plan. The robustness of the grouping will be discussed in Chapter 6. In practice, apart from the usual maintenance actions, there can be emergency maintenance. The emergency maintenance pertains to the equipment that must work continuously, e.g., the power electronic devices that guarantees the power supply of the building. Such equipment is excluded from the planning, as no deferred maintenance can be tolerated.

Taking advantage of the grouping, the major concern of the BRCMP problem becomes the aggregate energy and economy performances of each group. An aggregate population level optimisation model is thereby developed. Given the BRCMP a problem succeeding the retrofitting planning in chapter 2, the same objectives are employed, i.e., maximising the overall energy savings and internal rate of return (IRR) over the sustainability period. The major difference between the retrofitting planning and BRCMP is the decision variable. In retrofitting planning, the decision variables are the categories and number of the items to be applied with interventions, which are decided at the initial stage of the retrofitting project. The maintenance planning pays attention to the maintenance actions all over the sustainability project. The decision variables in BRCMP are the counts of the items to be restored by the maintenance actions at pre-decided time points from each group. The term 'maintenance intensity' is hereby employed to indicate a count of the restored items from one group at a time, and the term 'maintenance instant' to indicate a time point at which the maintenance actions are scheduled to take place. The maintenance instants constitute a successive sequence of time points all over the sustainability period and subject to the maintenance time schedule. Accordingly, the maintenance intensities are a sequence of integers with inherent dependence and subject to the maintenance instants. Consequently, the maintenance plan optimisation is a dynamic optimisation. The optimisation model formulation without taking into account the uncertainties is the first part of this chapter.

The existing optimisation models lack the ability to address the problem with the uncertainties. Given the dynamics nature of the BRCMP problem, the control system approach is introduced. The control system is an almost unexplored perspective for the building energy optimisation at the planning level. From the control system perspective, the totality of the retrofitted items constitute the control plant, the maintenance intensities become the control variables and the populations of each group of homogeneous items are the state variables. The measured output of the control system can be several long-term performances, e.g., the aggregate energy savings, capital investment, etc. The uncertainty factors are taken into account as the disturbances on the state variables or measured output. For simplicity, two further assumptions are made: 1) the disturbances are introduced to be a random noise on state variables; 2) the sampling errors are simplified as a random noise on the measured output. In this way, the BRCMP problem is cast into an optimal control problem. Taking advantage of the aforementioned weighted sum approach, the objective function can be formulated. Thereafter, the uncertainties, i.e., the disturbances, can be addressed by the control system approaches. A model predictive control (MPC) based approach is hereby employed. The MPC approach repeatedly optimises the optimal control inputs based on the predicted future from the present state of the system. The disturbances are included within each prediction, therefore the MPC is inherently robust against disturbances. The MPC approach is easy to implement by computers. It has been widely used in control problems in many fields, including the engineering, food processing, automotive applications, and aerospace applications [143], demand-side management [144] and dispatch of power generation [145]. The optimal control problem is the second part of this chapter.

The differential evolution (DE) algorithm with the binary neighbourhood field optimisation method is employed as the numerical solver for both the dynamic optimisation and the optimal control. A practical building retrofitting project is employed as the case study to test and verify the feasibility of the optimisation and control approaches.

3.2 MULTI-OBJECTIVE BRCMP

3.2.1 Variables definitions

Assuming that I groups of homogeneous items are involved in a retrofitting project. Let $t_k = kS, k = 0,1,2,...,T$ denote the sampling instants over the sustainability period $[0,TS)$, where $t_0 = 0$ and S indicates the sampling interval. Let $x_i(t_k)$ denote the population of item group i over the sampling period $[t_{k-1},t_k)$, which constitute the state variables:

$$\mathbf{x}(t_k) = (x_1(t_k), x_2(t_k), ..., x_I(t_k))^T. \tag{3.1}$$

Let $\mathbf{x}(t_0) = \mathbf{x}_0$ indicate the initial condition of the state variables. $\mathbf{x}_0$ is obtained from the retrofitting plan. In practice, $x_i(t_k)$ with $k > 0$ is obtained by the inspection at instant t_k. For the energy conservatism, the inspection result is considered to be the state over the last sampling interval. Let $u_i(t_k)$ denote the maintenance intensities at instant t_k, i.e., the count of maintenance actions subject to group i and take place over interval $[t_k, t_{k+1})$. The maintenance plan at t_k can be represented by:

$$\mathbf{u}(t_k) = (u_1(t_k), u_2(t_k), \ldots, u_I(t_k))^T. \tag{3.2}$$

For the convenience of further derivation, let $\mathbf{x}$ and $\mathbf{u}$ denote the system states and maintenance intensities respectively. $\mathbf{u}$ are thereby the decision variables of the BRCMP and control variables of the optimal control problem. Let Q denote the pre-decided maintenance time schedule:

$$Q = \{m_1, m_2, \ldots, m_\tau\}. \tag{3.3}$$

Q indicates the collection of the maintenance instants. The elements of Q are the indices of the sampling instants, selected from $k = 1, 2, \ldots, T$. Generally, the maintenance instants in our model are considered to be commensurate with the sampling instants t_k. According to the time schedule, $\mathbf{u}(t_k) = 0$ if $k \notin Q$.

Taking advantage of the population dynamics (2.11), the system state is updated by:

$$x_i(t_{k+1}) = G_i(x_i(t_k)) + x_i(t_k) + u_i(t_k). \tag{3.4}$$

$G_i(\cdot)$ denotes the population decay of the item group i over $[t_k, t_{k+1})$. From the control system perspective, $G_i(\cdot)$ is the system dynamics. In this chapter, the retrofitted items are also categorised into non-repairable items and repairable items. The population decay models are adopted from (2.12) and (2.13) accordingly.

3.2.2 Objective function formulation

The objective function formulation adopts the objectives from our retrofitting plan optimisation model: the energy savings as the energy performance indicator and IRR as the economy indicator. Taking advantage of the performance measures (2.3)-(2.7), the objectives are formulated as following:

$$\begin{cases} f_e(\mathbf{x}, \mathbf{u}) = \dfrac{ES|_{all}}{\alpha}, \\ f_r(\mathbf{x}, \mathbf{u}) = IRR, \end{cases} \tag{3.5}$$

where $f_e(\mathbf{x},\mathbf{u})$ is the energy performance objective and $f_r(\mathbf{x},\mathbf{u})$ is the economy performance objective. Similarly, $ES|_{all}$ denotes the aggregate energy savings:

$$ES|_{all} = \sum_{k=1}^{T} ES(\mathbf{x}(t_k),t_k) = \sum_{k=1}^{T}\sum_{i=1}^{I} a_i(t_k)x_i(t_k), \tag{3.6}$$

where α is the targeted energy saving amount. $ES|_{all}$ is the overall energy savings subject to the maintenance plan over the sustainability period. $ES(\mathbf{x}(t_k),t_k)$ is the aggregate energy savings from the retrofitting project over interval $[t_{k-1},t_k)$, where $\mathbf{x}(t_k)$ is to emphasise the connection between the energy savings and the group population, i.e., the system state. $a_i(t_k)$ denotes the energy savings that one item from group i contributes over $[t_{k-1},t_k)$. The aggregate cost savings $CS|_{all}$ can be computed accordingly:

$$CS|_{all} = \sum_{k=1}^{T} B(\mathbf{x}(t_k),t_k) = \sum_{k=1}^{T}\sum_{i=1}^{I} b_i(t_k)x_i(t_k), \tag{3.7}$$

where $B(\mathbf{x}(t_k),t_k)$ denotes the aggregate cost savings, i.e., the cash inflow over $[t_{k-1},t_k)$. $b_i(t_k)$ denotes the energy savings that one item from group i contributes over $[t_{k-1},t_k)$. In order to calculate IRR, the cash outflow must be obtained as well. The cash outflow mainly consists of the maintenance costs:

$$h|_{all} = h_0 + \sum_{k=1}^{T} h(\mathbf{u}(t_{k-1}),t_k) = h_0 + \sum_{k=1}^{T}\sum_{i=1}^{I} c_i(t_k)u_i(t_{k-1}), \tag{3.8}$$

where $h|_{all}$ denotes the overall capital investments of the project. h_0 denotes the initial investment for the implementation of the retrofitting plan. h_0 can be obtained according to (2.5). However, in the BRCMP problem, h_0 is considered to be a known a priori constant instead of a performance indicator to be adjusted. $h(\mathbf{u}(t_{k-1}),t_k)$ denotes the aggregate maintenance costs over $[t_{k-1},t_k)$, where $\mathbf{u}(t_{k-1})$ is applied over the same interval. $c_i(t_k)$ denotes the maintenance cost over $[t_{k-1},t_k)$ to restore one failed item from group i to working state. $h(\mathbf{u}(t_{k-1}),t_k)$ is thereby the cash inflow over $[t_{k-1},t_k)$. The net present value (NPV) which is computed taking advantage of the cash flows:

$$NPV = \sum_{k=1}^{T} \frac{B(\mathbf{x}(t_k),t_k) - h(\mathbf{u}(t_{k-1}),t_k)}{(1+d)^{n(t_k)-1}} - h_0, \tag{3.9}$$

and the IRR is the discount rate d that makes $NPV = 0$ over $[0,TS)$. $n(t_k)$ selects value from $1,2,...$ that indicates that the sampling interval $[t_{k-1},t_k)$ lies within the n-th year after t_0.

The constraints of the BRFMP problem include the system dynamics, targeted energy savings, maintenance budget limit, payback period limit, and the pre-decided maintenance time schedule:

$$\begin{cases} \mathbf{x}(t_{k+1}) = \mathbf{G}(\mathbf{x}(t_k))\triangle t + \mathbf{u}(t_k), \\ ES|_{all} \geq \alpha, \\ \sum_{k=1}^{T} h(t_k) \leq \beta, \\ T_p \leq T', \\ \mathbf{u}_p(t_k) = 0, \ k \notin Q, \end{cases} \tag{3.10}$$

where β denotes the maintenance budget limit. T_p denotes the payback period of the project, T' denotes the payback period limit. T_p is defined to be the last instant where NPV remains negative.

3.2.3 The BRCMP optimisation problem

The weighted sum approach is employed to formulate the objective function. Taking advantage of (3.5) and (3.10), the multi-objective optimisation problem is translated into a minimisation problem, which is the weighted sum of the objectives associated with a non-stationary penalty function:

$$J = -\lambda_1 f_e(\mathbf{x},\mathbf{u}) - \lambda_2 f_r(\mathbf{x},\mathbf{u}) + \omega \sum_{n=1}^{3} max(0, P_n), \tag{3.11}$$

subject to constraints (3.10). λ_1, λ_2 are positive constants, i.e., the weighting factors. ω is a large positive constant that amplifies the penalties of violating constraints. P_n are the penalty functions defined as following:

$$P_n = \begin{cases} \alpha - ES|_{all}, & n = 1, \\ \sum_{k=1}^{T} h(t_k) - \beta, & n = 2, \\ T_p - T', & n = 3 \end{cases} \tag{3.12}$$

The BRCMP optimisation problem is finding a maintenance plan $\mathbf{u}$ that minimises the objective function (3.11). The solver for this optimisation problem is the DE algorithm with the BNFO method that is introduced in Addendum A. The details of the solver will not repeat here.

3.3 CONTROL SYSTEM APPROACH WITH UNCERTAINTIES

3.3.1 The control system framework formulation

Taking advantage of the system states (3.1) and decision variable (3.2), a general form of control system formulation to describe the population dynamics in BRCMP is obtained by rewriting (3.4):

$$\begin{cases} \mathbf{x}(t_{k+1}) = \mathbf{G}(\mathbf{x}(t_k)) + \mathbf{x}(t_k) + \mathbf{u}(t_k) + \mathbf{d}(t_k), \\ \mathbf{y}(t_k) = ES(\mathbf{x}(t_k), t_k) + \mathbf{w}(t_k). \end{cases} \tag{3.13}$$

As aforementioned, the population dynamics is essential to describe the aggregate energy and economy performances at the planning level. Therefore, (3.13) will be a keystone to introduce the control system approaches to the building energy optimisation problems at the planning level. The aggregate energy savings are selected to be the measured output $\mathbf{y}(t_k)$ in this formulation. In large-scale projects, $\mathbf{y}(t_k)$ has to be measured by the sampling method. Ye *et al.* [106] figures out that the accuracy and confidential level of the sampling based measurement is determined by the sampling size. $\mathbf{d}(t_k)$ and $\mathbf{w}(t_k)$ are the disturbances on the system states and measured outputs respectively, which represents the impacts of the uncertainty factors.

Thereafter, the BRCMP can be cast into an optimal control problem that aims at finding an optimal control law $\mathbf{u}$ that minimises the performance index (3.11) subject to the system dynamics (3.13) and constraints (3.10). An MPC based approach is employed to solve the BRFCMP optimal control problem.

3.3.2 The MPC approach

In MPC approaches, a dynamic programming, i.e., an open-loop optimal control problem is repeatedly solved over a finite horizon, namely the control horizon, according to the prediction of the system states and performances. The obtained open-loop optimal control is then used to compute the control input to solve the BRCMP optimal control problem. The state variables executed over the next finite horizon are estimated taking advantage of the obtained control input. The optimal controller over the next finite horizon is actually a function of the system state from the previous control step. A closed-loop feedback is thereby obtained. Given the finite decision horizon ,i.e., the sustainability period in our model, the conventional MPC algorithm is modified as following: let t_m denote the current instant, consider a control horizon that covers $[t_m, TS)$, i.e., the rest of the sustainability period. The revised approach thereby introduces a risk that the computational burden grows along with the decision horizon T. Therefore, it only applies to problems with limited prediction steps. A mathematical transformation of the BRCMP optimal control problem is applied, and the dynamic programming over the control horizon $[t_m, TS)$ is accordingly defined to be the following minimisation problem:

$$min\ J' = -\lambda_1 f'_e|_m(\mathbf{x},\mathbf{u}) - \lambda_2 f'_r|_m(\mathbf{x},\mathbf{u}), \tag{3.14}$$

where $f'_r|_m(\mathbf{x},\mathbf{u})$ indicates the discount rate that makes $NPV'|_m = 0$, with

$$\begin{cases} f'_e|_m(\mathbf{x},\mathbf{u}) = \sum_{k=1}^{m} ES(\mathbf{x}(t_k),t_k) + \sum_{k=m+1}^{T} ES(\mathbf{x}|_m(t_k),t_k), \\ NPV'|_m = \sum_{k=1}^{m} \frac{B(\mathbf{x}(t_k),t_k) - h(\mathbf{u}(t_{k-1}),t_k)}{(1+d)^{n(t_k)-1}} \\ \quad + \sum_{k=m+1}^{T} \frac{B(\mathbf{x}|_m(t_k),t_k) - h(\mathbf{u}|_m(t_{k-1}),t_k)}{(1+d)^{n(t_k)-1}} - h_0, \end{cases} \tag{3.15}$$

subject to

$$\begin{cases} \mathbf{x}(t_{k+1}) = \mathbf{G}(\mathbf{x}(t_k)) + \mathbf{u}(t_k) + \mathbf{w}(t_k), \\ \sum_{k=1}^{m} ES(\mathbf{x}(t_k),t_k) + \sum_{k=m+1}^{T} ES(\mathbf{x}|_m(t_k),t_k) \geq \alpha, \\ \sum_{k=1}^{m} h(\mathbf{u}(t_k),t_k) + \sum_{k=m+1}^{T} h(\mathbf{u}|_m(t_k),t_k) \leq \beta, \\ T_p \leq T', \\ \mathbf{u}(t_k) = 0,\ k \notin Q, \end{cases} \tag{3.16}$$

where $\mathbf{x}|_m(t_k)$ denotes the predictive system states and $\mathbf{u}|_m(t_k)$ the scheduled control inputs after t_m. The employed MPC approach takes into account the existing system states and performances before t_m so that the global performance constraints are guaranteed to be satisfied. The DE algorithm with the BNFO method (As referred in Addendum A) is employed as the numerical solver to the dynamic optimisation problem (3.14)-(3.16).

Taking advantage of the results of the numerical solver, a series of optimal control inputs are obtained that are denoted by $\mathbf{u}'|_m = \{\mathbf{u}'|_m(t_k) : k = m, m+1, ..., T-1\}$. Only the optimal control input over the first interval $[t_m, t_{m+1})$ is applied, denoted by $\hat{\mathbf{u}}|_m = \{\mathbf{u}'|_m(t_m)\} = \{\hat{\mathbf{u}}|_m(\mathbf{x}(t_m), t_m)\}$, where the last equation is to emphasise the functional dependence of the optimal control on the initial state $\mathbf{x}(t_m)$ of the MPC formulation in (3.14)-(3.16). After $\hat{\mathbf{u}}|_m$ is applied, the predictive state $\mathbf{x}|_m(t_{m+1})$ can be obtained. Due to the impacts of uncertainty factors, i.e., the disturbances $\mathbf{d}(t_m)$, the actual state $\hat{\mathbf{x}}(t_{m+1}) = \mathbf{x}|_m(t_{m+1}) + \mathbf{d}(t_m)$. In practice, $\hat{\mathbf{x}}(t_{m+1})$ must be obtained from the inspection. $\hat{\mathbf{x}}(t_{m+1})$ then becomes the initial condition of the MPC formulation over the next control horizon $[t_{m+1}, TS)$. When $m \notin Q$, the control input $\mathbf{u}(t_m) = 0$. The optimal control inputs $\hat{\mathbf{u}}$ are thus obtained by consecutively implementing the above process over the sustainability period. The measured output $\mathbf{y}(t_k)$ is obtained by (3.13). $\mathbf{x}(t_{k+1})$ is also applied as the initial state for the open-loop optimal control problem over the next control horizon. In summary, the following MPC algorithm can be formulated:

3.3.3 The MPC Algorithm

Initialisation: Let initial state $\mathbf{x}(t_0) = \mathbf{x}_0$ and $m = 0$.
(i) Compute the open-loop optimal solution $\{\mathbf{u}'|_m(t_k)\}$ of the problem formulation (3.14)-(3.16), where $k = m, m+1, ..., T-1$.
(ii) The MPC controller $\hat{\mathbf{u}}|_m = \{\mathbf{u}'|_m(t_m)\}$ is applied after the sampling instant t_m. The remains of the open loop optimal solution $\{\mathbf{u}'|_m(t_k) : k = m+1, ..., T-1\}$ are discarded. The predictive state $\mathbf{x}|_m(t_{m+1})$ is then obtained according to:

$$\mathbf{x}|_m(t_{m+1}) = \mathbf{G}(\mathbf{x}(t_m)) + \mathbf{x}(t_m) + \mathbf{u}'|_m.$$

Given the impact of disturbance $\mathbf{d}(t_m)$ on system states, the actual state $\hat{\mathbf{x}}(t_{m+1}) = \mathbf{x}|_m(t_{m+1}) + \mathbf{d}(t_m)$.
(iii) Let $\hat{\mathbf{x}}(t_{m+1})$ be the initial state for the next predictive horizon, $m := m+1$ and go back to step (i).

According to the constraint (3.16), $\mathbf{u}(t_m) = 0$ when $m \notin Q$, where step (i) is skipped and $\hat{\mathbf{x}}(t_{m+1}) = \mathbf{G}(\mathbf{x}(t_m)) + \mathbf{d}(t_m)$. The above MPC algorithm will go over the sustainability period to solve out the optimal control law.

Generally, MPC is a closed-loop optimal control approach, as the input state variable $\mathbf{x}(t_{m+1})$ for each finite-horizon $[t_m, t_{m+N})$ is predicted according to the plant model and executed over the current sampling instant.

3.4 SIMULATION AND VERIFICATION

3.4.1 Case study

A practical retrofitting project is adopted to be our case study. In this study, the project scale is reduced in order to clearly illustrate population dynamics. The retrofitting plant is a fifteen-floor concrete office building for government affairs, erected in 1960s. A deep audit has been applied to identify the energy efficiency potentials and impacts of the interventions. The retrofitting plan is already decided, optimised based on the methodology in Chapter 2. The sustainability period is 10 years. The sampling interval is 6 months, the indices of the sampling instants are $k = \{0, 1, 2, ..., 24\}$. The baseline energy consumption is obtained from the history data which is 4,397,572 kWh per year. The targeted energy saving amount is 15% of the 10-year baseline consumptions, i.e., 6,596,358 kWh. In this project, the cash inflows are defined to be the amount of the cost savings. This is because the investor and the stakeholder of the project are the same party, i.e., the government as the building owner. The overall investment consists of the initial implementation costs and the maintenance costs. A full maintenance strategy is employed as the comparative strategy, where all the failed items are repaired.

The specifications of the retrofits are illustrated in Table 3.1. 5 categories of interventions are involved, including the motion sensors, the 20W retrofit Compact Fluorescent Lamps (CFL), the 23 inch LCD monitors, the 3kW heat-pumps and the 23L microwave ovens. The retrofitted items are grouped subject to the interventions. The motion sensors, 20W CFL and 23 inch LCD monitors are considered to be non-repairable items. The population decay of these item groups are estimated by (2.12). The heat-pumps and microwave ovens are considered to be repairable items, where the population decay of the corresponding item groups are estimated by (2.13). Note that (2.12) and (2.13) are discrete representations developed from continuous time survival rate models, as introduced in 2.2.3. The parameters of the respective population decay models are illustrated in Table 3.2.

Table 3.1 indicates several different performance characteristics of the items with respective interventions, where the currency unit is US dollars. The type column indicates the attribute of the item. Type I indicates the non-repairable items and type II indicates the repairable items. The retrofitting costs are illustrated to indicate the cost to implement one such intervention. The energy savings and cost savings are the the annual average values. The corrective costs are the average estimations of the costs

Table 3.1. Specifications of the involved retrofits

Pre-retrofitting	Retrofits	Type	Quantities	Retrofitting Costs ($)	Unit Energy Saving (kWh)	Unit Cost Saving ($)	Corrective Cost ($)
No motion sensor	Motion sensor	I	123	196	1140	121.1	196
Halogen Classic 75W	20W retrofit CFL	I	408	14	105.6	11.9	14
Old CRT Monitor	23 inch LCD Monitor	I	250	150	87.8	10.8	150
Electrical geyser	3kW Heat-pumps	II	85	1250	8640	973.3	201
Inefficient oven	23L Microwave oven	II	35	88	72	8.3	45

to restore one such item from failures. The quantities of the retrofitted item involved in this energy efficiency retrofitting project, i.e., the initial state $\mathbf{x}_0$. The quantities indicate the initial population of the item groups.

The maintenance actions are scheduled to take place at the end of each year except the last year, i.e., the maintenance time schedule $Q = \{2, 4, 6, ..., 22\}$. From the retrofitting costs, the initial investment h_0 can be obtained, which is \$176,650. The desired payback period is 3 years, i.e., $T' = 6$.

The maintenance planning aims at optimising a series of long-term, planning level performances. The maintenance actions scheduled over a 10-year period are involved in the case study. Waiting for actual operations over such a long period is infeasible. Therefore, the simulation of the population dynamics is hereby adopted. The simulation involves five different cases, including three optimal cases: the *Optimal balance* case where $\lambda_1 = 0.5$, $\lambda_2 = 0.5$, the *Energy prior* case where $\lambda_1 = 1.0$, $\lambda_2 = 0$, and the *Economy prior* case where $\lambda_1 = 0$, $\lambda_2 = 1.0$. The *Optimal balance* case takes into account the two objectives equally. The *Energy prior* case and *Economy prior* case actually cast the BRFCMP

Table 3.2. Parameters for the corresponding population deterioration models

Retrofits	type	MTTF /MTBF	μ_i	ν_i	η_i
Motion sensor	I	1.13	1.299	0.895	N/A
20W retrofit CFL	I	1.49	1.2165	0.9494	N/A
23 inch LCD Monitor	I	2.71	1.115	0.996	N/A
3kW Heat-pumps	II	2.08	N/A	N/A	0.24
23L Microwave oven	II	1.98	N/A	N/A	0.25

Table 3.3. Comparison of the performances of cases without disturbances

Cases	Budget limit ($)	Energy savings (kWh)	Percentage saved	IRR	Payback period (years)	NPV ($)	Maintenance cost ($)	Total investment ($)
No maintenance	N/A	2,065,742	4.69%	0.69%	N/A	-18,755.68	0	176,650
Full maintenance	N/A	8,830,340	20.08%	40.54%	2.71	314,556.3	179,223	355,873
Optimal balance	125,000	8,219,041	18.69%	40.56%	2.7	310,439.4	124,963	301,613
Optimal balance	200,000	8,827,172	20.07%	40.65%	2.7	315,168.6	178,233	354,883
Energy prior	125,000	8,219,041	18.69%	40.56%	2.7	310,439.4	124,963	301,613
Energy prior	200,000	8,830,340	20.08%	40.54%	2.71	314,556.3	179,223	355,873
Economy prior	125,000	8,219,041	18.69%	40.56%	2.7	310,439.4	124,963	301,613
Economy prior	200,000	8,737,285	19.87%	40.79%	2.69	318,225.4	162,328	338,978

problem into a constrained single objective optimisation problem, where one objective is taken into account. For the three cases, there are tight and sufficient maintenance budget limits. The tight budget for the whole sustainability period is $125,000, and the sufficient budget is $200,000. Two different contexts are introduced by the budget limits: the tight budget allows less capital investment than the costs of full maintenance strategy; the sufficient budget is enough to cover the full maintenance costs. The two budget limits are introduced to investigate the effectiveness of our method. Performances with different objectives under different budget limits will be given to illustrate the effectiveness of the proposed approach. In addition, two pre-decided maintenance strategies are included, namely the no maintenance strategy and full maintenance strategy. The no maintenance strategy illustrates the population dynamics without any maintenance. The full maintenance strategy selects all failed items at the current instant. The disturbances are represented by a random noise in the simulation. Given that the system state feedback is adopted in our MPC approach, the noise is added as a total on the system states. The range of the noise is $\pm 0.1\mathbf{x}(t_k)$.

3.4.2 Illustrative results and analysis

Table 3.3 illustrates the optimal maintenance plan performances without considering disturbances. The following information is included: the energy performance indicators including the aggregate energy savings (kWh) and percentage savings against the energy baseline; the economy performance indicators including the IRR, payback period (years) and NPV ($). The maintenance cost ($) and the total investments of the project ($) indicate the actual expenditures. The unacceptable no mainten-

Table 3.4. Comparison of the performances of cases including disturbances

Cases	Budget limit ($)	Energy savings (kWh)	Percentage saved	IRR	Payback period (years)	NPV ($)	Maintenance cost ($)	Total investment ($)
Balance open-loop	125,000	7,685,571	17.47%	38.43%	2.65	274,193.7	125,361	302,011
Balance with feedback	125,000	7,878,323	17.92%	38.78%	2.81	287,191.1	125,179	301,829
Balance open-loop	200,000	8,051,623	18.31%	39.24%	2.64	272,539.8	180,795	357,445
Balance with feedback	200,000	8,810,725	20.04%	40.97%	2.59	307,000.8	196,249	372,899
Energy open-loop	125,000	7,167,616	16.30%	33.54%	3.16	232,309.7	125,585	176,650
Energy with feedback	125,000	7,467,160	16.98%	35.29%	3.05	254,924	124,999	301,649
Energy open-loop	200,000	7,719,358	17.55%	37.33%	2.68	249,480	180,144	356,794
Energy with feedback	200,000	8,674,394	19.72%	39.63%	2.58	293,014.1	199,996	376,646
Economy open-loop	125,000	7,063,163	16.06%	36.69%	2.77	258,692	80,259	256,909
Economy with feedback	125,000	7,512,802	17.08%	37.60%	2.81	277,871.4	94,552	271,202
Economy open-loop	200,000	7,368,024	16.75%	36.04%	2.73	233,466.1	165,144	341,794
Economy with feedback	200,000	7,640,285	17.37%	39.55%	2.71	282,598.7	112,158	288,808

ance performances are illustrated in the first row. The important role of the maintenance is thereby manifested. Then full maintenance performances in the second row are thereby illustrated to be the performance baseline. After that, the *Optimal balance*, *Energy prior* and *Economy prior* performances under different budget limits are illustrated in the rest rows.

The sufficient budget limit cases reveal interesting results. The *Energy prior* performances are the same with the full maintenance solutions. The IRR from the *Optimal balance* performances is improved by slightly losing the energy savings. The *Economy prior* performances appear similar with the former two cases. Generally, the full maintenance strategy is close to the optima with sufficient budget. However, in practice, budget can often be insufficient. In tight budget limit cases, the maintenance plan optimisation plays an important role. In this case study, the same optimal maintenance plan is obtained in the three respective optimal cases with tight budget limits. An explanation of this situation is that the energy and economy performances objectives can be consistent in our case study, given that the cost savings mainly come from the cost of the saved energy consumptions. In summary, the maintenance costs are significantly reduced and the energy savings are still preserved, in comparison with the full maintenance strategy. Such performances reveals the potential for cost-effective maintenance planning, and the effectiveness of our optimisation method is thus verified.

Table 3.4 illustrates the results of the maintenance planning taking into account uncertainty factors.

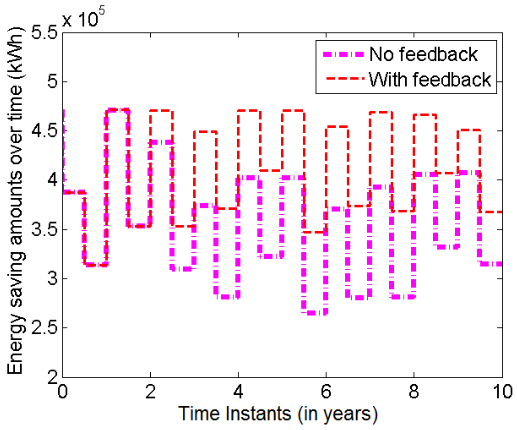

Figure 3.1. Energy performances of the maintenance plans with and without feedback in *Optimal Balance* case.

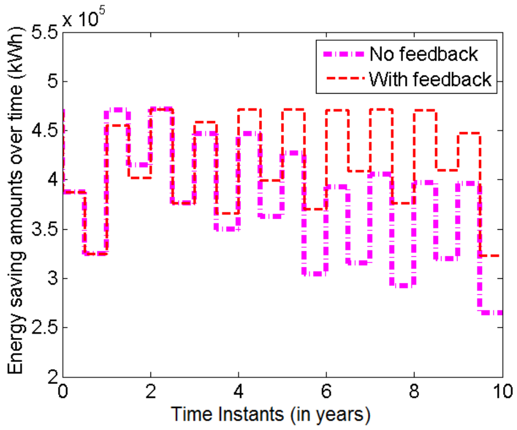

Figure 3.2. Energy performances of the maintenance plans with and without feedback in *Energy Prior* case.

The *Balance open-loop*, *Energy open-loop* and *Economy open-loop* are the cases where maintenance plans are obtained without considering uncertainties. The three cases are illustrated as the comparative performances. In contrary to the open-loop cases, *Balance with feedback*, *Energy with feedback* and *Economy with feedback* are the cases where the maintenance plan is optimised via the control system approach with state feedback. The disturbances in the with feedback cases and open-loop cases are the same for the sake of comparison. Generally, the performances in with feedback cases outperform the ones in open-loop cases, as Table 3.4 illustrates. This reveals that the robustness of the control system approach against uncertainty factors. The results can prove the control approach effectiveness when reducing the adverse impacts from the uncertainty factors during operation.

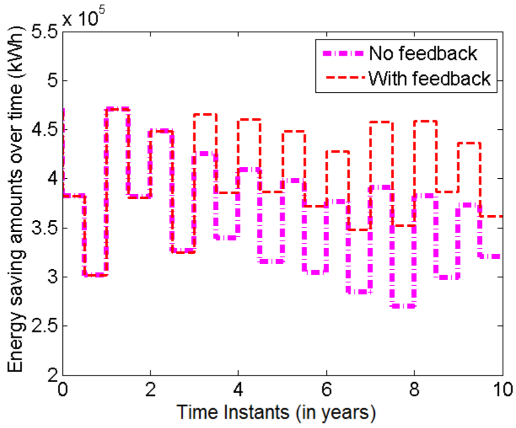

Figure 3.3. Energy performances of the maintenance plans with and without feedback in *Economy Prior* case.

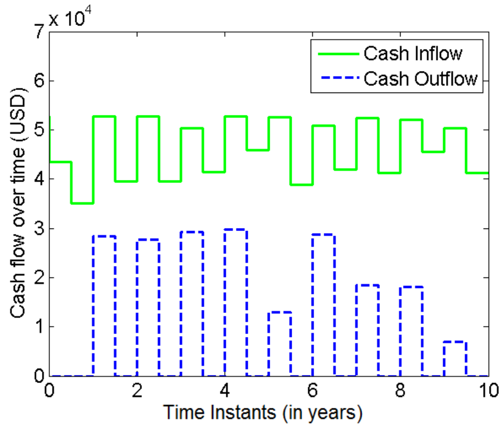

Figure 3.4. Cash flows of the maintenance plans with feedback in *Optimal Balance* case.

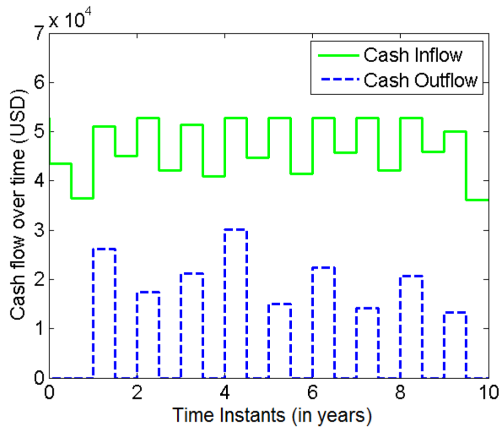

Figure 3.5. Cash flows of the maintenance plans with feedback in *Energy Prior* case.

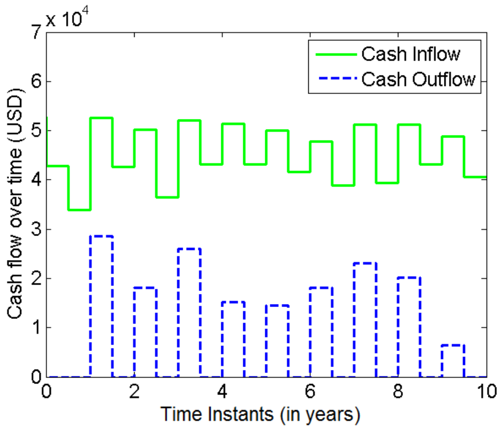

Figure 3.6. Cash flows of the maintenance plans with feedback in *Economy Prior* case.

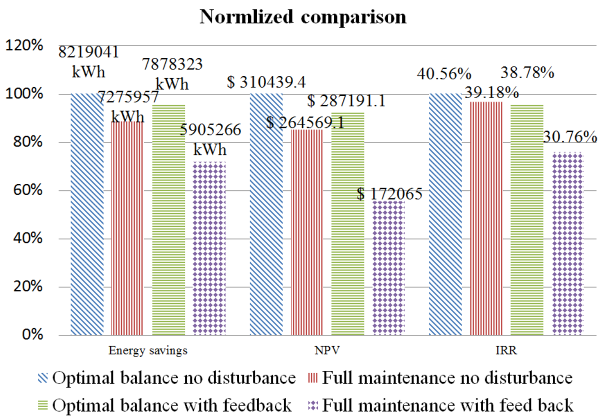

Figure 3.7. Performances comparison between the *Optimal Balance* and full maintenance under same budget condition.

The energy and economy performances of the *Balance with feedback*, *Balance with feedback* and *Economy with feedback* cases are illustrated in Figs. 3.1-3.6. The impacts of the uncertainty factors are included. There are two different types of illustrative system dynamics: the energy savings and cash flows over each sampling interval. In Figs 3.1-3.3, the performances in the with feedback cases are illustrated by the thin dashed lines. The thick dashdot lines represent the energy savings from the open-loop cases as the comparative trajectory. More energy savings are lost with uncertainties during operation in open-loop maintenance plans. The cash flows from the with feedback cases are selected in Figs. 3.4-3.6. The cash inflows are represented by the solid lines and the cash outflows are represented by the dashed line. The cash outflows reflect the maintenance intensities over the sampling interval. The performance measures of the cases under the tight budget limit are compared in Fig. 3.7. The *Optimal balance* without disturbance or with feedback control and the *Full maintenance* strategy without disturbance or with feedback control are selected for the comparison. The *Full maintenance* strategy is revised, where all failed items are restored until the budget limit is reached, thereafter the no maintenance strategy will be applied. The performance measures are normalised for the sake of clear illustration. From Fig. 3.7, the optimal maintenance plan outperforms the full maintenance strategy when budget limit is not sufficient. It further illustrates the effectiveness of the maintenance plan optimisation approach.

3.5 CONCLUSION

This chapter investigates the important role of maintenance in the building energy optimisation at the planning level. An aggregate population level optimisation model is proposed to address the BRCMP problem, with two different objectives: maximising the long-term aggregate energy savings over the sustainability period and maximising the internal rate of return of the project. A weighted sum approach is employed to formulate the objective function. Given the inherent dependence of the decision variable, i.e., the maintenance intensities, the optimisation problem is actually a dynamic optimisation. When taking into account the uncertainty factors, the dynamic optimisation is further developed into an optimal control problem, where a model predictive control based approach is employed to solve out the optimal control law.

The proposed optimal control model can be extended from various perspectives. The maintenance time schedule can be part of the optimisation; the interactions between the retrofitted items can be taken into account in the control system modelling; the preventive maintenance can also be incorporated. These topics will be discussed in the following chapters.

CHAPTER 4 MAINTENANCE PLANNING WITH INTERACTING ENERGY EFFECTS

4.1 INTRODUCTION

The existing studies have investigated the interacting energy efficiency effects among different equipment. For example, the *ASHRAE* [1] *2009 Fundamental Handbook* [146] introduces the complicated composition of the heating/cooling load for an air conditioning system in buildings, where the heat loss/gain from the heat transmission through the building envelope, the heat loss/gain through the ventilation, the heat gain from solar rays and the internal heat gain from the electrical appliances, e.g., lights and computers, are all involved in the computation of air conditioner heating/cooling loads. The energy consumptions of an air conditioning system are highly related to its heating/cooling loads. The heating/cooling loads can be significantly influenced by some appliances in the air conditioner working zone, e.g., the lights and computers. Sezgen [6] and Zmeureanu [147] evaluate such interactions between lighting and air conditioning systems in buildings. Ahn *et al.* [148] takes into account the lighting/HVAC interactions to design green buildings, where the convective heat from LED lighting is directed to reduce the air conditioner working loads. Consequently, the BRCMP optimisation model can be extended by incorporating such interactions to better reflect the practical situations.

Furthermore, the interacting reliability effects can also be taken into account in the population decay models. Breuker and Braun [149] investigates the common faults and their impacts for rooftop air conditioners, where several possible faults are resulted from improper air conditioner working load: if the working load is too high, the overloaded compressor motor can be damaged; if the working load is too low, liquid can flood back into the compressor, which increases the possibility of failures. In

[1] American Society of Heating, Refrigerating and Air-conditioning Engineers

practice, the design of building air conditioner systems takes into account the normal activities in its heating/cooling area. The selected capacity of the air conditioner system is often a little higher than the peak working load in its working space. However, the estimation of the peak working load can ignore the malfunctions of appliances. The population decay of both lighting and air conditioner groups can lead to abnormal working loads that can be either too low or too high compared to the air conditioning system rated capacities. Consequently, failures are more likely to happen among the air conditioners. The air conditioner reliability can deteriorate faster than usual depending on the status of the lighting and air conditioner groups. When taking into account such effects, the population dynamics must be formulated as a control system with coupled state equations.

When extending the BRCMP optimisation model by incorporating the interacting energy and reliability effects, the following assumptions are made to allow the population dynamics formulation:

1. There are only lights and air conditioners.

2. The retrofitted items are installed in a common space, i.e., all the lighting devices contribute to the working load of all the air conditioners.

3. The other heat sources are considered known a priori and independent of the lights and air conditioners.

The control system is then modelled based on the simplified population dynamics formulation. The state variables are a pair of coupled variables, i.e., the populations of the lighting group and the HVAC device group. The BRCMP problem is thereby extended to be an optimal control problem with a coupled system dynamics. A case study is used to test and verify the effectiveness of the proposed approach. A maintenance plan that is optimised without considering the interactions is employed as the comparative baseline.

4.2 PROBLEM FORMULATION

4.2.1 Variable definition

As aforementioned, the energy efficiency of the retrofitted lighting and air conditioners are the main concern. Assuming a project including two groups of homogeneous retrofitted items, i.e., the lighting group and air conditioner group. Let $t_k = kS, k = 0,1,2,...,T$ denote the sampling instants over the a finite decision horizon $[0,TS)$, namely the sustainability period, where S indicates the sampling interval. let $x_L(t_k)$ denote the population of lighting group and $x_{AC}(t_k)$ the population of air conditioner group over interval $[t_{k-1},t_k)$. The system state is represented by:

$$\mathbf{x}(t_k) = (x_L(t_k), x_{AC}(t_k))^T. \tag{4.1}$$

$\mathbf{x}(t_0) = (x_L^0, x_{AC}^0)^T$ indicates the initial state. The maintenance intensities at t_k for each group are represented by:

$$\mathbf{u}(t_k) = (u_L(t_k), u_{AC}(t_k))^T. \tag{4.2}$$

For convenience of further derivation, $\mathbf{x}$ and $\mathbf{u}$ are employed to represent the system states and maintenance intensities. $\mathbf{u}$ are the decision variables. Let $Q = \{m_1, m_2, ..., m_N\}$ denote a set of indices of the sampling instants, i.e., the maintenance instants. The elements of Q are selected from $k = 0,1,2,...,T$ as the maintenance instants are commensurate with sampling instants t_k. For t_k with $k \notin Q$, $u_L(t_k) = 0$ and $u_{AC}(t_k) = 0$. The maintenance instants are pre-decided and elements of Q are therefore constants.

4.2.2 Interacting energy effects modelling

Let $a_L(t_k)$ denote the average energy consumption per lighting unit over interval $[t_{k-1},t_k)$. The overall energy consumption of the lighting group is then indicated by $E_L(t_k) = a_L(t_k)x_L(t_k)$. The average power per lighting unit is generally consider constant during operation. According to [146], the instantaneous rate of sensible heat gain from the electric lighting can be formulated as the following:

$$q_{el} = 3.41WF_{ul}F_{sa}, \tag{4.3}$$

where q_{el} denotes the instantaneous heat gain (Btu/h), W the rated light wattage, F_{ul} the lighting use factor, F_{sa} the lighting special allowance factor and 3.41 the conversion factor. The lighting use factor indicates the ratio of lighting wattage in use to total installed wattage. The special allowance factor indicates the ratio of the lighting fixtures' power consumption, including lamps and ballast, to the nominal power consumption of the lamps [146]. Given (4.3), the average lighting heat gain $Q_L(t_k)$ that contributes to the air conditioner working load can be estimated by the following,

$$Q_L(t_k) = f_r E_L(t_k), \tag{4.4}$$

where f_r denotes a space fraction, i.e., the fraction of lighting heat gain goes into the room. [146] and [150] gives a series of reference values of the space fraction.

Taking advantage of (4.4), the average air conditioner working load during interval $[t_{k-1}, t_k)$ can also be estimated. The air conditioner working load includes heating and cooling loads. The energy consumption of an air conditioner is obtained from the heating/cooling load and the heating/cooling system energy efficiency. Let $Q_{HD}(t_k)$ denote the total heating load in the working zone during $[t_{k-1}, t_k)$ and $Q_{CD}(t_k)$ the total cooling load. $Q_{HD}(t_k)$ and $Q_{CD}(t_k)$ can be estimated by

$$\begin{aligned} Q_{HD}(t_k) &= Q'_{HD}(t_k) - Q_L(t_k), \\ Q_{CD}(t_k) &= Q'_{CD}(t_k) + Q_L(t_k), \end{aligned} \tag{4.5}$$

where $Q'_{HD}(t_k)$ indicates the overall heat loss from other resources and $Q'_{CD}(t_k)$ denotes the overall heat gain from other resources. The energy consumption of the lighting group is a part of the internal heat gain [146]. As aforementioned, $Q'_{HD}(t_k)$ and $Q'_{CD}(t_k)$ are considered known a priori and independent of $x_L(t_k)$ and $x_{AC}(t_k)$. In order to emphasise the interacting energy efficiency effects, the heating/cooling load is rewritten as $Q_{HD}(t_k, x_L(t_k))$ and $Q_{CD}(t_k, x_L(t_k))$. An assumption in our model is that the heating/cooling load is evenly distributed to the working air conditioners in the working zone. Thereafter, the energy consumption of an working air conditioner during $[t_{k-1}, t_k)$ is estimated by:

$$\begin{aligned} a_{AC}(t_k) =& \rho_h(t_k)\varepsilon_h(t_k)\frac{Q_{HD}(t_k, x_L(t_k))}{x_{AC}(t_k)} \\ &+ \rho_c(t_k)\varepsilon_c(t_k)\frac{Q_{CD}(t_k, x_L(t_k))}{x_{AC}(t_k)}, \end{aligned} \tag{4.6}$$

where $\rho_h(t_k)$ and $\rho_c(t_k)$ are constrained by

$$\begin{cases} \rho_h(t_k) + \rho_c(t_k) = 1, \\ \rho_h(t_k)\rho_c(t_k) = 0. \end{cases} \tag{4.7}$$

$\rho_h(t_k) = 1$ indicates that the air conditioners are working at heating mode and $\rho_c(t_k) = 1$ indicates the cooling mode. $\varepsilon_h(t_k)$ denotes the average heating efficiency and $\varepsilon_c(t_k)$ the average cooling efficiency of the working air conditioners during $[t_{k-1}, t_k)$. The estimation of $\varepsilon_h(t_k)$ and $\varepsilon_c(t_k)$ is not straightforward. The heating seasonal performance factor (HSPF) and seasonal energy efficiency ratio (SEER), defined in AHRI Standard 210/240[2], provide methodologies to measure the heating/cooling efficiency of an air conditioner. Generally, $\varepsilon_h(t_k)$ and $\varepsilon_h(t_k)$ are not constant and influenced by many factors including the difference between the actual heating/cooling load comparing with the rated capacity. The interacting energy efficiency effects thereby exist in the heating/cooling efficiency as well. $\varepsilon_h(t_k)$ and $\varepsilon_h(t_k)$ are rewritten into $\varepsilon_h(t_k, x_L(t_k), x_AC(t_k))$ and $\varepsilon_h(t_k, x_L(t_k), x_AC(t_k))$ accordingly. The overall energy consumption of the air conditioner group is then estimated by $E_{AC}(t_k) = a_{AC}(t_k)x_{AC}(t_k)$.

Let $S_L(t_k)$ and $S_{AC}(t_k)$ denote the energy savings from lighting and air conditioner groups respectively. Given the pre-implementation light wattage $\bar{a}_L(t_k)$ and pre-implementation energy consumption from the air conditioner group $\bar{E}_{AC}(t_k)$. Assuming that $a_L(t_k)$, $a_{AC}(t_k)$, $\bar{a}_L(t_k)$ and $\bar{E}_{AC}(t_k)$ are computed under the same weather, building environment, occupancy rate and operating schedule, the aggregated energy savings are calculated according to [119]:

$$\begin{aligned} S_L(t_k) &= x_L(t_k)(\bar{a}_L(t_k) - a_L(t_k)), \\ S_{AC}(t_k) &= \bar{E}_{AC}(t_k) - a_{AC}(t_k)x_{AC}(t_k), \end{aligned} \tag{4.8}$$

and corresponding cost saving:

$$\begin{aligned} C_L(t_k) &= p(t_k)S_L(t_k), \\ C_{AC}(t_k) &= p(t_k)S_{AC}(t_k), \end{aligned} \tag{4.9}$$

where $p(t_k)$ denotes the electricity price during $[t_{k-1}, t_k)$. Given the interactions between the two item groups in (4.5)-(4.9), the population dynamics are coupled as aforementioned and formulated in the following subsection.

4.2.3 Population dynamics modelling with interactions

Taking advantage of the modelling in the previous chapter, the population dynamics can be represented by:

$$\begin{bmatrix} x_L(t_{k+1}) \\ x_{AC}(t_{k+1}) \end{bmatrix} = \begin{bmatrix} G_L(x_L(t_k)) \\ G_{AC}(x_L(t_k), x_{AC}(t_k)) \end{bmatrix} + \begin{bmatrix} x_L(t_k) \\ x_{AC}(t_k) \end{bmatrix} + \begin{bmatrix} u_L(t_k) \\ u_{AC}(t_k) \end{bmatrix}, \tag{4.10}$$

where $x_L(t_0) = x_L^0$, $x_{AC}(t_0) = x_{AC}^0$ indicate the initial state. $G_L(x_L(t_k))$ indicates the population decay of lighting group and $G_{AC}(x_L(t_k), x_{AC}(t_k))$ the population decay of air conditioner group. $x_L(t_k)$ in $G_{AC}(x_L(t_k), x_{AC}(t_k))$ is to emphasise the coupling of the system states.

[2] Air Conditioning, Heating, and Refrigeration Institute in its 2008 standard AHRI 210/240, Performance Rating of Unitary Air-Conditioning and Air-Source Heat Pump Equipment.

Taking advantage of the population decay models, e.g.,(2.12) and (2.13), the interacting effects of the reliability between the lighting and air conditioner groups is estimated. At the current stage, the population decay model developed by Carstens *et al.* [109] is employed to formulate the lighting group decay. For the air conditioner group, Kwak *et al.* [151] claimed that the reliability of the main units of HVAC system in the period of life can be expressed by Weibull distribution, which is thereby employed to characterise the population decay of air conditioner group due to random failures. The population decay formulations are given as the following:

$$G_L(x_L(t_k)) = \frac{\mu_L \nu_L x_L(t_k)^2}{x_L^0}\triangle t - \mu_L x_L(t_k)\triangle t, \tag{4.11}$$

$$G_{AC}(x_L(t_k), x_{AC}(t_k)) = -\frac{\gamma t_k^{\gamma-1}\triangle t}{\eta^\gamma} x_{AC}(t_k). \tag{4.12}$$

where $\triangle t = t_{k+1} - t_k$. μ_L and μ_L are decay parameters, related to the average lighting life span from the group and can be identified according to section 2.2.3. $G_{AC}(x_L(t_k), x_{AC}(t_k))$ is developed taking advantage of the Weibull distribution [140]. γ is the shape parameter and η is the scale parameter of Weibull distribution. η is usually estimated by the mean time between failure (MTBF) that is obtained based on reliability statistical information. According to the aforementioned studies on air conditioner fault detection, failures are more likely to take place when the compressor is overloaded due to heavy loads or the cooling load is too small [149]. Therefore, η can vary during operation and is rewritten into $\eta(t_k, x_L(t_k), x_{AC}(t_k))$ to emphasise the interactions. The air conditioner reliability loss and damage quantification is not straightforward and therefore lacks relevant studies. At the current stage, a piecewise exponential estimator of the scale parameter $\eta(t_k, x_L(t_k), x_{AC}(t_k))$ is applied. Following the qualitative result in [149], an assumption is made that η of an air conditioner decreases when the air conditioner working load $q_{AC}(t_k, x_L(t_k), x_{AC}(t_k))$ becomes too large or too small, comparing to its rated heating/cooling capacity.

Let $p_h(t_k)$ denote the percentage heating load of an air conditioner during $[t_{k-1}, t_k)$ against the rated heating capacity $\bar{q}_h$. $p_c(t_k)$ denote the percentage cooling load based on its rated cooling capacity $\bar{q}_c$. From equations (4.5) and (4.6), $p_h(t_k)$ and $p_c(t_k)$ can be represented by:

$$\begin{cases} p_h(t_k) = \dfrac{Q_{HD}(t_k)}{\bar{q}_h x_{AC}(t_k)} * 100\%, \\ \quad = \dfrac{Q'_{HD}(t_k) - q_L(t_k)x_L(t_k)}{\bar{q}_h x_{AC}(t_k)} * 100\%, \ if \ \rho_h = 1, \\ p_c(t_k) = \dfrac{Q_{CD}(t_k)}{\bar{q}_c x_{AC}(t_k)} * 100\%,, \\ \quad = \dfrac{Q'_{CD}(t_k) + q_L(t_k)x_L(t_k)}{\bar{q}_c x_{AC}(t_k)} * 100\%, \ if \ \rho_c = 1. \end{cases} \tag{4.13}$$

Let η_0 denote the scale parameter estimated by MTBF in normal working conditions. If $p_h(t_k)$ and $p_c(t_k)$ deviate from 100%, $\eta(t_k, x_L(t_k), x_{AC}(t_k))$ is estimated according to the following equation:

$$\eta(t_k, x_L(t_k), x_{AC}(t_k)) = \begin{cases} \eta_0 \dfrac{1}{a_{h,l} + e^{-k_{h,l} p_h(t_k) + b_{h,l}}}, & p_h(t_k) < Th_{h,l}\%, \\ \eta_0, & Th_{h,l}\% \leq p_h(t_k) \leq Th_{h,r}\%, \\ \eta_0 \dfrac{1}{a_{h,r} + e^{k_{h,r} p_h(t_k) - b_{h,r}}}, & p_h(t_k) > Th_{h,r}\%, \end{cases} \tag{4.14}$$

$$\eta(t_k, x_L(t_k), x_{AC}(t_k)) = \begin{cases} \eta_0 \dfrac{1}{a_{c,l} + e^{-k_{c,l} p_c(t_k) + b_{c,l}}}, & p_c(t_k) < Th_{c,l}\%, \\ \eta_0, & Th_{c,l}\% \leq p_c(t_k) \leq Th_{c,r}\%, \\ \eta_0 \dfrac{1}{a_{c,r} + e^{k_{c,r} p_c(t_k) - b_{c,r}}}, & p_c(t_k) > Th_{c,r}\%, \end{cases} \tag{4.15}$$

where $a_{h,l}$, $b_{h,l}$, $k_{h,l}$, $a_{h,r}$, $b_{h,r}$, $k_{h,r}$, $a_{c,l}$, $b_{c,l}$, $k_{c,l}$, $a_{c,r}$, $b_{c,r}$ and $k_{c,r}$ are positive constants, i.e., the parameters of the piecewise exponential estimator. $Th_{h,l}$ and $Th_{h,r}$ denote the threshold points, i.e., a pair of percentage heating loads. If the actual percentage heating load $p_h(t_k) < Th_{h,l}\%$ or $p_h(t_k) > Th_{h,r}\%$, the scale parameter η starts decreasing. Similarly, $Th_{c,l}$ and $Th_{c,r}$ denote a threshold pair of such percentage cooling loads. Equation (4.14) applies when $\rho_h = 1$ and (4.15) applies when $\rho_c = 1$.

(4.10)-(4.15) constitute a control system formulation of coupled population dynamics.

4.2.4 Performance indicators formulation

The performance indicators for the optimisation problem is formulated as the following. Given the baseline energy consumption, the air conditioner working loads and maintenance costs per light and per air conditioner are known a priorigiven predecided from the pre-implementation audits and evaluation. Let $mc_L(t_k)$ denote the maintenance cost to restore a light and $mc_{AC}(t_k)$ the maintenance cost of an air conditioner. The aggregated energy savings during $[t_{k-1}, t_k)$ and the overall energy savings over the sustainability period $[0, TS)$ are:

$$\begin{cases} ES(t_k) = S_L(t_k) + S_{AC}(t_k), \\ ES|_{all} = \sum_{k=1}^{T} ES(t_k), \end{cases} \tag{4.16}$$

and the corresponding cost savings:

$$\begin{cases} C(t_k) = C_L(t_k) + C_{AC}(t_k), \\ C|_{all} = \sum_{k=1}^{T} C(t_k). \end{cases} \tag{4.17}$$

The maintenance cost at each time instant is obtained:

$$h(t_k) = mc_L(t_k)u_L(t_k) + mc_{AC}(t_k)u_{AC}(t_k), \tag{4.18}$$

and the overall investment of the retrofitting project is:

$$h|_{all} = h_0 + \sum_{k=1}^{T} h(t_k), \tag{4.19}$$

where h_0 denotes the initial expenditure of implementing the retrofitting project. The profit of the project is then obtained by $P = C|_{all} - h|_{all}$. The Net Present Value (NPV) of the project over $[0, TS)$ is formulated as the following,

$$NPV = \sum_{k=1}^{T} \frac{C(t_k) - h(t_k)}{(1+d)^{\phi(t_k)-1}} - h_0, \tag{4.20}$$

where $d \in (0,1)$ denotes the discount rate for NPV calculation. $\phi(t_k) = 1,2,3...$ indicates that the sampling instant t_k lies within a specific year after the implementation of the retrofitting project. Taking advantage of the NPV formulation, the IRR, denoted by $d_R|_T$ in the present model, can be obtained by solving the following equation:

$$\sum_{k=1}^{T} \frac{B(t_k) - h(t_k)}{(1+d_R|_T)^{\phi(t_k)-1}} - h_0 = 0, \tag{4.21}$$

which means to find the discount rate that makes NPV=0 over $[0, TS)$.

4.2.5 Optimal control problem formulation

In a control system formulation, the optimal control problem can be formulated.

Optimisation Problem $\mathcal{MPO}$: For a dynamic system described by (4.10)-(4.15) with a pair of coupled state variables $\mathbf{x}(t_k) = (x_L(t_k), x_{AC}(t_k))^T$ with $\mathbf{x}_0 = \mathbf{x}(t_0) = (x_L^0, x_{AC}^0)^T$, given a predetermined maintenance time schedule $Q = \{m_1, ..., m_N\}$, find the optimal maintenance plan $\mathbf{u} = \{u_L(t_{m_1}), u_{AC}(t_{m_1}), ..., u_L(t_{m_N}), u_{AC}(t_{m_N})\}$, which minimises the following performance index:

$$J(\mathbf{x}_0, Q, \mathbf{u}(\cdot)) = -\lambda_1 \frac{ES|_{all}}{\alpha} - \lambda_2 d_R|_T, \tag{4.22}$$

subject to (4.10)-(4.15) and

$$\begin{cases} ES|_{all} \geq \alpha, \\ \sum_{k=1}^{T} h(t_k) \leq \beta, \\ NPV|_0^{T_p} \geq 0, \\ x_L(t_k) \leq x_L^0,\ x_{AC}(t_k) \leq x_{AC}^0, \\ x_L(t_k) \geq x_L^0/3,\ x_{AC}(t_k) \geq x_{AC}^0/2. \end{cases} \tag{4.23}$$

where λ_1 and λ_2 denote the weighting factors. α denotes the targeted energy saving amount, and β the maintenance budget limit over $[0,TS)$. $NPV|_0^{T_p}$ denotes the NPV computed over $[0,T_pS)$ where T_p is the maximum acceptable payback period. The last two inequalities in (4.23) indicate the upper and lower bound of the state variables $x_L(t_k), x_{Ac}(t_k)$, where the lower bound is resulted from human comfort requirements. Given N the number of elements in Q, $\mathbf{u}(\cdot) \in \mathcal{R}^{2\times N}$, i.e., the minimisation problem (4.22)-(4.23) is a finite dimensional problem. The previously introduced MPC approach and the DE numerical solver can employed to solve the optimal control problem $\mathcal{MPO}$. The technical details are omitted in this chapter. They can be found in the previous chapters and the appendix.

4.3 SIMULATION AND VERIFICATION

4.3.1 Case study

A simulated case study is employed to verify the effectiveness of our approach. The simulation is established by taking advantage of the audit data from an actual retrofitting plan. The retrofitted building locates in South Africa. There are 480 retrofitted compact fluorescent lamp (CFL) lights and 16 retrofitted air conditioners in the building, i.e., $x_L^0 = 480$ and $x_{AC}^0 = 16$. The maintenance plan is scheduled for 10 years. As the maintenance plan optimisation involves long-term management level item group performances, it is infeasible to wait for actual operation during such a long time, therefore the simulation is selected. The operation starts from January, and the sampling interval is one month. Given the weather in Pretoria, the heating season includes May, June, July and August, the cooling season includes the rest months. The heating targeted temperature is 24^oC, and cooling targeted temperature is 26^oC.

Table 4.1. The estimated heating/cooling loads from other resources, the pre-retrofit light and air conditioner energy consumptions and the annual temperature profile

Month	Jan	Feb	Mar	Apr
Q'_{HD} (kWh)	n/a	n/a	n/a	n/a
Q'_{CD} (kWh)	4651.77	4560.96	4042.32	3971.5
$\bar{a}_L$ (kWh)	17.28	17.28	17.28	17.28
$\bar{E}_{AC}$ (kWh)	6340.34	6268.04	6309.68	6150.91
High ^oC	32	31	30	29
Low ^oC	17	17	16	12
Month	May	Jun	Jul	Aug
Q'_{HD} (kWh)	7856.72	9224.1	9473.4	7928.16
Q'_{CD} (kWh)	n/a	n/a	n/a	n/a
$\bar{a}_L$ (kWh)	17.28	17.28	17.28	17.28
$\bar{E}_{AC}$ (kWh)	0	0	0	0
High ^oC	20	17	15	16
Low ^oC	7	3	3	7
Month	Sep	Oct	Nov	Dec
Q'_{HD} (kWh)	n/a	n/a	n/a	n/a
Q'_{CD} (kWh)	4228.48	4342.72	4492.7	4542.7
$\bar{a}_L$ (kWh)	17.28	17.28	17.28	17.28
$\bar{E}_{AC}$ (kWh)	6111.19	6339.49	6421.05	6600.86
High ^oC	29	30	31	32
Low ^oC	11	14	15	16

Table 4.2. Retrofitted items specifications

	26W CFL lighting	8500 Btu/h air conditioner
Max possible quantities	480	16
Rated power heating (W)	26	926.8
Rated power cooling (W)	26	740
Rated heating capacity (Btu/h)	n/a	8500
Rated cooling capacity (Btu/h)	n/a	8500
Average monthly consumption (kWh)	6.24	n/a
Electricity price ($/kWh)	0.1661	0.1437
Installation price ($)	14.19	460
Maintenance cost ($)	14.19	180
MTBF (months)	11.9	18

For the convenience of the reader, the building specifications are omitted and some necessary information for the simulation is given in Table 4.1. The high ${}^oC$ indicates the highest temperature in a day and low ${}^oC$ indicates the lowest temperature in a day. As aforementioned, Q'_{HD} denote the total heat loss from the other resources other than lighting, Q'_{CD} denote the total heat gain from the other resources. The average estimations for each month are made according to the history occupancy profiles. $\bar{a}_L$ and $\bar{E}_{AC}$ denote the pre-retrofit energy consumption from the lighting and air conditioners, where $\bar{a}_L$ is the monthly consumption of one light and $\bar{E}_{AC}$ indicates the overall consumption of the whole pre-retrofit air conditioner system. The annual temperature profile is also illustrated in Table 4.1. The retrofitted item specifications are given in Table 4.2. The max possible quantities indicate the number of items included in the retrofitting, i.e., x_L^0 and x_{AC}^0. The average monthly consumption of one light is considered constant in this case, according to the history occupancy profile. The air conditioner consumptions are not illustrated in Table 4.2 but computed according to the energy modelling (4.5)-(4.9) and system dynamics (4.10)-(4.15). The installation prices indicate the respective cost of initially applying a retrofit. According to the install price and max possible quantities, h_0 is \$14,171.2. The maintenance costs indicate the respective cost of applying a maintenance action to a retrofitted item. The MTBF are given in months. Taking advantage of the MTBF information, the following population decay models are employed:

$$G_L(x_L(t_k)) = 0.0692 x_L(t_k)^2/68 - 0.1094 x_L(t_k) + x_L(t_k), \tag{4.24}$$

$$G_{AC}(x_L(t_k), x_{AC}(t_k)) = \left(1 - \frac{1}{\eta(t_k, x_L(t_k), x_{AC}(t_k))}\right) x_{AC}(t_k), \tag{4.25}$$

where the life expectancy of a lighting is 11.9 months, implying that $\mu_L = 0.0692$ and $\nu_L = 0.1094$ in (4.11). In equation (4.25), the shape parameter $\gamma = 1$, the MTBF of an air conditioner unit is 18 months, implying that $\eta_0 = 25.97$ in (4.12). During the heating season, η can be estimated by:

$$\eta(t_k, x_L(t_k), x_{AC}(t_k)) = \begin{cases} \dfrac{25.97}{0.835 + e^{-7.105 p_c(t_k) + 1.397}}, & p_h(t_k) < 45\%, \\ 25.97, \quad 45\% \le p_h(t_k) \le 100\%, \\ \dfrac{25.97}{0.719 + e^{1.195 p_c(t_k) + 2.465}}, & p_h(t_k) > 100\%, \end{cases} \tag{4.26}$$

and during cooling season:

$$\eta(t_k, x_L(t_k), x_{AC}(t_k)) = \begin{cases} \dfrac{25.97}{0.835 + e^{-7.105 p_c(t_k) + 1.397}}, & p_c(t_k) < 45\%, \\ 25.97, \quad 45\% \le p_c(t_k) \le 100\%, \\ \dfrac{25.97}{0.683 + e^{1.239 p_c(t_k) + 2.389}}, & p_c(t_k) > 100\%. \end{cases} \tag{4.27}$$

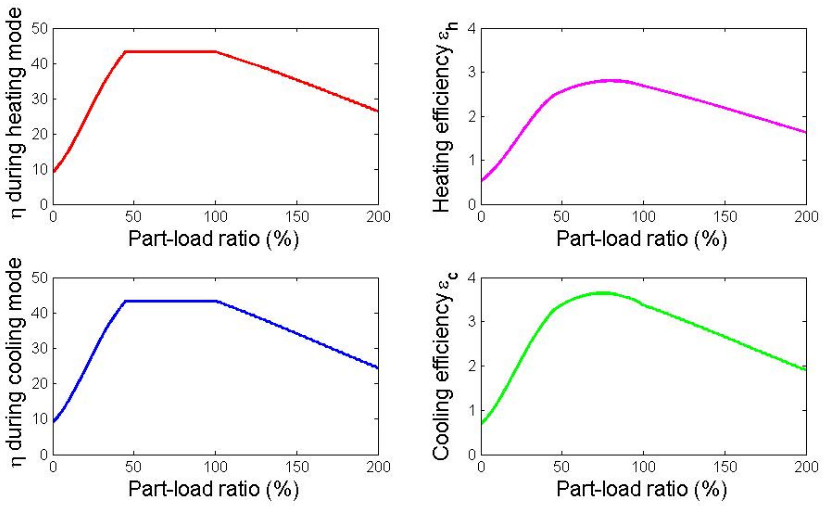

Figure 4.1. The shapes of η, ε_h and ε_c against the percentage part-load ratio.

The heating/cooling efficiency ε is estimated by:

$$\varepsilon_h(t_k,x_L(t_k),x_{AC}(t_k)) = \begin{cases} \dfrac{2.8}{0.9485+1.1364e^{-7.105p_c(t_k)+1.397}},\ p_h(t_k) < 45\%, \\ -2.7768p_h(t_k)^2+5.0672p_h(t_k)+1.0312, 45\% \leq p_h(t_k) \leq 100\%, \\ \dfrac{2.8}{0.7492+1.0417e^{1.1949p_c(t_k)+2.4649}},\ p_h(t_k) > 100\%, \end{cases} \tag{4.28}$$

$$\varepsilon_c(t_k,x_L(t_k),x_{AC}(t_k)) = \begin{cases} \dfrac{3.62}{0.9274+1.1e^{-7.105p_c(t_k)+1.397}},\ p_c(t_k) < 45\%, \\ -4.3386p_c(t_k)^2+6.4881p_c(t_k)+1.2167, 45\% \leq p_c(t_k) \leq 100\%, \\ \dfrac{3.62}{0.7348+1.0753e^{1.239p_c(t_k)+2.389}},\ p_c(t_k) > 100\%. \end{cases} \tag{4.29}$$

Fig. 4.1 depicts the shapes of η, ε_h and ε_c, where the part load ratio is a percentage of the actual working load against the rated capacity.

The baseline energy consumption is 1,500,743.6 kWh and the targeted energy saving is 671,380.1 kWh over 10 years. The discount rate for NPV calculation is 11% per year, and the desired payback period is 4 years. The maintenance time schedule is $Q = \{6, 12, 18, 24, ..., 114\}$. Several maintenance budget limits are applied: \$31,500, \$37,500 and \$42,500, from very tight to sufficient. The weights in objective function (4.22) are set to be $\lambda_1 = 0.5$ and $\lambda_2 = 0.5$.

There are two tests in the simulation. The first test excludes the uncertainties; the $\mathcal{MPO}$ problem is solved by the DE based numerical solver as an open loop dynamic programming problem over the whole sustainability period. To manifest the impact of the interacting effects, a maintenance plan is developed without considering the interactions, as we introduced in Chapter 3. The comparative maintenance plan is applied to the control system (4.10)-(4.15). The obtained performances are illustrated in Table 4.3 for comparison. The second test includes the uncertainties; in this test, the maintenance plan is developed by the MPC controller. The uncertainties are represented by a set of random variables that follow the even distribution in the range up to $\pm 10\%$ on the state variables $\mathbf{x}(t_k)$. The comparative maintenance plan is developed by solving the open loop problem. Thereafter, the two maintenance plans with or without taking into account the uncertainties are compared in Table 4.4 to manifest the effectiveness of the control system approach when addressing the $\mathcal{MPO}$ problem with uncertainties.

4.3.2 Illustrative results

The results in Table 4.3 and 4.4 are an average of 20-run results, where the 'Percentage savings' column denotes how much extra savings are obtained comparing with the targeted value. From Table 4.3, most performances are decreased by 2-3% if the maintenance plan is developed without taking into account the interacting effects. Up to 8.9% of the energy saving and up to 9.6% of the IRR can be improved relatively against the without interaction strategies (given that the no interaction strategy performances are 100%). We believe that this illustrates the impact of interacting effects in the case study: the interacting effects delivers an around 2% uncertainty to the performances with the given energy efficiency and reliability models. In Table 4.4, the open loop solution performances are decreased by 5-10% when comparing with closed-loop solutions. Thereby the effectiveness of the MPC controller can be illustrated. Such deterioration also indicate that the uncertainties deliver a significant impact to the final performances without the compensation of the feedback control in practice.

Fig. 4.2 illustrates the population dynamics in a few different cases. The air conditioner group population decay and lighting group population decay in the first row represent the population dynamics without any maintenance. At the end of the population dynamics without maintenance, all equipment are lost, suggesting a serious damage to the user comfort. The solid line indicates the estimation where interacting effects are excluded and the dashed dot line indicates the estimation taking into account the

Table 4.3. Comparison of solutions with or without taking into account the interacting effects with different budget limits

Cases	Budget limit ($)	Energy savings (kWh)	Percentage savings	IRR	Payback period (years)	NPV ($)	Maintenance cost ($)	Comfort violation
With interactions	31500	682461.3	1.65%	69.89%	1.52	37041.77	31414.17	Yes
Without interactions	31500	660406.1	-1.64%	67.84%	1.55	34737.33	31460.43	Yes
With interactions	37500	725261.8	8.02%	68.77%	1.52	35917.37	37379.22	No
Without interactions	37500	720228.5	7.27%	66.85%	1.54	36239.4	37473.3	No
With interactions	42500	822015.9	22.43%	70.76%	1.51	41791.32	42422.7	No
Without interactions	42500	818781.6	21.95%	70.59%	1.53	41584	42427.95	No

Table 4.4. Comparison of solutions with or without taking into account the uncertainties with different budget limits

Cases	Budget limit ($)	Energy savings (kWh)	Percentage savings	IRR	Payback period (years)	NPV ($)	Maintenance cost ($)	Comfort violation
Closed-loop solution	31500	669008.9	-0.35%	68.18%	1.53	36462.9	31526.3	Yes
Open loop solution	31500	607177.6	-9.56.%	62.34%	1.56	32020.5	31560.27	Yes
Closed-loop solution	37500	709476.3	5.67%	66.29%	1.54	35258.5	37487.1	No
Open loop solution	37500	666778.8	-0.685%	63.15%	1.54	33389.8	37479.3	Yes
Closed-loop solution	42500	795327.1	18.46%	67.95%	1.54	40791.4	42499.7	No
Open loop solution	42500	707188.9	5.33%	64.2%	1.53	36062.4	42417.6	No

interactions. The interacting effects deliver a significant impact to the air conditioner group population decay in our model. The cases in the second row depict the performances under maintenance effects. The air conditioner and lighting population dynamics respectively illustrate the population dynamics trajectories of the closed-loop solutions with $37500 budget limit.

4.4 CONCLUSION

In this chapter, the BRCMP problem from Chapter 3 is extended by taking into account the interactions of energy and reliability performances among items. The interactions between lighting and air conditioner systems are our major concern. From existing studies, the decrease in number of working lights and working air conditioners significantly change the cooling/heating load in the retrofitting plant, resulting in the changes of energy savings and reliability of the air conditioners. Such interactions

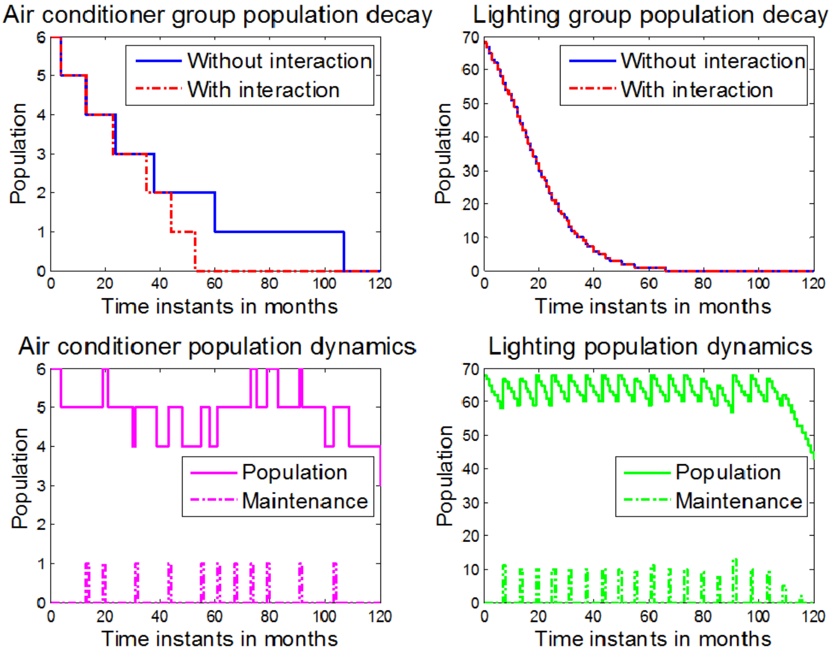

Figure 4.2. Population dynamics in a few different cases

are modelled as the coupled energy consumptions and reliability function scale parameters. A group of homogeneous lights and a group of homogeneous air conditioners, where items from the same group reveal similar energy and reliability performances, are selected to be our control object. The population dynamics of the two item groups is then formulated as a state-space model with coupled state equations. Thereafter, the maintenance plan optimisation problem is cast into an optimal control problem that aims at maximising the overall energy savings and internal rate of return of the retrofitting project during the sustainability period. According to the simulation results, up to 8.9% of the energy saving and up to 9.6% of the IRR can be improved against the without interaction strategies.

CHAPTER 5 MULTI-STATE BASED MAINTENANCE PLAN OPTIMISATION

5.1 INTRODUCTION

In the previous chapters, the control system modelling focuses on the corrective maintenance (CM) planning, the equipment deterioration effects are thereby omitted. In practice, equipment can deteriorate to a worse working state before malfunctions, e.g., air conditioners and heat pumps can consume more energy upon usage. Such a relationship has been revealed in relevant studies [152, 153]. To address such deterioration, the preventive maintenance (PM) must be incorporated into the maintenance plan optimisation (MPO) model. The multi-state system (MSS)approach is thereby investigated.

In reliability engineering, the multiple performance levels of a system can be characterised by the MSS approach [124]. The MSS is usually defined to be a system with multiple working state and failure states that range from perfectly functioning to complete failure. This is resulted from the deterioration and failure of some components in the system [125]. In the scope of the MSS model, CM restores the system from a failure state to working state, and PM restores the system to a better working state before the malfunction. The single deteriorating system with multiple working states has been the focus of many existing studies [126]. The system state-transition is taken into account to be governed by a Markov process, where the system states are defined to be a set of probabilities corresponding to the working states. As aforementioned, in our optimisation model, the major concern is the totality of the retrofitted items. The various categories of retrofitted items that are corresponding to different performance levels result in complicated aggregate performance dynamics. Therefore, the state of the totality of retrofitted items can become even more complicated than the one in a single deteriorating system. The grouping method is introduced to address this complexity. The homogeneous items from one group are further divided into several subsets subject to the item working state. Specifically, the term 'population' is hereby employed to represent the count of items within a homogeneous group under a specific working state. The populations of the subsets are commensurate with the probabilities of an individual item manifesting different working states. Population dynamics is thereby more complicated: it represents the transition of the items from one working state to another, resulting in the changes of the subset populations. Such population changes are commensurate with the individual item state-transition probabilities.

In this way, the homogeneous item group state can be described by an alternative MSS model. A state-space model is formulated based on the alternative MSS model. For simplicity, assuming the CM actions restore a number of items from the malfunctioning state to the best working state, and the PM actions the worse working state to the best state. The state variables in the MSS state-space model are the populations of the item subsets subject to different working states. The control inputs are the PM and CM maintenance intensities. The maintenance time schedule is known a priori, which is a fixed, pre-decided one. We do not take into account the installation of additional equipment apart from the retrofitted items, consequently, the system states are physically bounded. The uncertainty factors are also taken into account as the disturbances on the system states.

Thereafter, the population dynamics indicating the performance deterioration is modelled to be a control system, and the corresponding maintenance planning problem is cast into an optimal control problem. A weighted sum formulation is employed for the optimal control problem. There are two objectives: maximising the aggregate energy savings and maximising the internal rate of return (IRR) over the sustainability period. The targeted energy savings and the budget limit are involved in the optimal control problem as the constraints over the whole decision horizon. The model predictive control (MPC) approach that takes into account the history states is employed to satisfy the long term constraints. The state variables and control inputs are both integers as they represent the counts of retrofitted items. The differential evolution (DE) algorithm with the binary neighbourhood field optimisation (BNFO) method is employed as the numerical solver for the MPC approach. A simplification of a practical project is adopted as our case study.

5.2 CONTROL SYSTEM MODELLING

5.2.1 Control system framework for MSS based MPO

Let $t_k = kS, k = 0, 1, 2, ..., T$ denote the sampling instants over the sustainability period $[0, TS)$, where $t_0 = 0$ and S indicates the sampling interval. Given an item group l with N_l homogeneous items and M_l different working states subject to performance levels. Let $G_l(t_k)$ denote the performance level of an item at instant t_k. $G_l(t_k)$ takes value from the set

$$\mathbf{g}_l = \{g_{l,1}, g_{l,2}, ..., g_{l,M_l}\}. \tag{5.1}$$

The working state i is subject to performance level $g_{l,i}$. $\mathbf{g}_l$ is given in ascending order. g_{l,M_l} denotes the best working state, i.e., the state where an item can contribute maximum energy saving. Accordingly, $g_{l,1}$ denotes worst state where an item contributes the minimum saving. Thereafter, the homogeneous group l can be divided into M_l subsets subject to the working states. The subset i with $i = 1, 2, ..., M_l$ consists of all items from group l and under working state i, i.e., $G_l(t_k) = g_{l,i}$. Let $\mathbf{x}_l(t_k)$ denote the populations of all subsets in group l at t_k:

$$\mathbf{x}_l(t_k) = (x_{l,1}(t_k), x_{l,2}(t_k), ..., x_{l,M_l}(t_k))^T, \tag{5.2}$$

where $x_{l,i}(t_k)$ denotes the population of subset i at instant t_k, $\sum_{i=1}^{M_l} x_{l,i}(t_k) = N_l$. Let $\mathbf{u}_l(t_k)$ denote the maintenance intensities for group l during $[t_k, t_{k+1})$:

$$\mathbf{u}_l(t_k) = (u_1^l(t_k), u_2^l(t_k), ..., u_{M_l-1}^l(t_k), u_C^l(t_k))^T, \tag{5.3}$$

where $u_i^l(t_k)$ and $u_C^l(t_k)$ are a set of integers. $u_i^l(t_k)$ denotes the PM intensities, i.e., the count of items under state i that are restored to state M_l. $u_C^l(t_k)$ denotes the CM intensities, i.e., the count of malfunctioning items that are restored to state M_l. Let P denote the pre-decided PM time schedule and Q denote the pre-decide CM time schedule. $P = \{m_1^p, m_2^p, ..., m_{T_p}^p\}$ and $Q = \{m_1^c, m_2^c, ..., m_{T_c}^c\}$, The elements of P and Q are selected from the indices of sampling instants, i.e., $k = 0, 1, 2, ..., T$. This suggests that the maintenance instants are commensurate with the sampling instants t_k. For t_k with $k \notin P$, $u_i^l(t_k) = 0$ with $\forall i \in [1, M_l]$. For t_k with $k \notin Q$, $u_C^l(t_k) = 0$.

Given $\bar{N}$ item groups in the MPO problem, let $\mathbf{x}(t_k) = (\mathbf{x}_1(t_k), \mathbf{x}_2(t_k), ..., \mathbf{x}_{\bar{N}}(t_k))^T$ denote the state variable and $\mathbf{u}(t_k) = (\mathbf{u}_1(t_k), \mathbf{u}_2(t_k), ..., \mathbf{u}_{\bar{N}}(t_k))^T$ denote the control input. Let $G_l(\mathbf{x}_l(t_k), \mathbf{u}_l(t_k))$ denote the population dynamics in group l under the impacts of deteriorations and maintenances. A compact

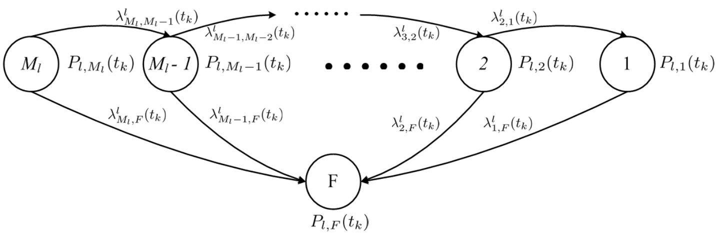

Figure 5.1. The state-transition diagram of an individual item from homogeneous group l with M_l working states and one malfunctioning state

form of the state-space model can be obtained:

$$\begin{bmatrix} \mathbf{x}_1(t_{k+1}) \\ \vdots \\ \mathbf{x}_{\bar{N}}(t_{k+1}) \end{bmatrix} = \begin{bmatrix} \mathbf{x}_1(t_k) \\ \vdots \\ \mathbf{x}_{\bar{N}}(t_k) \end{bmatrix} + \begin{bmatrix} G_1(\mathbf{x}_1(t_k),\mathbf{u}_1(t_k)) \\ \vdots \\ G_{\bar{N}}(\mathbf{x}_{\bar{N}}(t_k),\mathbf{u}_{\bar{N}}(t_k)) \end{bmatrix}, \tag{5.4}$$

where

$$G_l(\mathbf{x}_l(t_k),\mathbf{u}_l(t_k)) = [\triangle x_{l,M_l}(t_k), \triangle x_{l,M_l-1}(t_k), ..., \triangle x_{l,1}(t_k)]^T, \tag{5.5}$$

with $\triangle x_{l,i}(t_k)$ representing the population dynamics in subset i from group l. The initial state is $\mathbf{x}(t_0) = \mathbf{x}_0 = (\mathbf{x}_1^0, \mathbf{x}_2^0, ..., \mathbf{x}_{\bar{N}}^0)^T$.

5.2.2 Population dynamics formulation

In group l, $x_{l,i}(t_k)$ changes over each time. The state-transition of an individual group l item is illustrated in Fig. 5.1, where $P_{l,i}(t_k)$, $i \in [1, M_l]$ denotes the probability that this item works under state i and performance level $g_{l,i}$. $\lambda^l_{i,i-1}(t_k)$ indicates the state-transition from state i to state $i-1$ over the sampling interval $[t_k, t_{k+1})$. The circle F denotes the malfunctioning state and $P_{l,F}(t_k)$ denotes the probability of this item being malfunctioning. $\lambda^l_{i,F}(t_k)$ indicates the state-transition from state i to malfunctioning. As Fig. 5.1 illustrates, $P_{l,i}(t_k)$ increases due to transition $\lambda^l_{i+1,i}(t_k)$, decreases due to transition $\lambda^l_{i,i-1}(t_k)$ and transition $\lambda^l_{i,F}(t_k)$ simultaneously. $P_{l,M_l}(t_k)$ continuously decrease and $P_{l,F}(t_k)$ continuously increase without maintenance. Such state-transition can be formulated to be an Markov process. Given that the population dynamics of homogeneous group l is commensurate with the individual item state-transition, the population dynamics $G_l(\mathbf{x}_l(t_k),\mathbf{u}_l(t_k))$ in group l are formulated in (5.6), where $f^l_{i,i-1}(\mathbf{x}_{l,i}(t_k))$ denote the population dynamics from subset i to $i-1$ that is resulted from the transition $\lambda^l_{i,i-1}(t_k)$.

$$\begin{cases} \triangle x_{l,M_l}(t_k) = -f^l_{M_l,M_l-1}(\mathbf{x}_{l,M_l}(t_k)) - f^l_{M_l,F}(\mathbf{x}_{l,M_l}(t_k)) + \sum_{i=1}^{M_l-1} u^l_i(t_k) + u^l_C(t_k), \\ \triangle x_{l,M_l-1}(t_k) = f^l_{M_l,M_l-1}(\mathbf{x}_{l,M_l}(t_k)) - f^l_{M_l-1,Ml-2}(\mathbf{x}_{l,M_l-1}(t_k)) - f^l_{M_l-1,F}(\mathbf{x}_{l,M_l-1}(t_k)) - u^l_{M_l-1}(t_k), \\ \vdots \\ \triangle x_{l,2}(t_k) = f^l_{3,2}(\mathbf{x}_{l,3}(t_k)) - f^l_{2,1}(\mathbf{x}_{l,2}(t_k)) - f^l_{2,F}(\mathbf{x}_{l,2}(t_k)) - u^l_2(t_k), \\ \triangle x_{l,1}(t_k) = f^l_{2,1}(\mathbf{x}_{l,2}(t_k)) - f^l_{1,F}(\mathbf{x}_{l,1}(t_k)) - u^l_{1,M_l}(t_k), \end{cases} \tag{5.6}$$

The state-transition described in (5.6) is simplified by assuming that the transition exists only from the current state to malfunctioning state or between a pair of neighbour states. The population decay model denoted by $f^l_{i,i-1}(\mathbf{x}_{l,i}(t_k))$ can be obtained via the experimental data fitting or existing reliability models, as discussed in the previous chapters. Several assumptions are made to enable the employment of (5.6). The degradations of the maintained items and the maintenance downtime are ignored during the interval where maintenance actions take place. The state transition intensities of the items are known a priori. The inspection during operation can indicate the working states of the retrofitted items. Due to the energy conservatism principles, the inspections are considered as the actual states of the item groups from the last sampling instant to the current one.

5.3 CONTROLLER DESIGN

5.3.1 Objective function formulation

In the maintenance plan optimisation (MPO) problem for a building retrofitting project, the retrofitted items can be further categorised into two types. The type-I retrofitted items undertake no preventive maintenance over the life-cycle. The corrective replacement takes place after the breakdown of a type-I item, e.g., an energy efficient globe or motion sensor, etc. The old malfunctioning item is thereby scrapped. The energy saving degradation of the type-I retrofits are not taken into account. The type-II retrofitted items are more complicated. The performance levels of a type-II item, e.g., an air conditioner or heat pump, are indicated by the estimated energy savings, computed following the M&V principles [119]. For a type-II item, the performance degradation before the malfunctions is incorporated into the energy modelling. In order to restore a type-II item to a better state, the PM actions must be applied.

The CM actions are also needed to restore the item from malfunctions. The type-I item is a binary state system, which is actually a special case of the MSS. Therefore, (5.2) is employed to describe items of both types.

The overall energy savings and IRR over the sustainability period are introduced to be the control objectives. The targeted energy saving amount limit, budget limit and payback period limit are adopted to be the constraints. The performance characteristics are known a priori via pre-implementation audit and simulation:

$$\begin{cases} \mathbf{a}_l(t_k) = \{a_{l,1}(t_k), a_{l,2}(t_k), ..., a_{l,M_l}(t_k)\}, \\ \mathbf{b}_l(t_k) = \{b_{l,1}(t_k), b_{l,2}(t_k), ..., b_{l,M_l}(t_k)\}, \\ \mathbf{C}_l(t_k) = \{C_1^l(t_k), C_2^l(t_k), ..., C_{M_l}^l(t_k), C_C^l(t_k)\}. \end{cases} \tag{5.7}$$

Similar to the notations in the previous chapters, $\mathbf{a}_l(t_k)$ denotes the average energy savings over $[t_{k-1}, t_k)$ and $\mathbf{b}_l(t_k)$ denotes the average cost savings. $\mathbf{C}_l(t_k)$ denotes the maintenance costs. In (5.7), for $i \in [1, M_l]$, $a_{l,i}(t_k)$ and $b_{l,i}(t_k)$ denote the performance characteristics of an individual item with $G_l(t_k) = g_{l,i}$. $C_i^l(t_k)$ denotes the PM costs and $C_C^l(t_k)$ denotes the CM cost. Thereafter, the aggregate energy savings can be formulated:

$$\begin{cases} ES(t_k) = \sum_{l=1}^{\bar{N}} \sum_{i=1}^{M_l} a_{l,i}(t_k) x_{l,i}(t_k), \\ ES|_{all} = \sum_{k=1}^{T} ES(t_k), \end{cases} \tag{5.8}$$

and the corresponding cost savings:

$$\begin{cases} B(t_k) = \sum_{l=1}^{\bar{N}} \sum_{i=1}^{M_l} b_{l,i}(t_k) x_{l,i}(t_k), \\ B|_{all} = \sum_{k=1}^{T} B(t_k), \end{cases} \tag{5.9}$$

the aggregate maintenance cost at each time instant:

$$h(t_k) = \sum_{l=1}^{\bar{N}} (\sum_{i=1}^{M_l} C_i^l(t_k) u_i^l(t_k) + C_C^l(t_k) u_C^l(t_k)), \tag{5.10}$$

and the retrofitting project investment:

$$h|_{all} = h_0 + \sum_{k=1}^{T} h(t_k), \tag{5.11}$$

where h_0 denotes the initial investment of the retrofitting project. The net present value (NPV) over $[0, TS)$ is formulated taking advantage of $B(t_k)$ and $h(t_k)$:

$$NPV = \sum_{k=1}^{T} \frac{B(t_k) - h(t_k)}{(1+d)^{n-1}} - h_0, \tag{5.12}$$

where d denotes the discount rate. $n = 1, 2, \ldots$ indicates that the sampling interval $[t_{k-1}, t_k)$ lies within the n-th after t_0. The IRR is thereby obtained by solving out the discount rate that makes $NPV = 0$ over $[0, TS)$.

5.3.2 Optimal control problem formulation

Given the initial state $\mathbf{x}(t_0) = \mathbf{x}_0$, the pre-decided PM time schedule $P = \{m_1^p, m_2^p, \ldots, m_{T_p}^p\}$ and CM time schedule $Q = \{m_1^c, m_2^c, \ldots, m_{T_c}^c\}$, the optimal control problem is to find a control law, i.e., the sequence of maintenance intensities $\mathbf{u}(\cdot) = \{\mathbf{u}(t_1), \mathbf{u}(t_2), \ldots, \mathbf{u}(t_T)\}$ that subjects to P and Q and minimises the following performance index over the sustainability period:

$$J(\mathbf{x}_0, \mathbf{u}(\cdot)) = -\lambda_1 \frac{ES|_{all}}{\alpha} - \lambda_2 IRR, \tag{5.13}$$

subject to (5.4)-(5.6), and

$$\begin{cases} ES|_{all} \geq \alpha, \\ \sum_{k=1}^{T} h(t_k) \leq \beta, \\ T_p \leq T', \\ \mathbf{0} \leq \mathbf{x}(t_k) \leq \mathbf{x}_0, \\ u_i^l(t_k)(t_k) = 0, \ k \notin P, \\ u_C^l(t_k)u(t_k) = 0, \ k \notin Q, \end{cases} \tag{5.14}$$

where λ_1 and λ_2 are the weighting factors. α denotes the target energy saving amount, and β denotes the maintenance budget limit over $[0, TS)$. T_p denotes the payback period and T' is the payback period limit.

5.3.3 MPC controller

A mathematical transformation is applied to the optimal control problem (5.13)-(5.14) to allow the employment of the MPC approach. The predictive horizon at instant t_m covers the rest of the sustainability period $[t_m, TS)$, and a dynamic programming is formulated to minimise the following performance index:

$$J'(\mathbf{x}(t_m), \mathbf{u}'|_m(\cdot)) = -\lambda_1 \frac{ES'|_m}{\alpha} - \lambda_2 IRR', \tag{5.15}$$

where IRR' is the discount rate that makes $NPV'|_m = 0$, with

$$\begin{cases} ES'|_m = \sum_{k=1}^{m} \bar{ES}(t_k) + \sum_{k=m+1}^{T} ES(t_k), \\ NPV'|_m = \sum_{k=1}^{m} \frac{\bar{B}(t_k) - \bar{h}(t_k)}{(1+d)^{n-1}} + \sum_{k=m+1}^{T} \frac{B(t_k) - h(t_k)}{(1+d)^{n-1}} - h_0, \end{cases} \tag{5.16}$$

subject to (5.4)-(5.6), and

$$\begin{cases} ES'|_m \geq \alpha, \\ h'|_m \leq \beta',\ m \in R, \\ T_p \leq T', \\ \mathbf{0} \leq \mathbf{x}(t_m) \leq \mathbf{x}_0, \\ u_i^l(t_k)(t_k) = 0,\ k \notin P, \\ u_C^l(t_k)u(t_k) = 0,\ k \notin Q, \end{cases} \tag{5.17}$$

where

$$\begin{cases} h'|_m = \sum_{k=m+1}^{T} h(t_k), \\ \beta' = \beta - \sum_{k=1}^{m} \bar{h}(t_k), \end{cases} \tag{5.18}$$

The $\bar{ES}(t_k)$, $\bar{B}(t_k)$ and $\bar{h}(t_k)$ respectively denote the aggregation of the existing energy savings, cost savings and maintenance costs prior to t_m. T_p is obtained by figuring our the last instant that $NPV'|_m$ remains negative.

Let $\mathbf{d}(t_k) = (\mathbf{d}_1(t_k), \mathbf{d}_2(t_k), ..., \mathbf{d}_{\bar{N}}(t_k))^T$ denote the impacts of uncertainty factors, i.e., the disturbance on state variables. The actual state $\hat{\mathbf{x}}(t_{m+1}) = \mathbf{x}(t_{m+1}) + \mathbf{d}(t_k)$, which can be measured from inspections. The actual state is utilised to be the initial condition of prediction horizon $[t_{m+1}, TS)$. The detailed discussions pertaining to the MPC can be found in Chapter 3. The MPC algorithm is then formulated as following:

MPC Algorithm

Initialisation: Let initial state $\mathbf{x}(t_0) = \mathbf{x}_0$ and $m = 0$.

(i) Compute the open loop optimal solution $\{\mathbf{u}'|_m(t_k)\}$ of the problem formulation (5.15)-(5.18), where $k = m, m+1, ..., T-1$.

(ii) The MPC controller $\bar{\mathbf{u}}|_m = \{\mathbf{u}'|_m(t_m)\}$ is applied after the sampling instant t_m. The remains of the open loop optimal solution $\{\mathbf{u}'|_m(t_k) : k = m+1, ..., T-1\}$ are discarded. The predicted $\mathbf{x}(t_{m+1})$ are then obtained according to (5.4)-(5.6). As a result of the uncertainties, the actual system state over the next sampling period is updated according to:

$$\begin{bmatrix} \hat{\mathbf{x}}_1(t_{m+1}) \\ \vdots \\ \hat{\mathbf{x}}_{\bar{N}}(t_{m+1}) \end{bmatrix} = \begin{bmatrix} \mathbf{x}_1(t_{m+1}) \\ \vdots \\ \mathbf{x}_{\bar{N}}(t_{m+1}) \end{bmatrix} + \begin{bmatrix} \mathbf{d}_1(t_m) \\ \vdots \\ \mathbf{d}_{\bar{N}}(t_m) \end{bmatrix},$$

which is inspected at t_{m+1} and executed over $[t_m, t_{m+1})$.

(iii) Let $\hat{\mathbf{x}}(t_{m+1}) = (\hat{\mathbf{x}}_1(t_{m+1}), ..., \hat{\mathbf{x}}_{\bar{N}}(t_{m+1}))^T$ be the initial state for the next predictive horizon, $m := m+1$ and go back to step (i).

According to the pre-decided maintenance time schedules P and Q, $\mathbf{u}(t_m) = 0$ when $m \notin P$ and $m \notin Q$, where step (i) is skipped and $\hat{\mathbf{x}}(t_{m+1})$ is obtained by

$$\begin{bmatrix} \hat{\mathbf{x}}_1(t_{m+1}) \\ \vdots \\ \hat{\mathbf{x}}_{\bar{N}}(t_{m+1}) \end{bmatrix} = \begin{bmatrix} \mathbf{x}_1(t_m) \\ \vdots \\ \mathbf{x}_{\bar{N}}(t_m) \end{bmatrix} + \begin{bmatrix} G_1(\mathbf{x}_1(t_m), 0) \\ \vdots \\ G_{\bar{N}}(\mathbf{x}_{\bar{N}}(t_m), 0) \end{bmatrix} + \begin{bmatrix} \mathbf{d}_1(t_m) \\ \vdots \\ \mathbf{d}_{\bar{N}}(t_m) \end{bmatrix}.$$

The above MPC algorithm will go over the sustainability period to solve out the optimal control strategy. The DE algorithm based numerical solver can be found at Algorithm 1 in addendum A.

5.4 SIMULATION AND VERIFICATION

The case study involves a simplification of a retrofitting project for a government building. The sustainability period is 10 years, where the sampling interval is one month, i.e., there are 120 sampling instants, $k = 1, 2, ..., 120$. The PM actions take place before the end of each year, i.e., the PM time schedule is $P = \{11, 23, 35, 47, ..., 119\}$. The CM actions take place every three months, therefore the CM time time schedule is $Q = \{2, 5, 8, 11, ..., 119\}$. Table 5.2 illustrates the specifications of the 5 categories of retrofitted items, i.e., the groups of homogeneous items, which are all in good conditions at the initial stage. The motion sensors, 20W Light Emitting Diode (LED) bulbs and 180W new projectors are considered to be type-I items, i.e., the binary state systems. The 3kW heat-pumps and new air conditioners are considered to be type-II items, i.e., the MSS. The 3kW heat-pumps and new air conditioners are type-II items. Fig. 5.2 illustrates the state transition diagram for type-II items, where preventiveA indicates the PM action that restores the item state from average to good, preventiveB from bad to good, and corrective from failed to good.

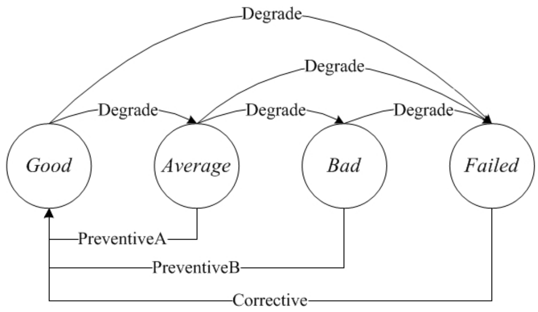

Figure 5.2. The state transition diagram for type-II items in the case study.

Table 5.1. Transition intensities of involved retrofits (in months)

Retrofitted Items	Type	MTBF (months)	t1 (good to average) (months)	t2 (average to bad) (months)
Motion sensor	I	33.5	N/A	N/A
20W retrofit LED	I	27.2	N/A	N/A
180W new projector	I	32.8	N/A	N/A
3kW heat-pumps	II	52	25.2	100
New air conditioner	II	43.8	21.6	86.4

The subset population dynamics are estimated by an exponential decay model with constant transition intensities [140]. Let $\theta^l_{i,i-1}$ denote the transition intensity from state i to state $i-1$ for an item from homogeneous group l, and $\eta^l_{i,i-1} = 1/\theta^l_{i,i-1}$. The subset population dynamics $f^l_{i,i-1}(\mathbf{x}_{l,i}(t_k))$ is:

$$f^l_{i,i-1}(\mathbf{x}_{l,i}(t_k)) = \eta^l_{i,i-1} x_{l,i}(t_k). \quad (5.19)$$

Table 5.1 illustrates the known a priori transition intensities for each category of retrofitted items. The mean time between failure (MTBF) indicates the transition intensity for an item from an arbitrary working state to failure state, $t1$ indicates the one from good to average and $t2$ from average to bad.

Table 5.2 gives the following specifications. The Type column indicates the type of the items. The Quantities column represents the initial populations of the homogeneous groups, which are regulated by the corresponding retrofitting project. The unit prices column indicates the the purchase and installation costs of an retrofitted item. The unit energy saving column and cost saving column illustrates measures of the monthly average. The aforementioned savings are considered to be constant over the sustainability period. The preventiveA cost, preventiveB cost and corrective cost hereby represent the averages of the respective maintenance costs. The targeted energy saving amount is

Table 5.2. Specifications of the retrofitted items

Retrofitted Items	Type	Quantities	Unit Energy Saving (kWh)	Unit Cost Saving ($)	Corrective Cost ($)	PreventiveA Cost ($)	PreventiveB Cost ($)
Motion sensor	I	125	95.08	11.26	196	N/A	N/A
20W retrofit LED	I	382	8.5	0.91	14.19	N/A	N/A
23 inch LCD Monitor	I	48	19.2	2.16	263.28	N/A	N/A
3kW Heat-pumps	II	86	720	81.11	201	47	65
New air conditioner	II	111	148.5	16.3	175	26	35

Table 5.3. Performance characteristics of obtained maintenance plan in different cases

Cases	Energy savings (kWh)	Percentage saved	IRR	Payback period (months)	NPV ($)	Maintenance cost ($)	Total investment ($)
No maintenance	3517093	38.70%	13.62%	62.77	33277.99	0	270758
Full maintenance	10687010	117.86%	33.18%	40.62	338954.1	255249.6	526007.6
Optimal Balance	10367170	114.31%	35.06%	39.33	366320.5	164992.1	435750.1
Energy Prior	10381420	114.49%	34.92%	39.32	366461.8	164989.6	435747.6
Economy Prior	10256830	113.11%	35.23%	39.34	364942	156841.6	427599.6

9,067,921.6 kWh. The initial investment is \$270,760, which can be computed by the quantities and unit prices of the retrofitted items. The maintenance budget limit is \$165,000 over the sustainability period. The payback period limit is 40 months, and the discount rate for NPV computation is 9%. The impact of the uncertainty factors are represented by a series of bounded random noises ranging within $\pm 5\%$ of the state variables.

There are 5 cases with different maintenance strategies: the *no maintenance* and *full maintenance* are cases without taking into account uncertainties, and the *optimal balance*, *energy prior* and *economy prior* are three optimal case, where uncertainty factors deliver impacts and the control approach must be applied. Different weighting factors are employed in these cases. In the optimal balance case, the energy and economy objectives are equally considered, therefore $\lambda_1 = 0.5$ and $\lambda_2 = 0.5$; in the energy prior case, only the energy savings are considered, therefore $\lambda_1 = 1.0$ and $\lambda_2 = 0$; in the economy prior case, only the economy performance is considered, therefore $\lambda_1 = 0$ and $\lambda_2 = 1.0$. The MPO problem becomes a constrained single-objective optimisation problem in the *energy prior*and *economy prior* cases.

The performances of the maintenance strategies in the 5 cases are illustrated in Table 5.3. The performances of the *no maintenance* case illustrate the impact of the deterioration. The performances of the *full maintenance* case are also illustrated for comparison, where all the degraded and failed items are restored without taking the budget limit into account. Due to the budget limits, the full maintenance strategy can be infeasible in some cases. The performances of the three optimal cases are then illustrated and compared with the *full maintenance* case. In summary, the energy savings in the three optimal cases are very close to the *full maintenance* case, and the IRR and NPV values are even larger. However, the full maintenance strategy incurs a much larger overall investment while the three optimal cases keep the expenditure within the budget limit. All the illustrative performances are the mean values of 10-run results taking into account the uncertainties.

Fig. 5.3 draws the system dynamics trajectories from the three optimal cases. In addition to the population dynamics, the cash flows are also illustrated, which can reflect the maintenance intensities over each interval. Furthermore, Fig. 5.4 draws the energy savings over time in these cases. The black solid line indicates the ideal energy savings without deterioration, which cannot be achieved in practice. The other four curves respectively represent the energy savings in the full maintenance case and the three optimal maintenance cases. In addition, two different population dynamics trajectories are illustrated in Fig. 5.5, subject to no maintenance and full maintenance strategies. The curves respectively represent the population dynamics from all 5 categories of retrofitted items that are under good, average, bad and failed states. According to Fig. 5.5 and Table 5.3, if there are no maintenance actions, the energy efficiency of the plant cannot sustain against the deterioration, and the economy of the retrofitting project is seriously damaged as well. This reveals the important role of the maintenance for a retrofitting project from both energy efficiency and economy perspectives.

The magnitude of difference is limited in the optimal cases according to Table 5.3 and Fig. 5.3. One possible reason is that, in our case study, the government is the owner and the user of the retrofitted building. Therefore the cost savings are proportional to the energy savings. Given that the cash inflow mainly consists of the cost savings, the more energy savings are achieved, the more cash inflow can be earned. As a result, the energy saving objective plays a very important role in the MPO problem. However, when various stakeholders are involved, the performances can be very different.

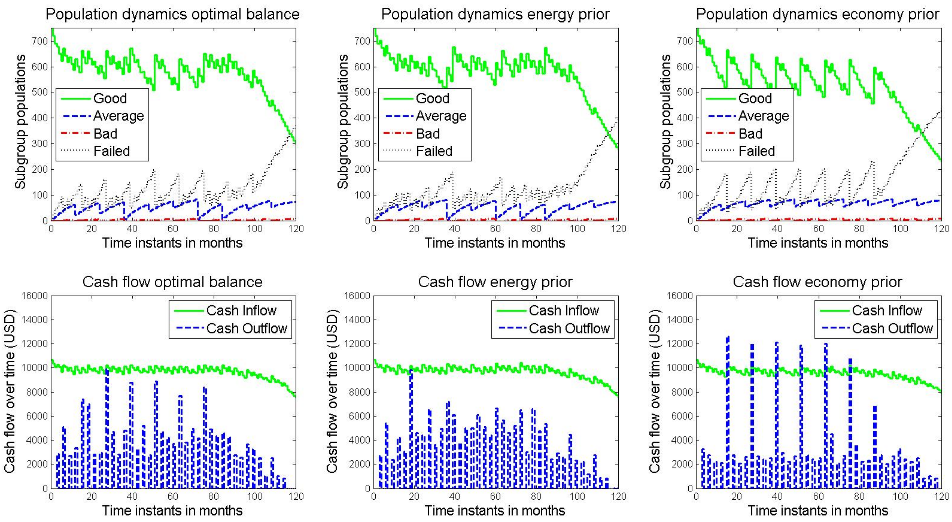

Figure 5.3. The performances of the three optimal cases. Both the population dynamics and the cash flows are illustrated.

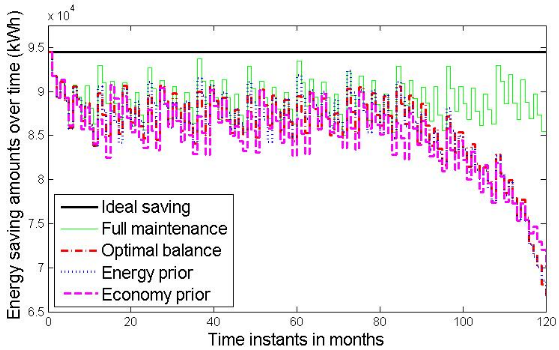

Figure 5.4. The energy saving dynamics over the sustainability period in all cases

5.5 CONCLUSION

In this chapter, both the preventive and corrective maintenances are incorporated into the maintenance plan optimisation model for the building energy retrofitting project. The multi-state system model is taken into account to characterise the performance deterioration of retrofitted items during operation. The totality retrofitted items can manifest complicated state during operation. This complexity is addressed by introducing a grouping method, where retrofitted items are categorised into several homogenous groups, each can be divided into several subgroups subject to the item working states. The subset population dynamics follows the state-transition of an individual item. Thereafter, the

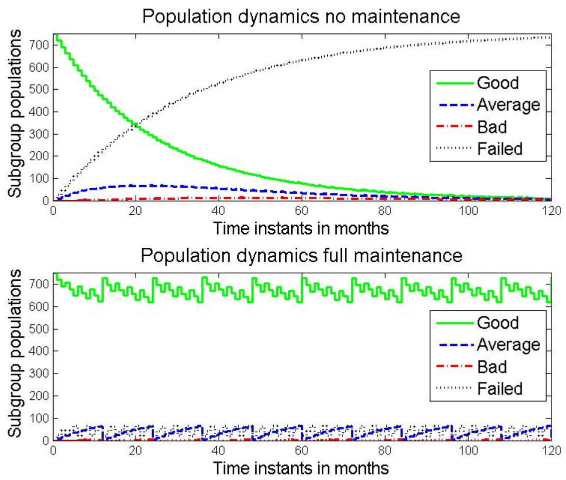

Figure 5.5. The population dynamics of no maintenance and full maintenance.

maintenance plan optimisation problem is improved to be an optimal control problem with multi-state system dynamics, which allows the employment of the model predictive control approach. The effectiveness of the proposed optimisation model and control approach is illustrated in the case study, where the comparative maintenance strategies are outperformed.

CHAPTER 6 MAINTENANCE INSTANTS AND INTENSITIES OPTIMISATION

6.1 INTRODUCTION

In the previous chapters, a control system framework is proposed to incorporate the maintenance planning into retrofitting planning, where the maintenance plan optimisation is cast into an optimal control problem. Such an optimal control problem aims at finding a series of maintenance intensities to maximise the aggregate energy savings and internal rate of return (IRR) [81] over a finite decision horizon, namely the sustainability period. The maintenance intensities are subject to a pre-determined, fixed collection of maintenance instants, namely the maintenance time schedule. In chapter 5, a multi-state system approach is further employed, where items can deteriorate to a worse working state or even worse, the malfunctioning state, during operation. Accordingly, two types of maintenance actions are introduced: the preventive maintenance (PM) and corrective maintenance (CM). The PM time schedule and CM time schedule are pre-determined and fixed as well. Such a time schedule is determined via the expertise of decision makers. In this way, the optimal control problem is parameterised to find the optimal combination of maintenance intensities. The impacts of maintenance instants are excluded. However, the maintenance instants also deliver significant impacts to the aggregate energy and economic performances, due to their dynamic natures. Adjusting the maintenance instants can further influence the aggregate performances. Additional energy efficiency potentials are expected from the maintenance time schedule optimisation, especially when limited budget and manpower are applied. Therefore, incorporating the maintenance time schedule optimisation into the investment decision is the main topic at the current stage.

In order to simultaneously take into account the maintenance intensities and instants into the retrofitting and maintenance planning, the parameterisations of the optimal control problem must be modified. However, adjusting the maintenance instants in the existing control system framework is an uneasy task, due to the interplay between the maintenance intensities and instants. An impulsive and switched system modelling is introduced to characterise such an interplay. Actually, the effects of maintenance are different with the conventional control inputs. Firstly, the maintenance implementation time is usually much smaller than the sustainability period, consequently, the maintenance actions are considered to take place instantaneously. Secondly, the item group population grows to a larger number under the impact of maintenance. As a result, the state variables, i.e., the item group populations are considered to jump under the effects of maintenance. The performance dynamics can be modelled as a hybrid system with impulsive effects and switching phenomena, i.e., an impulsive switched system [154]. According to the impulsive and switched system modelling, the maintenance intensities and instants are parameterised to be a set of coupled decision variables. Thereafter, the influences that maintenance actions deliver to the system dynamics can be characterised, and the optimal control problem is translated into a parameter optimisation problem such that the gradient method can be employed to find the numerical solution [154].

The main contribution of this chapter is introducing an impulsive and switched system modelling to the control system framework for the investment decision of retrofitting and maintenance planning. Comparing with the previous chapters, the impulsive and switched system modelling allows simultaneous optimisation of the maintenance intensities and instants, which are a pair of coupled parameters in the control framework. Specifically, a maintenance plan optimisation (MPO) is hereby investigated. Some preliminary results have been presented in [155], where the discrete form of the control system framework is employed. For the sake of generality, a continuous form is developed, instead of the previous discrete form. Furthermore, the system states are modified to be the ratios of the current item group population to the initial population, and the maintenance intensities are the ratios of the restored item to the total failed item from the same item group. In this way, the maintenance strategy actually becomes a proportional feedback control. The objective function is the weighted sum of the aggregate energy savings and IRR over the sustainability period. The MPO problem is subject to the impulsive and switched system dynamics and a series of constraints, e.g., the targeted energy savings, maintenance budget limit and payback period limit. Given that the IRR is a non-analytic function rather than a simple integral of the utility function [156], the gradient method is an unsuitable solver for the present optimal control problem. Therefore, a differential evolution (DE) algorithm based numerical solver is introduced to the MPO problem. A case study retrofitting project is illustrated to test and verify the effectiveness of the proposed approach.

6.2 CONTROL PROBLEM FORMULATION

6.2.1 Impulsive and switched system modelling:

Given the finite decision horizon, i.e., the sustainability period $[0,T)$. Let the following continuous dynamical system over $[0,T)$ represent the impulsive and switched system dynamics of MPO:

$$\dot{x}(t) = g(x(t),t), t \neq k_i, i = 1,2,...,S, \tag{6.1}$$

where x denotes the state variables, i.e., the ratio of current item group population to the initial item population. x ranges from 0 to 1, where $x(0) = 1$. $g(\cdot)$ is a continuously differentiable function, which denotes the population decay of the item group. Assumed that there are S maintenance instants over $[0,T)$, let $k = k_1, k_2, ..., k_S$ denote the maintenance instants. The system states jump at k, therefore the system dynamics under the impulsive maintenance effects is given as follows:

$$\begin{cases} \vec{x}(k_i) = x(k_i) + \triangle x(k_i), i = 1,2,...S, \\ \dot{x}(k_i) = g(\vec{x}(k_i), k_i), \end{cases} \tag{6.2}$$

where $\triangle x(k_i)$ denotes an impulsive effect prior to k_i that incurs an impulsive jump of the system state. $\triangle x(k_i)$ denotes the impulsive effect at instant k_i, and ranges from 0 to $1 - x(k_i)$. $x(k_i)$ denotes the system state prior to the impulsive jumps and $\vec{x}(k_i)$ denotes the system state after the impulsive jump. The continuous dynamical system (6.1)-(6.2) is thereby an impulsive switched system.

In a multi state control system framework, given an item group l with M_l working states and N_l items. M_l denotes the best working states and 1 denotes the worst. The impulsive and switched system dynamics of group l is formulated as (6.3), where the system state $x_{l,i}(t)$, $i = 1,2,...,M_l$ denotes the ratios of the population of items under state i to the initial population of item group l. $f^l_{i,j}(x_{l,i}(t),t)$ denotes the portion of items that degrade from state i to a worse state j, $g_{l,i}(x_{l,i}(t),t)$ denotes the portion of items under state i and become malfunctioning. For simplicity, assuming that an item under working state i can only degrade to the next worse state $i-1$. For convenience, let $\mathbf{x}_l(t) = (x_{l,M_l}(t), x_{l,M_l-1}(t), ..., x_{l,1}(t))^T$, $\dot{\mathbf{x}}_l(t) = F(\mathbf{x}_l(t))$ denote (6.3). $\mathbf{x}_l(k)$ jumps at k as (6.4) illustrates. where $x_{l,0}(t)$ is especially employed to indicate the portion of malfunctioning items from group l at t. Similar with (6.2), $\triangle x_{l,i}(t)$ denotes the impulsive effect that incurs the impulsive jump of system states. $\vec{\mathbf{x}}_l(t) = (\vec{x}_{l,M_l}(t), \vec{x}_{l,M_l-1}(t), ..., \vec{x}_{l,1}(t))^T$ denotes the system states after the

$$\begin{cases} \dot{x}_{l,M_l} = -f^{l}_{M_l,M_l-1}(x_{l,M_l}(t),t) - g_{l,M_l}(x_{l,M_l}(t),t), t \neq kc, \\ \dot{x}_{l,M_l-1} = f^{l}_{M_l,M_l-1}(x_{l,M_l}(t),t) - f^{l}_{M_l-1,M_l-2}(x_{l,M_l-1}(t),t) - g_{l,M_l-1}(x_{l,M_l-1}(t),t), t \neq kp, \\ \qquad \vdots \\ \dot{x}_{l,1} = f^{l}_{2,1}(x_{l,2}(t),t) - g_{l,1}(x_{l,1}(t),t),\ t \neq kp, \\ \dot{x}_{l,M_l}(0) = 1, \\ \dot{x}_{l,n}(0) = 0, n = 1,2,...,M_{l-1}. \end{cases} \tag{6.3}$$

$$\begin{cases} \triangle x_{l,M_l}(t) = u^{c}_{l}(t) x_{l,0}(t),\ t = kc, \\ \triangle x_{l,M_l}(t) = \sum_{i=1}^{M_l-1} u_{l,i}(t) x_{l,i}(t),\ t = kp, \\ \triangle x_{l,M_l-1}(t) = -u_{l,M_l-1}(t) x_{l,M_l-1}(t),\ t = kp, \\ \qquad \vdots \\ \triangle x_{l,1}(t) = -u_{l,1}(t) x_{l,1}(t),\ t = kp, \\ \vec{x}_{l,i}(t) = x_{l,i}(t) + \triangle x_{l,i}(t),\ 1 \leq i \leq M_l,\ t = kp, kc, \\ \dot{\mathbf{x}}_l(t) = F(\vec{\mathbf{x}}_l(t)),\ t = kp, kc, \\ x_{l,0}(t) = 1 - \sum_{i=1}^{M_l} x_{l,i}(t), \end{cases} \tag{6.4}$$

impulsive jumps. Such impulsive effects are resulted from the maintenance intensities. As introduced above, there are two types of maintenance: PM and CM, and accordingly, two types of switching instants: $kp_i, i = 1,2,...,S_p$ the preventive maintenance instants, and $kc_i, i = 1,2,...,S_c$ the corrective maintenance instants. Let $Q_p = \{kp_1, kp_2, ..., kp_{S_p}\}$ and $Q_c = \{kc_1, kc_2, ..., kc_{S_c}\}$ denote the respective collections of preventive and corrective maintenance instants, where the elements are distributed over the sustainability period $[0,T)$. S_p denotes the horizon of Q_p and S_c denotes the horizon of Q_c. Q_p and Q_c therefore represent the preventive and corrective maintenance time schedule. For the convenience of derivation, let kp denote the arbitrary element of Q_p and kc denote the arbitrary element of Q_c.

Let $\mathbf{u}_{l,i}(t)$ and $\mathbf{u}^{c}_{l}(t)$ denote the control inputs for the impulsive and switched system (6.3)-(6.4) over $[0,T)$. $\mathbf{u}_{l,i}(t)$ with $i = 1,2,...,M_{l-1}$ represent the PM intensities, $\mathbf{u}^{c}_{l}(t)$ represents the CM intensities. These maintenance intensities are actually a series of ratios corresponding to $\mathbf{x}_l(t)$, where a portion of $x_{l,i}(t)$, $i = 1,2,...,M_{l-1}$ are added to $x_{l,M_l}(t)$, as illustrated in (6.4). This reveals a fact that the maintenance strategy is actually a kind of proportional feedback control. $\mathbf{u}_{l,i}(t)$ and $\mathbf{u}^{c}_{l}(t)$ are computed as follows,

$$\begin{cases} \mathbf{u}_l^p(t) = (u_{l,1}(t), u_{l,2}(t), ..., u_{l,M_l-1}(t))^T, t = kp, \\ \mathbf{u}_l^p(t) = \mathbf{0}, t \neq kp, \\ \mathbf{u}_l^c(t) = u_l^c(t), t = kc, \\ \mathbf{u}_l^c(t) = 0, t \neq kc. \end{cases} \tag{6.5}$$

Given that $\mathbf{u}_l^p(t)$ and $\mathbf{u}_l^c(t)$ are $\mathbf{0}$ when $t \neq kp$ and $t \neq kc$, the control of (6.3)-(6.4) is to determine the pairs of $u_{l,i}(kp)$ and kp, $u_{l,c}(kc)$ and kc. In this way, the control problem is translated into a parameter optimisation problem. The population decay formulations are difficult to obtain. Currently, the population decay statistical laws that have been confirmed in existing studies [140] are employed as follows:

$$\begin{cases} f_{i,i-1}^l(x_{l,i}(t), t) = \zeta_{l,i}^p x_{l,i}(t), i > 1 \\ g_{l,i}(x_{l,i}(t), t) = \zeta_{l,i}^c x_{l,i}(t), \end{cases} \tag{6.6}$$

where the decay rates are assumed to be constant. $\zeta_{l,i}^p$ and $\zeta_{l,i}^c$ are usually small positive constants close to 0. For some item categories where preventive maintenance cannot apply, e.g., the lamps, only one working state is considered. The population decay is obtained from the experimental data fitting results [109]:

$$g_{l,1}(x_{l,1}(t), t) = \mu_l x_{l,1}(t) - \mu_l \nu_l x_{l,1}(t)^2. \tag{6.7}$$

The parameter determinations for these decay models can be found in our relevant studies [53, 109].

6.2.2 Objective function formulation

The performance indicators are given in this subsection. Given a building energy efficiency retrofitting project including $\bar{N}$ groups of homogeneous retrofitted items. The average energy savings, cost savings, and maintenance costs per item are known a priori. These characteristics can be obtained from pre-implementation audits. Let P_l denote the initial population for item group l, and the performance characteristics are represented as follows,

$$\begin{cases} \mathbf{a}_l(t) = \{a_{l,1}(t), a_{l,2}(t), ..., a_{l,M_l}(t)\}, \\ \mathbf{b}_l(t) = \{b_{l,1}(t), b_{l,2}(t), ..., b_{l,M_l}(t)\}, \\ \mathbf{C}_l(t) = \{C_{1,1}(t), C_{l,2}(t), ..., C_{l,M_l-1}(t), C_l^c(t)\}, \end{cases} \tag{6.8}$$

where $\mathbf{a}_l(t)$ denotes the energy savings from an item at instant t. $\mathbf{b}_l(t)$ denotes the cost savings. $a_{l,i}(t)$ and $b_{l,i}(t)$ are corresponding with $x_{l,i}(t)$. $\mathbf{C}_l(t)$ denotes the maintenances costs per item, where $C_{1,i}(t)$ is pertaining to PM intensity $u_{l,i}(t)$ and $C_l^c(t)$ the CM intensity $u_l^c(t)$. The overall energy savings over the sustainability period $[0,T)$ are then represented by (6.9),

$$\begin{cases} ES(t) = \sum_{l=1}^{\bar{N}} \sum_{i=1}^{M_l} a_{l,i}(t) x_{l,i}(t) P_l, \\ ES|_{all} = \int_{t=0}^{T} ES(t) dt, \end{cases} \tag{6.9}$$

and the corresponding cost savings are obtained:

$$\begin{cases} B(t) = \sum_{l=1}^{\bar{N}} \sum_{i=1}^{M_l} b_{l,i}(t) x_{l,i}(t) P_l, \\ B|_{all} = \int_{t=0}^{T} B(t) dt, \end{cases} \tag{6.10}$$

the maintenance cost at each time instant is obtained:

$$\begin{aligned} h(t) = & \sum_{l=1}^{\bar{N}} \sum_{i=1}^{M_l-1} C_{l,i}(t) u_{l,i}(t) \\ & + \sum_{l=1}^{\bar{N}} C_l^c(t) u_l^c(t) + M_c(t), \end{aligned} \tag{6.11}$$

where $M_c(t)$ denotes a minimal cost that is charged when a maintenance action takes place at t. $M_c(t) = 0$ if $t \notin Q_c \bigcup Q_p$. $M_c(t)$ is introduced to reflect the actual situation, where the maintenance manpower must be taken into account. The overall investment of the retrofitting project is then represented by:

$$h|_{all} = h_0 + \int_{t=0}^{T} h(t) dt, \tag{6.12}$$

where h_0 denotes the initial expenditure of the retrofitting project. The Net Present Value (NPV) [81] of the project over $[0,T)$ is computed from $B(t)$ and $h(t)$. In order to compute NPV from a continuous system model, the yearly cash inflow and cash outflow must be obtained. Let B_n denote the cash inflow and h_n denote the cash outflow of the *n-th* year. The formulation of B_n and h_n are illustrated as follows:

$$\begin{cases} B_n = \int_{t_{n-1}}^{t_n} B(t) dt, \\ h_n = \int_{t_{n-1}}^{t_n} h(t) dt, \end{cases} \tag{6.13}$$

where t_n denotes the instant that separates the *n-1-th* year and *n-th* year. $t_0 = 0$. Assuming that there are N_T years within the sustainability period, the NPV can be computed as follows,

$$NPV = \sum_{n=1}^{N_T} \frac{B_n - h_n}{(1+d)^n} - h_0, \tag{6.14}$$

where d denotes the discount rate for NPV calculation. The IRR, denoted by $d_R|_T$, is defined to be the discount rate that makes $NPV = 0$ over $[0,T)$. The IRR cannot be represented analytically, but still a bounded value with finite initial investment h_0 [156].

Let $\mathbf{P} = \{P_1, P_2, ..., P_{\bar{N}}\}$ denote the initial populations of the respective item groups, $\mathbf{u}_p(\cdot)$ denote the collection of $\mathbf{u}_l^p(kp)$, $\mathbf{u}_c(\cdot)$ denote the collection of $\mathbf{u}_l^c(kc)$, $l = 1, 2, ..., \bar{N}$. Taking advantage of the weighted sum approach, the objective function for the MPO problem is obtained as follows,

$$J(\mathbf{P}, Q_p, Q_c, \mathbf{u}_p(\cdot), \mathbf{u}_c(\cdot)) = -\lambda_1 \frac{ES|_{all}}{\alpha} - \lambda_2 d_R|_T, \tag{6.15}$$

where α is the targeted saving value, $d|_R^T$ is the IRR. λ_1 and λ_2 denote the weighting factors. The objective function formulation indicates that the energy and economic performances are simultaneously taken into account, where the weighting factors adjust the importance of the two objectives.

6.2.3 Optimal Control Problem

Taking advantage of the aforementioned impulsive and switched system modelling (6.3)-(6.7) and objective function formulation (6.15), the optimal control problem can be formulated as follows:

Optimization Problem $\mathcal{MPO}$: For a dynamical system consisting of $\bar{N}$ subsystems in (6.3)-(6.7) with state variables $\mathbf{x}(t) = \{\mathbf{x}_1(t), ..., \mathbf{x}_l(t), ..., \mathbf{x}_{\bar{N}}(t)\}$ and initial state $\mathbf{x}(0)$, find the optimal maintenance time schedule Q_p and Q_c, PM intensities $\mathbf{u}_p(\cdot) = \{\mathbf{u}_1^p(kp), ..., \mathbf{u}_l^p(kp), ..., \mathbf{u}_{\bar{N}}^p(kp)\}$ and CM intensities $\mathbf{u}_c(\cdot) = \{\mathbf{u}_1^c(kc), ..., \mathbf{u}_l^c(kc), ..., \mathbf{u}_{\bar{N}}^c(kc)\}$, which minimise the performance index (6.15) that is subject to system dynamics 6.3-6.7 and the following constraints

$$\begin{cases} ES|_{all} \geq \alpha, \\ \int_{t=0}^{T} h(t)dt \leq \beta, \\ T_p \leq T', \end{cases} \tag{6.16}$$

where β is the maintenance budget limit over $[0, T)$, T' is the payback period limit. T_p is the payback period, which is computed from the last t_n that makes $NPV < 0$. Let $M_{\bar{N}}$ denote the total number of working states for the $\bar{N}$ item groups, $\mathbf{u}_p(\cdot) \in \mathcal{R}^{(M_{\bar{N}} - \bar{N}) \times S_p}$ and $\mathbf{u}_c(\cdot) \in \mathcal{R}^{\bar{N} \times S_c}$, i.e., the minimisation problem (6.15)-(6.16) is a finite dimensional problem. (6.15)-(6.16) is different with the conventional optimal control problem. Firstly, the control inputs to be solved are a set of parameters. Secondly, the objective function is a weighted sum of two different performance indicators, instead of the quadratic performance index. Finally, $d_R|_T$ is non-analytic, as a result, the gradient method becomes infeasible to (6.15)-(6.16). Therefore, a differential evolution (DE) algorithm can be employed as the numerical solver to the minimisation problem, as introduced in previous chapters and the appendix.

6.2.4 Feasibility and Boundedness

Feasibility of the optimisation and stability of the closed-loop system can be given by the following theorem.

Theorem 1 *Consider the population dynamics described by the impulsive switched system* (6.3)–(6.7). *If β in* (6.16) *is selected large enough, then,*

1. *system states are bounded;*

2. *the optimisation problem $\mathcal{P}$ is feasible.*

Proof.

1. With $0 < \zeta^p_{l,i} < 0.5$ and $0 < \zeta^c_{l,i} < 0.5$ (which are usually satisfied in practice) in (6.6), it is apparent that $x_{l,i}$ with $i > 1$ decreases to zeros if there are no maintenance.

   Moreover, according to the constraints (6.16), $h(t)$ is bounded, indicating that $\mathbf{u}_p(\cdot)$ and $\mathbf{u}_c(\cdot)$ are bounded. It then follows from (6.4) that $\Delta x_{l,i}$ are always bounded.

   Consequently, it can be concluded that system states are bounded.

2. Boundedness of system states indicates that $-\lambda_1 \frac{ES|_{all}}{\alpha}$ in (6.15) is bounded; the IRR $d_{R|T}$ is bounded since $0 < d < 1$ and $h_0 > 0$, indicating that $-\lambda_2 d_R|_T$ in (6.15) is bounded. Consequently, the performance index J is lower bounded.

   In another aspect, according to [117], there exists at least one feasible solution that satisfies all the constraints from (6.15)–(6.16). Moreover, constraints given by (6.16) indicates a closed set of solution. As a result, it can be concluded that the optimisation problem $\mathcal{MPO}$ is feasible, with the optimal solution either equal to or superior over the existing solution in [117].

$\square$

6.3 SIMULATION AND ANALYSIS

6.3.1 A case study

A case study is investigated to test and verify the energy efficiency potentials of maintenance time schedule optimisation. For simplicity, a subset of two retrofitted item groups from a large retrofitting project is employed as the case study. One item group consists of a series of compact fluorescent lamps (CFLs) that manifest binary working state. The other group consists of the air conditioner fan coil units, where three working states are involved. The specifications and some performance characteristics of the involved retrofitted items are illustrated in Table 6.2. The new fan coil unit 3, 2 and 1 denote the three working states that correspond with different savings and maintenance costs. The energy saving and cost saving are the annual average value obtained from the energy auditing. The preventive cost indicates the costs of restoring a fan coil unit from working state 2 or 1 to the best working state 3. The corrective cost indicates the costs of restoring one item from failure to normal working. The state transition and the population dynamics of the fan coil unit group is characterised by the multi state model in (6.6). The CFL population decay is governed by the statistical law as confirmed in (6.7). The parameters in (6.6)-(6.7) are given in Table 6.1.

The sustainability period is 10 years, where $T = 10$. Given that the sustainability period is a very long time, it is infeasible to wait the actual operation results. Therefore the simulation instead of the filed test is implemented here. The targeted energy saving is 1,042,237.44 kWh. The initial cost h_0 is \$28,692. The minimal cost is \$200. The discount rate for NPV calculation is 11% per year, and the payback period limit is 3 years. In order to investigate the performances of the approach, a series of scenarios are introduced, where different maintenance budget limits are involved: \$35,000, \$39,000, \$45,000, \$49,500, \$55,000, and \$60,000, from very tight to sufficient. There are 19 preventive maintenance instants and 9 corrective maintenance instants. A pair of fixed preventive and corrective time schedules $Q_p = \{0.5, 1, 1.5, 2, ..., 9.5\}$ and $Q_c = \{1, 2, 3, ..., 9\}$ are employed to be the baseline performances, where the maintenance instants are expected to be evenly distributed over sustainability period. The adopted weight factors are $\lambda_1 = 0.5$ and $\lambda_2 = 0.5$, implying that the two objectives are equally considered.

Table 6.1. Parameters for the corresponding population deterioration models

Retrofits	μ_i	ν_i	ζ_i^p	ζ_i^c
15W retrofit CFL	1.1364	0.7746	N/A	N/A
New fan coil units 3	N/A	N/A	1.2500	0.4545
New fan coil units 2	N/A	N/A	0.8333	0.5348
New fan coil units 1	N/A	N/A	N/A	0.7576

Table 6.2. Characteristics of retrofitted items

Retrofits	Quantities	Unit Price ($)	Unit Energy Saving (kWh)	Unit Cost Saving ($)	Preventive Cost ($)	Corrective Cost ($)
15W retrofit CFL	338	14	105.6	11.9	N/A	14
New fan coil units 3	42	380	4320	486.65	N/A	175
New fan coil units 2	0	380	3542.3	397.95	52	N/A
New fan coil units 1	0	380	2651.75	278.35	70	N/A

6.3.2 Results and analysis

Table 6.3 illustrates the optimisation results as well as the comparative results. The optimal maintenance time schedule is shown in Table 6.4. The following performances are selected in Table 6.3: the overall energy savings during the sustainability period (given in kWh), the percentage savings that indicate the ratios against the targeted energy savings, the IRR, the payback period (given in years), the NPV, the total maintenance cost and the overall investment (given in USD). The investigated MPO problem is complicated as there are significant interplays between the decision variables, furthermore, a non-linear and non-analytic item is involved in the objective function. Due to this complexity, multiple runs with sufficient iterations are applied to obtain the optimal solutions.

According to Table 6.3, for all six different scenarios, the collaborative optimisation approach outperforms the maintenance plan with fixed time schedule. The energy savings from two approaches are very close, while notable improvements on the economic performances, i.e., the IRR, payback period and NPV, can be observed. When comparing with the fixed time schedule, the IRR are improved by from 17.5% to 20.81% (considering the fixed time schedule solutions to be 100%), the payback period are improved by from 18.03% to 21.03%, and NPV are improved by from 4.2% to 6.9%. The significant improvements of the economic performances are resulted from its time sensitivity. The

Table 6.3. Maintenance plan performances with optimal and fixed time schedule and under different budget limits

Cases	Budget limit ($)	Energy savings (kWh)	Percentage saved	IRR	Payback period (years)	NPV ($)	Maintenance cost ($)	Total investment ($)
Optimal time schedule	35,000	1256843.42	120.59%	34.80%	2.1	44926.19	35000	63692
Fixed time schedule	35,000	1254194.99	120.33%	29.26%	2.57	42488.31	34997	63689
Optimal time schedule	39,000	1324389.81	127.07%	35.15%	2.08	46847.46	38991	67683
Fixed time schedule	39,000	1324431.62	127.07%	29.92%	2.63	44961.26	38983	67675
Optimal time schedule	45,000	1443808.05	138.53%	36.45%	2.1	51029.96	44993	73685
Fixed time schedule	45,000	1443137.27	138.47%	30.57%	2.63	48272.56	44994	73686
Optimal time schedule	49,500	1523456.37	146.17%	36.92%	2.08	52872.58	49488	78180
Fixed time schedule	49,500	1507740.41	144.66%	30.69%	2.63	49431.04	49481	78173
Optimal time schedule	55,000	1592895.84	152.83%	36.66%	2.09	53721.8	54983	83675
Fixed time schedule	55,000	1586436.17	152.21%	30.39%	2.65	50545.11	54993	83685
Optimal time schedule	60,000	1628414.85	156.24%	37.18%	2.09	54113.05	59475	88167
Fixed time schedule	60,000	1626898.5	156.10%	30.78%	2.62	50937.89	59285	87977

optimal maintenance time schedule adjust the yearly cash flows that significantly influence the financial paybacks.

Fig. 6.1 depicts the optimal trajectories during the sustainability period under different budget limits. The three figures in the first row indicate the population dynamics and the three figures in the second row indicate the cash flows. Given that one air conditioner fan coil unit contributes much larger energy and cost savings than one CFL, the budget is firstly used on the maintenance of the fan coil units when the budget limit is tight. From Table 6.3 and Fig. 6.1, two facts are verified: according to our model, the evenly distributed maintenance instants and intensities result in higher energy savings, yet the time schedule optimisation reveals significant economic efficiency potentials comparing with the fixed maintenance time schedule. Fig. 6.2 depicts and compares the solutions from Table 6.3. Fig. 6.3 shows the timely energy savings under the three budget limits.

Furthermore, an extra set of six scenarios with same budget limit but 2.5 year payback period limit are investigated to further identify the advantages of the collaborative optimisation approach. The payback period limit is relatively tight in the extra six scenarios. Table 6.5 illustrates the corresponding solutions. According to Table 6.5, when comparing the optimal the fixed time schedule, the energy savings are improved by from 1.88% to 3.36%, the IRR are improved by from 19.12% to 23.09%. Due

Table 6.4. Optimal maintenance time schedules (in years)

Time schedule	Budget limit ($)	Maintenance Number	Maintenance Instants
Q_p	35,000	19	{0.4824 1.0000 1.5053 2.0066 2.5504 3.0015 3.5750 4.0005 4.4987 5.0222 5.4288 6.0105 6.4904 7.0005 8.0359 8.3516 8.4361 8.9501 9.5853}
Q_c		9	{1.0014 2.0097 3.0001 4.0089 5.0388 6.0175 7.0012 8.0329 9.0041}
Q_p	39,000	19	{0.4994 1.0021 1.6362 2.0170 2.4896 3.0686 3.4937 4.0103 4.3531 4.9908 5.4922 6.0241 6.3516 6.9791 7.1393 7.3216 7.9012 9.3183 9.6936}
Q_c		9	{1.0035 2.0199 2.7400 4.0174 4.9930 6.0200 6.9680 8.2087 9.0544}
Q_p	45,000	19	{0.5639 1.0001 1.4966 2.0033 2.3821 3.0064 3.5911 4.0084 4.4965 4.7379 5.4728 6.0174 6.5339 7.0084 7.1204 8.0067 8.4721 9.0470 9.3255}
Q_c		9	{1.0004 2.0000 3.0005 4.0001 5.0186 6.0159 7.0015 8.0001 8.7736}
Q_p	49,500	19	{0.1648 1.0001 2.0000 2.0006 3.0023 3.5163 4.0100 4.2250 4.6346 5.0061 5.4174 5.4338 6.0066 7.0042 7.7697 8.2473 9.0150 9.3649 9.6464}
Q_c		9	{1.0027 2.0097 3.0000 4.0000 5.0014 6.0000 7.0094 7.9781 8.6827}
Q_p	55,000	19	{0.4913 1.0307 1.4698 2.0153 2.4907 3.0012 3.5345 4.0069 4.5019 5.0000 5.4813 6.0190 6.4916 7.0386 7.7634 7.9394 8.4522 8.9935 9.4889}
Q_c		9	{1.0364 2.0185 3.0052 4.0074 4.9905 6.0184 7.0390 8.0494 8.9953}
Q_p	65,000	19	{0.5011 1.1385 1.4726 2.0539 2.3032 3.1412 3.6526 4.1384 4.5511 5.0707 5.6281 6.3182 6.8380 7.4386 7.8842 8.2963 8.8296 9.3070 9.6213}
Q_c		9	{1.0695 2.0515 3.1388 4.1875 5.2676 6.0573 7.1144 8.0477 9.1108}

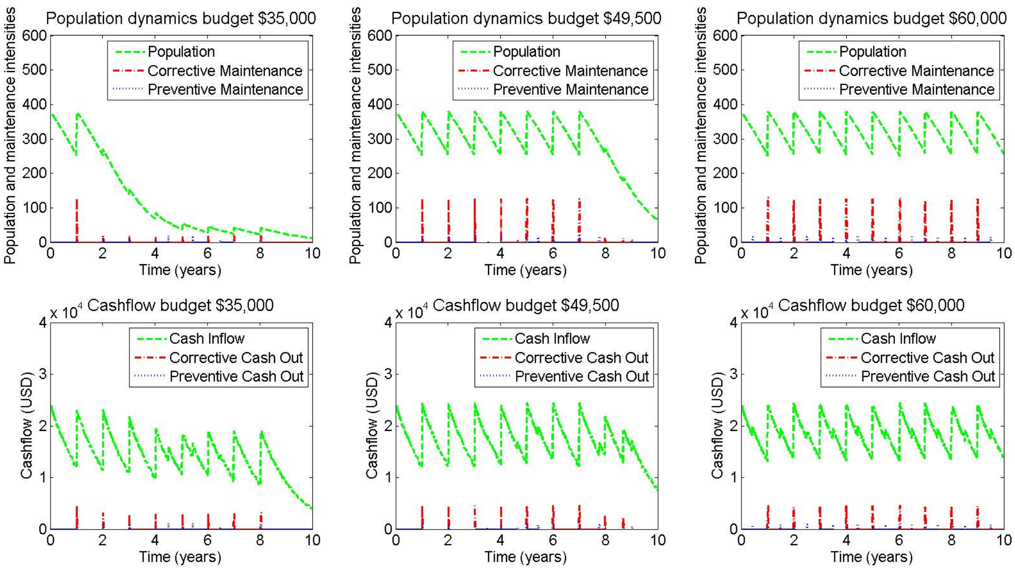

Figure 6.1. The population and cash flows under the optimal maintenance time schedule with different budget limit.

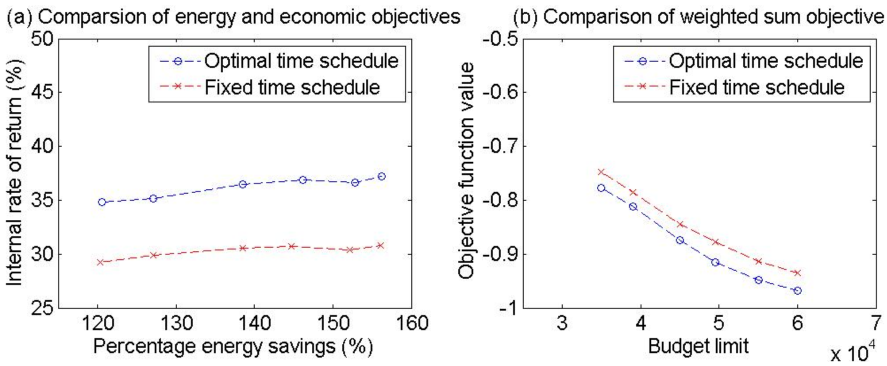

Figure 6.2. Comparison of the optimal and fixed time schedule solutions. (a) depicts the IRR and percentage energy savings in six scenarios, each circle indicates a solution from optimal time schedule and each cross indicates a solution from fixed time schedule. (b) depicts the value of our weighted sum objective function in six scenarios. Similarly, the circles indicate the optimal time schedule solutions and crosses indicate fixed time schedule solutions.

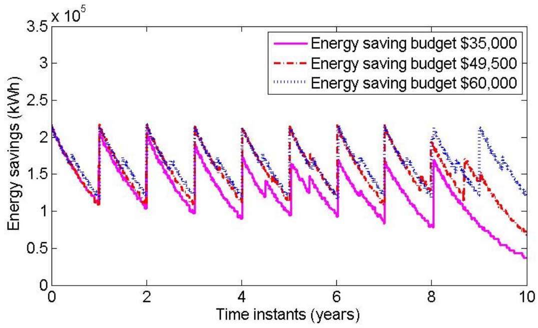

Figure 6.3. The timely energy savings over the sustainability period.

to the tight payback period limit, some energy savings are compromised in the fixed time schedule solutions. This illustrates the further advantage of the collaborative optimisation against the fixed time schedule when tight constraints are applied.

6.4 CONCLUSIONS AND FUTURE WORKS

In this chapter, the maintenance time schedule optimisation is incorporated into the maintenance plan optimisation for building energy retrofitting projects. The aggregate energy and economic performances of the retrofitting project manifest significant dynamics under the joint effects of the item performance deterioration, item failures and maintenance. Such dynamics is addressed via a control

Table 6.5. Maintenance plan performances with optimal and fixed time schedule and tight payback period limit

Cases	Budget limit ($)	Energy savings (kWh)	Percentage saved	IRR	Payback period (years)	NPV ($)	Maintenance cost ($)	Total investment ($)
Optimal time schedule	35,000	1256843.42	120.59%	34.80%	2.1	44926.19	35000	63692
Fixed time schedule	35,000	1216033.51	116.68%	29.22%	2.496	41053.05	34997	63689
Optimal time schedule	39,000	1324389.81	127.07%	35.15%	2.08	46847.46	38991	67683
Fixed time schedule	39,000	1298216.07	124.56%	29.40%	2.49	42957.73	38905	67597
Optimal time schedule	45,000	1443808.05	138.53%	36.45%	2.1	51029.96	44993	73685
Fixed time schedule	45,000	1404030.34	134.71%	29.80%	2.47	45676.87	44983	73675
Optimal time schedule	49,500	1523456.37	146.17%	36.92%	2.08	52872.58	49488	78180
Fixed time schedule	49,500	1482095.11	142.20%	30.03%	2.46	47445.9	49493	78185
Optimal time schedule	55,000	1592895.84	152.83%	36.66%	2.09	53721.8	54983	83675
Fixed time schedule	55,000	1562903.36	149.96%	30.14%	2.496	49031.11	54989	83681
Optimal time schedule	60,000	1628414.85	156.24%	37.18%	2.09	54113.05	59475	88167
Fixed time schedule	60,000	1598405.83	153.36%	30.21%	2.5	49094.4	58883	87575

system framework, where the retrofitted items are categorized into several groups. Each group consists of items that are considered to be homogeneous, and the item group populations are selected to be the state variables of the control system. Given that the system states jump under the instantaneous effect of the maintenance, the performance dynamics is modelled to be an impulsive and switched system. Both the preventive and corrective maintenance is involved in the control system framework. Thereafter, the maintenance intensities and instants are simultaneously and collaboratively optimised. The optimisation aims at maximising the aggregate energy savings and internal rate of return over the sustainability period subject to the impulsive and switched system dynamics, targeted energy saving limit, maintenance budget limit and payback period limit. A case study is investigated to test and verify the effectiveness of the proposed approach. From the simulation results, up to 20.8% of the IRR and up to 6.9% of the NPV can be improved against the fixed maintenance time schedule under the same budget limit with relaxed payback period limit (considering fixed time schedule solution to be 100%). When tight payback period limit is applied, up to 3.36% of the energy savings and up to 23.09% of the IRR can be improved. Therefore, further energy efficiency and economic efficiency opportunities are identified via the collaborative optimisation of maintenance intensities and instants over a finite time period subject to limited budget and manpower.

The current stage work calls for further studies. The number of maintenance instants can deliver further impacts to the aggregate performances. Incorporating the maintenance time schedule scale optimisation into the current control system framework will be a focus of our next step studies.

CHAPTER 7 GROUPING ROBUSTNESS ANALYSIS

7.1 INTRODUCTION

The building retrofitting and maintenance planning problems is inherently complex as they can involve multiple time scales and substantial magnitude. A retrofitting plan is usually evaluated on a large time scale, e.g., 10-15 years. However, the population and performances can manifest significant changes within 1-2 years depending on the type of the retrofitted items, e.g., the lights [109]. The performances of the retrofitted items are often evaluated within a short period, e.g., a few days even several hours. Furthermore, the population of the involved retrofitted items can be so large that it is very difficult and expensive to evaluate and control each individual item from the perspective of the decision makers. Therefore, a simplification method, namely grouping, is implemented in the previous optimisation models to address the above complexity. The retrofitted items are categorised into several homogeneous groups, where items from the same group are considered to be homogeneous ones that manifest the same energy and economy performances, furthermore, the homogeneous group population decreases in a manner consistent with the individual item reliability. The term 'reliability' is from the reliability engineering, which specifically refer to the ability of a system or component to perform its required functions under stated conditions for a specified period of time [140]. In this way, the overall performances can be evaluated by investigating the homogeneous group population and the performances of an individual homogeneous item. The grouping has been implemented in some other management level optimisation problems. Ye *et al.* [108] implements the grouping to figure out an optimal metering plan for a large number of lights to achieve the M&V accuracy cost-effectively.

However, grouping is an inherently subjective approach. Different decision makers can have different opinions on how to implement groupings. A question is thereby raised: How will different groupings influence the performances of the maintenance plan in a maintenance plan optimisation (MPO)? A kind of grouping based MPO problems are hereby employed as the basis of the discussion. The concept 'performance robustness' is hereby introduced to facilitate the evaluation of the impacts from applying different grouping. For the MPO, performance robustness refers to the ability that the control system output sustains when an alternative grouping is applied. More specifically, given a set of same retrofitted items and two different groups, if the results (performances) of an arbitrary maintenance plan based on one grouping remain accessible when the other grouping is applied, the performance robustness is satisfied, and the two groupings are considered equivalent. The satisfaction of the performance robustness provides the decision makers a method to evaluate alternative groupings.

This chapter presents a preliminary study on the robustness of grouping based maintenance plan optimisation in building retrofitting. A mathematical description of the grouping as well as the grouping based control system formulation is illustrated. Taking advantage of the open loop performances of a control system under full maintenance and no maintenance policy, a distance of performance is defined to evaluate the performances of alternative groupings. Thereafter, a distance of different groupings is defined within the scope of the retrofitting and maintenance planning (RMP) problems in the building energy retrofitting context. The distance of grouping provides a criterion to evaluate the similarity of two alternative groups. Based on the two distances, a theorem is proved to characterise the relationship of groupings and performances for the RMP problems. A theoretical characterisation of grouping robustness is given, and a case study is shown for the effectiveness of the characterisation.

7.2 MATHEMATICAL DESCRIPTION OF ITEM GROUPING

7.2.1 What is grouping

The general idea of item grouping is dividing the retrofitted items into several groups. For each group, instead of investigating the performances of each individual item, a representative item is selected from the group to indicate the average of the totality of the individual items. The individual items and the representative item are thereby considered homogeneous. The homogeneous items manifest same energy efficiency and reliability performances. In this way, the overall energy and reliability performances of the totality of the retrofitted items are evaluated by management level characteristics, i.e., the population of the homogeneous item group.

Let the information system $\mathbf{I} = \{\mathbb{U}, \mathbb{A}, \{V_a | a \in \mathbb{A}\}, \{M_a | a \in \mathbb{A}\}\}$ describe the totality of retrofitted items. These retrofitted items are assumed to be the same type of facilities, e.g., lights or air conditioners. This implies that the items can be described by a series of common properties. Let $\mathbb{U}$ denote a non-empty set of finite objects p, i.e., the retrofitted items of the same type. $\mathbb{A}$ is a non-empty finite set of attributes $a \in \mathbb{A}$ and V_a denotes the set of values that attribute a may take. $M_a(p)$ denotes a mapping that assign a value $a(p)$ from V_a to each attribute a and object p, i.e., $M_a(p) = a(p)$. Let $\doteq$ denote an equivalence relation between two objects. Given $i \neq j$, if $\forall a \in \mathbb{A}, a(p_i) = a(p_j)$, then $p_i \doteq p_j$, i.e., p_i and p_j are homogeneous objects.

Let $\mathbb{P}(\mathbb{U})$ denote a grouping method that divides $\mathbb{U}$ into several groups, and n the number of groups. $\mathbb{P}(\mathbb{U})$ results in the following n partitions:

$$\begin{Bmatrix} \mathbb{I}_1 \\ \vdots \\ \mathbb{I}_n \end{Bmatrix} = \begin{Bmatrix} \mathbb{U}_1, \mathbb{A}, \{V_a | a \in \mathbb{A}\}, \{\tilde{M}_a | a \in \mathbb{A}\}, \tilde{p}^1, m_1 \\ \vdots \\ \mathbb{U}_n, \mathbb{A}, \{V_a | a \in \mathbb{A}\}, \{\tilde{M}_a | a \in \mathbb{A}\}, \tilde{p}^n, m_n \end{Bmatrix}, \tag{7.1}$$

where $\mathbb{U}_i \cap \mathbb{U}_j = \varnothing$ with $i \neq j$, and $\mathbb{U}_1 \cup \mathbb{U}_2 \cup \ldots \cup \mathbb{U}_m = \mathbb{U}$. Let $\mathbb{U}_i = \{p^{i,1}, p^{i,2}, \ldots, p^{i,m_i}\}$ and $\tilde{x}^i$ denote the representative object for $\mathbb{U}_i$, m_i the number of the objects in $\mathbb{U}_i$. Let $M_a(\tilde{p}^i) = \tilde{a}^i$, $\tilde{a}^i \in V_a$. Given $k = 1, 2, \ldots, m_i$, $\tilde{M}_a(p^{i,k})$ denotes a new mapping that assigns $\tilde{a}^i$ to each attribute a and object $p^{i,k} \in \mathbb{U}_i$, i.e., $\tilde{M}_a(p^{i,k}) = \tilde{a}^i$. Let $\triangle a(p^{i,k}) = \|a(p^{i,k}) - \tilde{a}^i\|$ denote the deviation from $a(p^{i,k})$ to $\tilde{a}^i$, where $\|\cdot\|$ is defined to be a certain distance. $\tilde{a}^i$ is selected such that $\sum_{k=1}^{m_i} \triangle a(p^{i,k})$ is minimised. Let $\cong$ denote such a relation that the two objects are considered homogeneous under the grouping $\mathbb{P}(\mathbb{U})$. Given $k \neq l$, if $\forall a \in \mathbb{A}$, $\tilde{M}_a(p_k) = \tilde{M}_a(p_l)$, then $p_k \cong p_l$. According to the grouping method, $\tilde{M}_a(p^{i,k}) = \tilde{M}_a(\tilde{p}^i)$, i.e., all objects from the same partition $\mathbb{U}_i$ are considered homogeneous. However, there lacks a guarantee that $p_k \doteq p_l$ as $a(p_k)$ and $a(p_l)$ can be different. Additional uncertainty can be introduced when $\mathbb{P}(\mathbb{U})$ is applied to describe $\mathbb{U}$.

7.2.2 Grouping based control system modelling

As aforementioned, the grouping is applied to obtain the control system framework taking account of the population dynamics of the totality of the retrofitted items. The RMP is accordingly cast into an optimal control problem. The general idea of the control system and optimal control problem formulation is introduced in this section.

Given a grouping $\mathbb{P}(\mathbb{U})$ with n partitions, i.e., n groups of homogeneous retrofitted items. Let $\mathbf{x}(t_k) = \{x_1(t_k), x_2(t_k), ..., x_n(t_k)\}$ denote the respective populations for each group during sampling interval $[t_{k-1}, t_k)$, i.e., $\mathbf{x}(t_k)$ is the state variable. $\mathbf{x}_0 = \{x_1(t_0), x_2(t_0), ..., x_n(t_0)\}$ denotes the initial population as well as the maximum possible population. According to the common notation of control system, the notation 'x' now refers to the population instead of a single object of an information system I. The maintenance actions consist of two factors: the maintenance intensities and maintenance instants. The term 'maintenance intensities' indicates the count of the maintained devices during a maintenance action, and 'maintenance instants' indicates the time instant at which a maintenance action takes place. Let $\mathbf{u}(t_k) = \{u_1(t_k), u_2(t_k), ..., u_n(t_k)\}$ denote the maintenance intensities at maintenance instant t_k. Given the nature of the maintenance, $\mathbf{u}(t_k)$ can be considered as a kind of proportional feedback control, i.e., $u_i(t_k) = \omega_i(t_k)(x_i(t_0) - x_i(t_k))$, where $\omega_i(t_k)$ denotes a proportion between 0 and 1. A compact form of the control system can be obtained:

$$\begin{bmatrix} x_1(t_{k+1}) \\ \vdots \\ x_n(t_{k+1}) \end{bmatrix} = \begin{bmatrix} G_1(t, x_1(t_k), u_1(t_k)) \\ \vdots \\ G_n(t, x_n(t_k), u_n(t_k)) \end{bmatrix} + \begin{bmatrix} d_1(t_k) \\ \vdots \\ d_n(t_k) \end{bmatrix}, \tag{7.2}$$

where $G_i(t, x_i(t_k), u_i(t_k))$ denotes the population decay formulations for each homogeneous group. $G_i(t, x_i(t_k), u_i(t_k))$ can be obtained from various resources, e.g., a simplified linear assumption [121] or experimental data fitting [109], an extension of the equipment reliability function [140] or multi-state transition model [117]. Uncertainties can be resulted from complicated resources, e.g., sampling, measurement and modeling efforts. They are inevitable to all these models. $d_i(t_k)$ denotes a set of random variables that represents the impact of the uncertainties.

In the aforementioned RMP problems, several contradictory considerations that leads to conflicting objectives can be involved, e.g., maximising energy savings, minimising capital costs, maximising human comfort, etc. As a result, the control objective is formulated by a weighted sum approach to take into account multiple objectives in the control system framework. Assuming that s objectives are involved in the RMP problem. An optimal control problem for the RMP can be formulated as following: given the initial state $\mathbf{x}_0$, find the control law, i.e., the maintenance plan $\mathbf{u}|_{t_0}^{t_f}$ over a finite period $[t_0, t_f)$ to minimise the following performance index:

$$\begin{aligned} J(\mathbf{x}_0, \mathbf{u}|_{t_0}^{t_f}) \triangleq & \lambda_1 O_1(\mathbf{x}|_{t_0}^{t_f}, P_1(\mathbf{x}|_{t_0}^{t_f})) + \lambda_2 O_2(\mathbf{x}|_{t_0}^{t_f}, P_2(\mathbf{x}|_{t_0}^{t_f})) + \\ & \ldots + \lambda_s O_s(\mathbf{x}|_{t_0}^{t_f}, P_s(\mathbf{x}|_{t_0}^{t_f})), \end{aligned} \tag{7.3}$$

subjects to (7.2) and a series of constraints:

$$\begin{cases} \psi_j^i(\mathbf{x}(t_f)) \geq 0, \ j = 1, 2, \ldots, n_\psi^i, \\ \psi_j^e(\mathbf{x}(t_f)) = 0, \ j = 1, 2, \ldots, n_\psi^e, \\ \kappa_j^i(t, \mathbf{x}|_{t_0}^{t_f}, \mathbf{u}|_{t_0}^{t_f}) \geq 0, \ j = 1, 2, \ldots, n_\kappa^i, \\ \kappa_j^e(t, \mathbf{x}|_{t_0}^{t_f}, \mathbf{u}|_{t_0}^{t_f}) = 0, \ j = 1, 2, \ldots, n_\kappa^e, \\ \mathbf{u} \in [\mathbf{u}^L, \mathbf{u}^U], \end{cases} \tag{7.4}$$

where $\mathbf{x}|_{t_0}^{t_f} = \{\mathbf{x}(t_0), \mathbf{x}(t_1), \ldots, \mathbf{x}(t_f)\}$, $\mathbf{u}|_{t_0}^{t_f} = \{\mathbf{u}(t_0), \mathbf{u}(t_1), \ldots, \mathbf{u}(t_f)\}$, $O_1(\cdot), \ldots, O_s(\cdot)$ denote the objective functions for each single objective,$\lambda_1, \ldots, \lambda_n$ denote the corresponding weighting factors. $[\mathbf{u}^L, \mathbf{u}^U]$ denotes the boundary of the maintenance intensities $\mathbf{u}$. $P_1, \ldots, P_s \subseteq \mathbb{A}$ denote the corresponding attributes, e.g., the item energy savings that contribute to the overall energy efficiency, the cost savings that contribute to the overall economic performance, etc.

Taking advantage of the aforementioned grouping method, each single objective $O_i(\cdot)$ and the objective function (7.3) can be obtained from the group population $\mathbf{x}|_{t_0}^{t_f}$ and the representative object attributes $\tilde{a}^i$ subject to grouping $\mathbb{P}(\mathbb{U})$.

7.2.3 Performance evaluation between groupings

Given a grouping $\mathbb{P}(\mathbb{U})$, the performances of a maintenance plan $\mathbf{u}|_{t_0}^{t_f}$ can evaluated by the single objectives $O_1(\cdot), \ldots, O_s(\cdot)$ according to the objective function formulation (7.3). However, due to the dynamical nature of the RMP problem, i.e., the optimal control problem (7.2)-(7.4), the performance evaluation of different groupings is not that straightforward. Different groupings can result in different state variables and different boundary of the control variables. Furthermore, if two groupings have different number of partitions, the dimension of the state variables and control variables are different accordingly. As a result, it is infeasible to find a same maintenance plan to compare the performances of two groupings.

In the aforementioned existing studies, given a fixed set of pre-determined maintenance instants, namely maintenance time schedule, there are two kinds of baseline maintenance policy: the full maintenance policy and no maintenance policy [157]. The full maintenance policy indicates that all failed items are maintained at and only at each maintenance instant. The no maintenance policy indicates that none of the failed items are maintained at any instant. The full maintenance policy is intuitive and common in practice. The no maintenance policy can be applied to verify the population decay model. Both policies are feasible to an arbitrary grouping method.

Hypothesis 1 *Given that the full maintenance and no maintenance policies are often selected to be the baseline maintenance strategies, the performances from full maintenance and no maintenance policies are considered to be benchmark performances for the grouping robustness investigation. Given a totality of retrofitted item $\mathbb{U}$ and a corresponding RMP problem that is described by the optimal control problem* (7.2)-(7.4)*. Two alternative groupings $\mathbb{P}_1(\mathbb{U})$ and $\mathbb{P}_2(\mathbb{U})$ are applied to formulate the control systems in this RMP problem. Despite the number of partitions with the two groupings, i.e., the dimension of the control system, the full maintenance or no maintenance performances of the same RMP problem subject to the same maintenance time schedule can be compared to evaluate the performance distance between the two groupings.*

Taking advantage of Hypothesis 1 and the objective function formulation (7.3), the performance distance between two alternative groupings is accordingly defined:

Definition 1 *Given a totality of retrofitted items $\mathbb{U}$ and a corresponding grouping $\mathbb{P}(\mathbb{U})$. An RMP based optimal control problem is formulated subject to $\mathbb{U}$ and $\mathbb{P}(\mathbb{U})$ as* (7.2)-(7.4) *indicate. Let $O_i^F(\mathbb{P}(\mathbb{U}))$ denote the value of single objective i under grouping $\mathbb{P}(\mathbb{U})$ and the full maintenance policy, $O_i^0(\mathbb{P}(\mathbb{U}))$ denote the value of single objective i under the no maintenance policy. Given two alternative groupings $\mathbb{P}_1(\mathbb{U})$ and $\mathbb{P}_2(\mathbb{U})$, let $J(\mathbb{P}_1(\mathbb{U}))$ and $J(\mathbb{P}_2(\mathbb{U}))$ denote their respective performances under the same maintenance plan. The distance between $J(\mathbb{P}_1(\mathbb{U}))$ and $J(\mathbb{P}_2(\mathbb{U}))$ is formulated by the following equation:*

$$\begin{aligned} D_p(\mathbb{P}_1(\mathbb{U}),\mathbb{P}_2(\mathbb{U})) &\triangleq \|J(\mathbb{P}_1(\mathbb{U}))-J(\mathbb{P}_2(\mathbb{U}))\| \\ &= \sqrt{\frac{\sum_{i=1}^{s}\lambda_i(O_i^F(\mathbb{P}_1(\mathbb{U}))-O_i^F(\mathbb{P}_2(\mathbb{U})))^2}{\sum_{i=1}^{s}\lambda_i}}+\sqrt{\frac{\sum_{i=1}^{s}\lambda_i(O_i^0(\mathbb{P}_1(\mathbb{U}))-O_i^0(\mathbb{P}_2(\mathbb{U})))^2}{\sum_{i=1}^{s}\lambda_i}} \end{aligned} \tag{7.5}$$

In general, if $\|J(\mathbb{P}_1(\mathbb{U})) - J(\mathbb{P}_2(\mathbb{U}))\| < \varepsilon$, where ε is a small enough positive, it can be considered that the difference between the performance of the two alternative groupings is small, i.e., $\mathbb{P}_1(\mathbb{U})$ and $\mathbb{P}_2(\mathbb{U})$ result in very similar performances on the same RMP problem.

7.3 ROBUSTNESS OF GROUPING IN BUILDING RETROFITTING CONTEXT

In this section, the performance robustness of the grouping method is discussed based on a common formulation of RMP problems in the building retrofitting context. Such a formulation have been employed in most of the aforementioned studies. Before the discussion of the performance robustness, the RMP problem formulation is briefly introduced.

7.3.1 Population decay dynamics modelling

The population decay dynamics modelling is fundamental to the RMP problems. At the current stage, two population decay models are established for non-repairable items and repairable items. Generally, building energy appliance are categorised into reparable and non-reparable ones. A repairable appliance can have multiple minor failures and be repaired before becoming salvaged. Air conditioners, heat pumps or printers are repairable appliances. A non-repairable item can only experience one catastrophic failure before the salvage. A replacement is required to remove such failure. CFLs or motion sensors are non-repairable appliances. The failure rates of the repairable and non-repairable items are usually different. The population decay dynamics models investigated here are merely a small part of a broad field of the reliability engineering. There are many other available classifications in different scenarios, which remain uninvestigated, and consequently many other available models, corresponding to different categories of retrofitted items.

For the repairable items, an exponential degradation model is investigated to model the repairable failures in [140] and applied in the studies [157], as shown in (7.6),

$$x(t_k) = x(t_k)e^{-\zeta \triangle t}. \tag{7.6}$$

The state space form of (7.6) is

$$x(t_{k+1}) = x(t_k)(1 - \zeta \triangle t), \tag{7.7}$$

or in continuous time,

$$\dot{x} = -\zeta x,$$

where θ denotes the Mean Time between Failures (MTBF) of the retrofitted items, and ζ is calculated by:

$$\zeta = (\theta)^{-1}. \tag{7.8}$$

It is assumed that such retrofitted items have constant failure rate ζ.

For the non-repairable items, a lighting population decay dynamics that is obtained from experimental data fitting is employed [109]. A general form of the population decay dynamics model by re-calibrating existing models established from biological population dynamics study or from reliability engineering experiments [158] is proposed. The general form of the model is provided in (7.9):

$$x(t_k) = \frac{x_0}{\nu + \sigma e^{\mu t_k}}, \tag{7.9}$$

where $x(t)$ is the survived devices at time t_k for a lighting project, x_0 is the initial value, t_k is counted from the implementation of a lighting retrofit project. $\sigma = e^{-L}$, where L denotes the rated average life span of a certain model of the retrofitted item. The rated average life span is declared by the manufacturer or responsible vendor as being the expected time at which 50% of any large number of devices reach the end of their individual lives [121]. μ is the slope of decay and ν is the initial percentage lamp survival at $t = 0$. Thus, with a given L, ν and μ can be obtained by solving the following equations:

$$\begin{cases} x(t_0) = x_0, \\ x(L - t_0) = 0.5x_0, \end{cases} \tag{7.10}$$

a state space of (7.9) can thus be obtained:

$$x(t_{k+1}) = x(t_k) - \mu x(t_k)\triangle t + \mu\nu x(t_k)^2/x(t_0)\triangle t, \tag{7.11}$$

or in continuous time,

$$\dot{x} = \mu\nu x^2/x_0 - \mu x.$$

Models (7.6)- (7.11) indicate the system dynamics of the control system (7.2). For repairable items, the system dynamics is a linear one; for the non-repairable systems, the system dynamics is a quadratic one. Let $\triangle A$ denote the deviation of the system parameters, i.e., ζ in (7.7) or μ, ν in (7.11), $\triangle\mathbf{x}$ denote the deviation of the state trajectory. Obviously, for an RMP problem that is defined over a finite interval of time, given the same controller, if $\|\triangle A\| < \varepsilon$ where ε is a small enough positive, the control system with system dynamics (7.7) or (7.11) remains stable, and $\|\triangle\mathbf{x}\|$ remains small as well.

7.3.2 Objective function formulation

For a retrofitting project, the energy efficiency is evaluated by the energy savings against the baseline energy consumption. The energy savings cannot be directly measured, since they represent the absence of energy use. Instead, savings are determined by comparing measured use before and after implementation of a project, making appropriate adjustments for changes in conditions [67, 119]. The economic performance is evaluated by the net present value (NPV) or internal rate of return (IRR). The IRR is defined to be the discount rate at which the net present value of cash flows in a retrofitting project equal zero. The cash inflows mainly come from the cost savings corresponding to the energy savings, or the incentive policies, if applicable. The cash outflow comes from the retrofitting costs at the initial stage and the maintenance costs during operation. Obviously, IRR is a non-analytic indicator. In the previous chapters, IRR is commonly employed to be an objective. As a result, the evolutionary algorithm based numerical solver is widely employed in these relevant studies. The NPV is computed based on a discount rate that is pre-determined by the decision maker, it is analytic but more subjective than IRR. At the current stage, we assume that the objective function is analytic and smooth for the grouping robustness discussion, therefore, the NPV is employed to be one of the control objectives.

Taking advantage of a lighting retrofitting project as an example, where a number of lights in an office building are involved. The modelling of the RMP problem is generally employed from chapter 3. Given that a grouping $\mathbb{P}(\mathbb{U})$ results in n lighting groups. The sustainability period is $[0,TS)$. A series of sampling instants t_k with $k = 0,1,2,...,T$ are evenly distributed over $[0,TS)$ and S denotes the sampling interval. The state variable $\mathbf{x}(t_k)$, i.e., the item group population over $[t_{k-1},t_k)$ is represented by the following equation:

$$\mathbf{x}(t_k) = (x_1(t_k), x_2(t_k), ..., x_n(t_k))^T. \tag{7.12}$$

The maintenance intensities $\mathbf{u}(t_k)$ are accordingly represented by the following equation:

$$\mathbf{u}(t_k) = (u_1(t_k), u_2(t_k), ..., u_n(t_k))^T, \tag{7.13}$$

subject to the maintenance time schedule Q. $Q = \{k_1, k_2, ..., k_\tau\}$ indicates a collection of the maintenance instants. The elements of Q are selected from $k = 1,2,...,T$, i.e., the indices of the sampling instants. These maintenance instants are considered to be commensurate with the sampling instants t_k. According to the time schedule, $\mathbf{u}(t_k) = 0$ if $k \notin Q$.

The objectives are formulated as following:

$$\begin{cases} f_e(\mathbf{x},\mathbf{u}) = \dfrac{ES|_{all}}{\alpha}, \\ f_r(\mathbf{x},\mathbf{u}) = \dfrac{NPV}{h_0}, \end{cases} \tag{7.14}$$

where $f_e(\mathbf{x},\mathbf{u})$ is the energy performance objective and $f_r(\mathbf{x},\mathbf{u})$ is the economic performance objective. $ES|_{all}$ denotes the aggregate energy savings:

$$ES|_{all} = \sum_{k=1}^{T} ES(\mathbf{x}(t_k),t_k) = \sum_{k=1}^{T}\sum_{i=1}^{n} a_i(t_k)x_i(t_k), \tag{7.15}$$

where α is the targeted energy saving amount. $ES|_{all}$ is the overall energy savings subject to the maintenance plan over the sustainability period. $ES(\mathbf{x}(t_k),t_k)$ is the aggregate energy savings from the retrofitting project over interval $[t_{k-1},t_k)$, where $\mathbf{x}(t_k)$ is to emphasise the connection between the energy savings and the group population, i.e., the system state. $a_i(t_k)$ denotes the energy savings that one item from group i contributes over $[t_{k-1},t_k)$. The aggregate cost savings $CS|_{all}$ can be computed accordingly:

$$CS|_{all} = \sum_{k=1}^{T} B(\mathbf{x}(t_k),t_k) = \sum_{k=1}^{T}\sum_{i=1}^{n} b_i(t_k)x_i(t_k), \tag{7.16}$$

where $B(\mathbf{x}(t_k),t_k)$ denotes the aggregate cost savings, i.e., the cash inflow over $[t_{k-1},t_k)$. $b_i(t_k)$ denotes the energy savings that one item from group i contributes over $[t_{k-1},t_k)$. In order to calculate IRR, the cash outflow must be obtained as well. The cash outflow mainly consists of the maintenance costs:

$$h|_{all} = h_0 + \sum_{k=1}^{T} h(\mathbf{u}(t_{k-1}),t_k) = h_0 + \sum_{k=1}^{T}\sum_{i=1}^{n} c_i(t_k)u_i(t_{k-1}), \tag{7.17}$$

where $h|_{all}$ denotes the overall capital investments of the project. h_0 denotes the initial investment for the implementation of the retrofitting plan. $h(\mathbf{u}(t_{k-1}),t_k)$ denotes the aggregate maintenance costs over $[t_{k-1},t_k)$, where $\mathbf{u}(t_{k-1})$ is applied over the same interval. $c_i(t_k)$ denotes the maintenance cost over $[t_{k-1},t_k)$ to restore one failed item from group i to working state. $h(\mathbf{u}(t_{k-1}),t_k)$ is thereby the cash inflow over $[t_{k-1},t_k)$. The net present value (NPV) is computed taking advantage of the cash flows:

$$NPV = \sum_{k=1}^{T} \frac{B(\mathbf{x}(t_k),t_k) - h(\mathbf{u}(t_{k-1}),t_k)}{(1+d)^n} - h_0. \tag{7.18}$$

Taking advantage of the aforementioned performance indicators, the RMP optimal control problem is established by a weighted sum approach, where the multi-objective optimisation problem is translated into a minimisation problem. The objective function is a weighted sum of the objectives. In this way, the multi-objective problem is converted into a minimisation problem. The performance index is given in (7.19):

$$J = -\lambda_1 f_e(\mathbf{x},\mathbf{u}) - \lambda_2 f_r(\mathbf{x},\mathbf{u}) \tag{7.19}$$

subject to the system dynamics and the following constraints:

$$\begin{cases} \mathbf{x}(t_{k+1}) = \mathbf{G}(\mathbf{x}(t_k)) + \mathbf{u}(t_k), \\ ES|_{all} \geq \alpha, \\ \sum_{k=1}^{T} h(t_k) \leq \beta, \\ T_p \leq T', \\ \mathbf{u}(t_k) = 0,\ k \notin Q, \end{cases} \tag{7.20}$$

where λ_1, λ_2 are positive constants, i.e., the weighting factors. The constraints of the RMP problem include the system dynamics, targeted energy savings α, maintenance budget limit β, payback period limit T', and the pre-decided maintenance time schedule Q. T_p denotes the payback period of the project, which is the last instant where NPV remains negative. The RMP optimal control problem is then finding a maintenance plan $\mathbf{u}$ subject to pre-decided maintenance time schedule Q and the system dynamics to minimise the performance index (7.19). The technical details of the MPC controller design and corresponding numerical solver can be found in the previous chapters and the appendix.

7.3.3 Grouping robustness

Based on the above RMP problem in building retrofitting context, the criteria of the grouping robustness is hereby investigated. A few assumptions are made before the discussion:

1. Items that are from different types of EE devices cannot be categorised into one group, e.g., a heat pump and a CFL are distinguished to be two types, for they have different structure of the population decay models and different common properties, i.e., different types of items cannot be characterised by one information system.

2. Based on the above assumption, only the robustness of different groupings for a totality of the same type of retrofitted items is investigated. This suggests that different groupings mainly result in parameter deviations in the models, e.g., system dynamics (7.7), (7.11), and objective functions (7.14)-(7.19).

3. Only the performances without the disturbance in the control system are employed to be the grouping robustness criteria at the current stage.

The general idea of grouping robustness can be interpreted as following: if two alternative groupings are similar according to a certain criterion, the two groupings result in very similar performances on the same RMP problem under equivalent maintenance plan. The similarity of the performances is verified by the distance of performances in Definition 1.

The similarity of two alternative groupings is given by the following distance:

Definition 2 *Given two alternative groupings $\mathbb{P}_1(\mathbb{U})$ with n_1 partitions and $\mathbb{P}_2(\mathbb{U})$ with n_2 partitions. The representative objects from the two groupings are indicated by $\{\tilde{p}_1^i|i=1,2,...,n_1\}$ and $\{\tilde{p}_2^j|j=1,2,...,n_2\}$ respectively. m_1^i and m_2^j denote the number of items from each group respectively. Given the same totality $\mathbb{U}$, obviously, $\sum_{i=1}^{n_1} m_1^i = \sum_{j=1}^{n_2} m_2^i$. The two groupings can be described by the same information system and have a finite set of common properties $\mathbb{A}$ with the value space $\{V_a|a \in \mathbb{A}\}$. $\mathbb{A}$ and V_a comprise a metric space, namely $\bar{\mathbb{A}}$. $\{\tilde{p}_1^i\}$ and $\{\tilde{p}_2^j\}$ are considered to be two sets of mass points in metric space $\bar{\mathbb{A}}$. Let $\vec{r}_1^i$ denote the position vector for $\tilde{p}_1^i$ and $\vec{r}_2^j$ for $\tilde{p}_2^j$, and $\|\vec{r}_1^i - \vec{r}_2^j\|$ the distance between $\tilde{p}_1^i$ and $\tilde{p}_2^j$. Assuming that there are l attributes in $\mathbb{A}$, denoted by $\{a_1, a_2, ..., a_l\}$. Taking advantage of* (7.1)*, $\vec{r}_1^i$ and $\vec{r}_2^j$ are thereby defined by the following equation:*

$$\begin{aligned}\vec{r}_1^i &= \{\frac{\partial J(\mathbf{x}_1,\mathbf{u}_F)}{\partial a_1}\tilde{M}_{a_1}(p_1^i), \frac{\partial J(\mathbf{x}_1,\mathbf{u}_F)}{\partial a_2}\tilde{M}_{a_2}(p_1^i), ..., \frac{\partial J(\mathbf{x}_1,\mathbf{u}_F)}{\partial a_l}\tilde{M}_{a_l}(p_1^i)\} \\ \vec{r}_2^j &= \{\frac{\partial J(\mathbf{x}_2,\mathbf{u}_F)}{\partial a_1}\tilde{M}_{a_1}(p_2^j), \frac{\partial J(\mathbf{x}_2,\mathbf{u}_F)}{\partial a_2}\tilde{M}_{a_2}(p_2^j), ..., \frac{\partial J(\mathbf{x}_2,\mathbf{u}_F)}{\partial a_l}\tilde{M}_{a_l}(p_2^j)\},\end{aligned} \tag{7.21}$$

and the mass of such a point $\tilde{p}_1^i$ or $\tilde{p}_2^j$ is defined by the following equation:

$$\begin{aligned}\bar{m}_1^i &= m_1^i \frac{\partial J(\mathbf{x}_1,\mathbf{u}_F)}{\partial \mathbf{x}_1^i}, \\ \bar{m}_2^j &= m_2^j \frac{\partial J(\mathbf{x}_2,\mathbf{u}_F)}{\partial \mathbf{x}_2^j},\end{aligned} \tag{7.22}$$

where $\mathbf{x}_1$ and $\mathbf{x}_2$ denote the state trajectory under full maintenance policy $\mathbf{u}_F$. $\mathbf{x}_1^i$ and $\mathbf{x}_1^i$ denote the state trajectory of state variable x_1^i and x_2^j. $\tilde{M}_{a_k}(p_1^i)$ denotes the representative object p_1^i's value of attribute a_k. $\frac{\partial J(\mathbf{x}_1,\mathbf{u}_F)}{\partial a_k}$ hereby indicates the weights of this attribute. According to sensitivity analysis theory [159], attribute a_k is a more sensitive parameter if $\frac{\partial J(\mathbf{x}_1,\mathbf{u}_F)}{\partial a_k}$ is larger, i.e., attribute a_k is more important to objective function $J(\mathbf{x},\mathbf{u})$. Taking advantage of (7.21) *and* (7.22)*, let $\tilde{p}_{1,c}$ and $\tilde{p}_{2,c}$ denote the respective barycenter of the mass point sets $\{\tilde{p}_1^i\}$ and $\{\tilde{p}_2^j\}$, the position vectors of $\tilde{p}_{1,c}$ and $\tilde{p}_{2,c}$ can be computed by:*

$$\begin{aligned}\vec{r}_{1,c} &= \frac{\sum_{i=1}^{n_1} \bar{m}_1^i \vec{r}_1^i}{\sum_{i=1}^{n_1} \bar{m}_1^i}, \\ \vec{r}_{2,c} &= \frac{\sum_{j=1}^{n_2} \bar{m}_2^j \vec{r}_2^j}{\sum_{j=1}^{n_2} \bar{m}_2^j}.\end{aligned} \tag{7.23}$$

Let $\breve{d}_1^i$ denote the minimal distance between $\tilde{p}_1^i$ and all representative objects from $\mathbb{P}_2(\mathbb{U})$. Similarly, $\breve{d}_2^j$ denotes the minimal distance between $\tilde{p}_2^j$ and all representative objects from $\mathbb{P}_1(\mathbb{U})$, i.e.,

$$\begin{aligned} \breve{d}_1^i &= min\{\|\vec{r}_1^i - \vec{r}_2^j\|, j = 1,2,...,n_2\}, \\ \breve{d}_2^j &= min\{\|\vec{r}_2^j - \vec{r}_1^i\|, i = 1,2,...,n_1\}. \end{aligned} \tag{7.24}$$

Taking advantage of (7.22)-(7.24)*, the distance between $\mathbb{P}_1(\mathbb{U})$ and $\mathbb{P}_2(\mathbb{U})$ is defined as the following:*

$$\begin{aligned} D_u(\mathbb{P}_1(\mathbb{U}),\mathbb{P}_2(\mathbb{U})) &\triangleq \|\mathbb{P}_1(\mathbb{U}) - \mathbb{P}_2(\mathbb{U})\| \\ &= \|\vec{r}_{1,c} - \vec{r}_{2,c}\| + \frac{1}{n_1+n_2}(\sum_{i=1}^{n_1} \breve{d}_1^i + \sum_{j=1}^{n_2} \breve{d}_2^i). \end{aligned} \tag{7.25}$$

According to Definition 2, some properties can be more sensitive than the others subject to the form of the objective function. Such properties are referred to as the ‘important parameters’. For an RMP problem that is defined by the optimal control problem (7.2), (7.7), (7.11) and (7.12)-(7.20), the important parameters include the rated MTBF or life span L, the unit energy savings $a_i(t_k)$, the unit cost savings $b_i(t_k)$ and the maintenance cost $c_i(t_k)$. These parameters are computed from a series of data, e.g., the baseline consumptions, rated power, operating hour, labor cost, equipment price, energy price, etc. Some data are relatively irrelevant to the important parameters, e.g., the color of the device, the noise during operation, etc. The interplay between the data are complicated. In our previous studies, the important parameters have been extracted from the processed auditing data. Accordingly, the following discussion only employs the four important parameters to establish the information system.

Theorem 2 *For the RMP problem defined by* (7.2)*,* (7.7)*,* (7.11) *and* (7.12)-(7.20)*, given two alternative groupings $\mathbb{P}_1(\mathbb{U})$ and $\mathbb{P}_2(\mathbb{U})$. For any small $\varepsilon > 0$, $\exists \delta > 0$, if $\mathbb{P}_1(\mathbb{U})$ and $\mathbb{P}_2(\mathbb{U})$ are closed enough, i.e., $\|\mathbb{P}_1(\mathbb{U}) - \mathbb{P}_2(\mathbb{U})\| \leq \delta$, then they result in similar performances, i.e., $\|J(\mathbb{P}_1(\mathbb{U})) - J(\mathbb{P}_2(\mathbb{U}))\| < \varepsilon$.*

Proof.

1. $n_1 = n_2$:

Taking advantage of (7.14)-(7.19), according to the Taylor series, the deviation of the respective objectives between the two groupings can be converted as the following:

$$\begin{aligned}\triangle f_e^F &= f_e(\mathbf{x}_2^0, \mathbf{s}_{2,F}, \mathbf{a}_2) - f_e(\mathbf{x}_1^0, \mathbf{s}_{1,F}, \mathbf{a}_1) \\ &= f_e(\mathbf{x}_1^0 + \triangle\mathbf{x}_1^0, \mathbf{s}_{1,F} + \triangle\mathbf{s}_{1,F}, \mathbf{a}_1 + \triangle\mathbf{a}_1) - f_e(\mathbf{x}_1^0, \mathbf{s}_{1,F}, \mathbf{a}_1) \\ &= Jf_e(\mathbf{x}_1^0, \mathbf{s}_{1,F}, \mathbf{a}_1)h^T + \frac{1}{2}hHf_e(\mathbf{x}_1^0, \mathbf{s}_{1,F}, \mathbf{a}_1)h^T + R(f_e(\mathbf{x}_1^0, \mathbf{s}_{1,F}, \mathbf{a}_1)),\end{aligned} \tag{7.26}$$

where $h = (\triangle\mathbf{x}_1^0, \triangle\mathbf{s}_{1,F}, \triangle\mathbf{a}_1)$, Jf_e denotes the Jacobian matrix and Hf_e denotes the Hessian matrix. R denotes the remainder. $\mathbf{s}$ denotes the percentage survival rate of the retrofitted items, where $\mathbf{x} = \mathbf{x}_0\mathbf{s}$. $\mathbf{s}_{1,F}$ thus denotes the open loop percentage survival rate under full maintenance strategy. Similarly,

$$\begin{aligned}\triangle f_e^0 &= Jf_e(\mathbf{x}_1^0, \mathbf{s}_{1,0}, \mathbf{a}_1)h^T + \frac{1}{2}hHf_e(\mathbf{x}_1^0, \mathbf{s}_{1,0}, \mathbf{a}_1)h^T + R(f_e(\mathbf{x}_1^0, \mathbf{s}_{1,0}, \mathbf{a}_1)), \\ \triangle f_r^F &= Jf_r(\mathbf{x}_1^0, \mathbf{s}_{1,F}, \mathbf{a}_1)h^T + \frac{1}{2}hHf_r(\mathbf{x}_1^0, \mathbf{s}_{1,F}, \mathbf{a}_1)h^T + R(f_r(\mathbf{x}_1^0, \mathbf{s}_{1,F}, \mathbf{a}_1)), \\ \triangle f_r^0 &= Jf_r(\mathbf{x}_1^0, \mathbf{s}_{1,0}, \mathbf{a}_1)h^T + \frac{1}{2}hHf_r(\mathbf{x}_1^0, \mathbf{s}_{1,0}, \mathbf{a}_1)h^T + R(f_r(\mathbf{x}_1^0, \mathbf{s}_{1,0}, \mathbf{a}_1)).\end{aligned} \tag{7.27}$$

Generally, it is assumed that the Jacobian and Hessian matrices exist and bounded for the RMP problem. Given that the RMP problem is bounded by nature, and (7.19) is a simple linear combination of the state variables, the assumption applies to the investigated RMP problems. From the above equations and Definition 2, the performance distance is a function of the parameter deviations in initial population $\mathbf{x}^0$, survival rate $\mathbf{s}_F$ or $\mathbf{s}_0$, and model parameters $\mathbf{a}$, therefore the vector of deviations h is the focus of grouping robustness investigation. Given that:

$$\|J(\mathbb{P}_1(\mathbb{U})) - J(\mathbb{P}_2(\mathbb{U}))\| = \sqrt{\frac{\lambda_1 \triangle f_e^{F\,2} + \lambda_2 \triangle f_r^{F\,2}}{\lambda_1 + \lambda_2}} + \sqrt{\frac{\lambda_1 \triangle f_e^{0\,2} + \lambda_2 \triangle f_r^{0\,2}}{\lambda_1 + \lambda_2}}. \tag{7.28}$$

Obviously, for any small $\varepsilon > 0$, if $|\triangle f_e^F| < \frac{1}{2}\varepsilon$, $|\triangle f_e^0| < \frac{1}{2}\varepsilon$, $|\triangle f_r^F| < \frac{1}{2}\varepsilon$ and $|\triangle f_r^0| < \frac{1}{2}\varepsilon$, $\|J(\mathbb{P}_1(\mathbb{U})) - J(\mathbb{P}_2(\mathbb{U}))\| < \varepsilon$.

From (7.26), given that $\frac{1}{2}hHf_e(\mathbf{x}_1^0, \mathbf{s}_{1,F}, \mathbf{a}_1)h^T$ is positive and the remainder $R(f_e(\mathbf{x}_1^0, \mathbf{s}_{1,F}, \mathbf{a}_1))$ is trivial, obviously, $|Jf_e(\mathbf{x}_1^0, \mathbf{s}_{1,F}, \mathbf{a}_1)h^T| < \frac{1}{2}\varepsilon$, therefore, $|h| < \frac{\varepsilon}{2|Jf_e(\mathbf{x}_1^0, \mathbf{s}_{1,F}, \mathbf{a}_1)|}$. Similarly, from (7.27), $|h| < \frac{\varepsilon}{2|Jf_e(\mathbf{x}_1^0, \mathbf{s}_{1,0}, \mathbf{a}_1)|}$, $|h| < \frac{\varepsilon}{2|Jf_r(\mathbf{x}_1^0, \mathbf{s}_{1,F}, \mathbf{a}_1)|}$, $|h| < \frac{\varepsilon}{2|Jf_r(\mathbf{x}_1^0, \mathbf{s}_{1,0}, \mathbf{a}_1)|}$. Let δ' denote the smallest one of the right part of the above inequalities. As a result, $|h| < \delta'$, thus $|\triangle\mathbf{x}_1^0| < \delta'$, $|\triangle\mathbf{s}_{1,F}| < \delta'$ and $|\triangle\mathbf{a}_1| < \delta'$.

According to robust control theory [160, 161], for system dynamics (7.7) and (7.11), it can be considered that $|\triangle L| < f(\eta)$ if $|\triangle\mathbf{s}_{1,F}| < \eta$, where $f(\eta)$ is a bounded function and $\lim_{\eta\to 0} f(\eta) = 0$. With $|\triangle\mathbf{s}_{1,F}| < \delta'$, $|\triangle L| < f(\delta')$, and with $|\triangle\mathbf{a}_1| < \delta'$, it is easy to figure out that $|\frac{1}{n_1+n_2}(\sum_{i=1}^{n_1}\check{d}_1^i + \sum_{j=1}^{n_2}\check{d}_2^i)| < f(\delta') + \delta'$. Furthermore,

$|\triangle \mathbf{x}_1^0| < \delta'$, i.e., $\forall i$, $\exists j$ such that $\|m_1^i - m_2^j\| < \delta'$. According to Definition 2, obviously, $\|\vec{r}_{1,c} - \vec{r}_{2,c}\| = \|\frac{\sum_{i=1}^{n_1} \bar{m}_1^i \vec{r}_1^i - \sum_{j=1}^{n_2} \bar{m}_2^j \vec{r}_2^j}{\sum_{i=1}^{n_1} m_1^i}\| < n_1\delta'$. Therefore, $\|\mathbb{P}_1(\mathbb{U}) - \mathbb{P}_2(\mathbb{U})\| = \|\vec{r}_{1,c} - \vec{r}_{2,c}\| + \frac{1}{n_1+n_2}(\sum_{i=1}^{n_1} \breve{d}_1^i + \sum_{j=1}^{n_2} \breve{d}_2^i) < f(\delta') + \delta' + n_1\delta'$, i.e., $\forall \varepsilon > 0$, $\exists \delta = f(\delta') + \delta' + n_1\delta'$, if $\|\mathbb{P}_1(\mathbb{U}) - \mathbb{P}_2(\mathbb{U})\| \leq \delta$, then $\|J(\mathbb{P}_1(\mathbb{U})) - J(\mathbb{P}_2(\mathbb{U}))\| < \varepsilon$.

2. $n_1 \neq n_2$:

Taking advantage of (7.2), (7.7), (7.11) and (7.12)-(7.20), for a group of homogeneous item x with the initial population x_0, it can be divided into l subgroups x_i with the initial population x_0^i, $x_0 = \sum_{i=1}^{l} x_0^i$. Each x_i consists of the same homogeneous items as x. The performances f_e^F, f_r^F, f_e^0 and f_r^0 of group x can thus be rewritten into a linear combination of the performances of subgroups x_i:

$$\begin{aligned}
f_e^F(x, u_F) &= \sum_{k=1}^{T} a(t_k) x^F(t_k) = x_0 \sum_{k=1}^{T} a(t_k) s^F(t_k) \\
&= (\sum_{i=1}^{l} x_0^i) \sum_{k=1}^{T} a(t_k) s^F(t_k) = \sum_{i=1}^{l} f_e^F(x_i, u_F) \\
f_r^F(x, u_F) &= \frac{1}{(1+d)^n} \sum_{k=1}^{T} (b(t_k) x^F(t_k) - c(t_k) u^F(t_k)) = \frac{x_0}{(1+d)^n} \sum_{k=1}^{T} (b(t_k) s^F(t_k) - c(t_k) \omega^F(t_k)) \\
&= \frac{\sum_{i=1}^{l} x_0^i}{(1+d)^n} \sum_{k=1}^{T} (b(t_k) s^F(t_k) - c(t_k) \omega^F(t_k)) = \sum_{i=1}^{l} f_r^F(x_i, u_F).
\end{aligned} \tag{7.29}$$

Similarly,

$$\begin{aligned}
f_e^0(x, u_0) &= \sum_{i=1}^{n} f_e^0(x^i, u_0) \\
f_r^0(x, u_0) &= \sum_{i=1}^{n} f_r^0(x^i, u_0).
\end{aligned} \tag{7.30}$$

As a result, x and the summation of x_i can be considered as equivalent groupings.

Assuming that $n_1 < n_2$. Some groups from $\mathbb{P}_1(\mathbb{U})$ can be further divided into several subgroups, each consists of the same homogeneous items. According to above discussion, such a dividing results in the same performances as the old grouping $\mathbb{P}_1(\mathbb{U})$. Given that $\mathbb{P}_1(\mathbb{U})$ is further divided into n_2 groups in this way, i.e., a new grouping $\mathbb{P}_1'(\mathbb{U})$ with n_2 partitions is obtained. Obviously, $\|\mathbb{P}_1(\mathbb{U}) - \mathbb{P}_1'(\mathbb{U})\| = 0$, $\|J(\mathbb{P}_1(\mathbb{U})) - J(\mathbb{P}_1'(\mathbb{U}))\| = 0$.

Given that both $\mathbb{P}_2(\mathbb{U})$ and $\mathbb{P}'_1(\mathbb{U})$ has n_2 partitions, taking advantage of proof 1, $\forall\varepsilon > 0$, $\exists\delta > 0$ such that if $\|\mathbb{P}'_1(\mathbb{U}) - \mathbb{P}_2(\mathbb{U})\| < \delta$, $\|J(\mathbb{P}'_1(\mathbb{U})) - J(\mathbb{P}_2(\mathbb{U}))\| < \varepsilon$. $\|\mathbb{P}_1(\mathbb{U}) - \mathbb{P}'_1(\mathbb{U})\| = 0$, therefore, $\|\mathbb{P}_1(\mathbb{U}) - \mathbb{P}_2(\mathbb{U})\| < \delta$; $\|J(\mathbb{P}_1(\mathbb{U})) - J(\mathbb{P}'_1(\mathbb{U}))\| = 0$, therefore $\|J(\mathbb{P}_1(\mathbb{U})) - J(\mathbb{P}_2(\mathbb{U}))\| < \varepsilon$, i.e., $\forall\varepsilon > 0$, $\exists\delta > 0$ such that if $\|\mathbb{P}_1(\mathbb{U}) - \mathbb{P}_2(\mathbb{U})\| < \delta$, $\|J(\mathbb{P}_1(\mathbb{U})) - J(\mathbb{P}_2(\mathbb{U}))\| < \varepsilon$.

□

7.3.4 Case study

A case study is illustrated to investigate the utilisation of Definition 2 in projects. There are totally 3000 compact fluorescent lights (CFLs) in this project. There are five different groupings for the 3000 CFLs, as Table 7.1 indicates. The illustrative parameters in Table 7.1 are the average of the items of each subgroup. Due to the different operating environment and occupant behaviors, some performance characteristics of the lights can be different, e.g., the energy savings, cost savings and lifespan (given in years). The energy savings and cost savings are the annual averages. The unit price indicates the average cost of purchasing and installing one CFL. The maintenance cost indicates the cost of applying corrective maintenance, i.e., the replacement to one failed CFL.

In accordance with the groupings, there are five different grouping based system dynamics, each corresponding to a same collection of CFLs. The five state space formulations are illustrated in Table

Table 7.1. Five different groupings for a lighting retrofitting project

Groupings	Quantities	Unit Price ($)	Unit Energy Saving (kWh)	Unit Cost Saving ($)	Maintenance Cost ($)	Lifespan (MTTF)
Grouping I 1	1910	14	99.5	11.28	14	1.67
Grouping I 2	1090	22	205	23.9	22	1.5
Grouping II 1	1830	13.8	99	11.2	13.8	1.67
Grouping II 2	1200	21.5	199.7	22.75	21.5	1.51
Grouping III 1	1570	14.2	101.5	11.7	14.2	1.69
Grouping III 2	1430	19.7	178.6	20.8	19.7	1.55
Grouping IV 1	1910	14	99.5	11.28	14	1.67
Grouping IV 2	570	22.1	204	23.8	22.1	1.49
Grouping IV 3	520	21.9	205.9	24.02	21.9	1.52
Grouping V 1	3000	17	127.5	13.1	17	1.61

Table 7.2. System dynamics of different grouping methods

Grouping	System dynamics formulations	model parameters
I	$x_1(t_{k+1}) = x_1(t_k) - \mu_1 x_1(t_k) + \mu_1 \nu_1 x_1^2(t_k)/x_1(t_0) + u_1(t_k), x_1(t_0) = 1910,$	$\mu_1 = 1.1033, \nu_1 = 0.8118$
	$x_2(t_{k+1}) = x_2(t_k) - \mu_2 x_2(t_k) + \mu_2 \nu_2 x_2^2(t_k)/x_2(t_0) + u_2(t_k), x_2(t_0) = 1090,$	$\mu_2 = 1.1343, \nu_2 = 0.7769$
II	$x_1(t_{k+1}) = x_1(t_k) - \mu_1 x_1(t_k) + \mu_1 \nu_1 x_1^2(t_k)/x_1(t_0) + u_1(t_k), x_1(t_0) = 1830,$	$\mu_1 = 1.1033, \nu_1 = 0.8117$
	$x_2(t_{k+1}) = x_2(t_k) - \mu_2 x_2(t_k) + \mu_2 \nu_2 x_2^2(t_k)/x_2(t_0) + u_2(t_k), x_2(t_0) = 1200,$	$\mu_2 = 1.1322, \nu_2 = 0.7791$
III	$x_1(t_{k+1}) = x_1(t_k) - \mu_1 x_1(t_k) + \mu_1 \nu_1 x_1^2(t_k)/x_1(t_0) + u_1(t_k), x_1(t_0) = 1570,$	$\mu_1 = 1.1002, \nu_1 = 0.8155$
	$x_2(t_{k+1}) = x_2(t_k) - \mu_2 x_2(t_k) + \mu_2 \nu_2 x_2^2(t_k)/x_2(t_0) + u_2(t_k), x_2(t_0) = 1430,$	$\mu_2 = 1.1242, \nu_2 = 0.7877$
IV	$x_1(t_{k+1}) = x_1(t_k) - \mu_1 x_1(t_k) + \mu_1 \nu_1 x_1^2(t_k)/x_1(t_0) + u_1(t_k), x_1(t_0) = 1910,$	$\mu_1 = 1.0328, \nu_1 = 0.8117$
	$x_2(t_{k+1}) = x_2(t_k) - \mu_2 x_2(t_k) + \mu_2 \nu_2 x_2^2(t_k)/x_2(t_0) + u_2(t_k), x_2(t_0) = 570,$	$\mu_2 = 1.1364, \nu_2 = 0.7746$
	$x_3(t_{k+1}) = x_3(t_k) - \mu_3 x_3(t_k) + \mu_3 \nu_3 x_3^2(t_k)/x_3(t_0) + u_3(t_k), x_3(t_0) = 520,$	$\mu_3 = 1.1301, \nu_3 = 0.7813$
V	$x_1(t_{k+1}) = x_1(t_k) - \mu_1 x_1(t_k) + \mu_1 \nu_1 x_1^2(t_k)/x_1(t_0) + u_1(t_k), x_1(t_0) = 3000,$	$\mu_1 = 1.1223, \nu_1 = 0.7899$

7.2. Such a state space model employs the population decay of a lamp group that is governed by a statistical law. The statistical law is obtained from the experimental data fitting [109]. The model parameters are identified as introduced in chapter 2.

Taking advantage of (7.12)-(7.20), the corresponding RMP problem subject to the system dynamics in Table 7.2 is established. The sustainability is 10 years. The sampling interval is one month, i.e., the time period between t_{k+1} and t_k is one month. Thereafter, a finite decision horizon $k = \{0, 1, 2, ..., 120\}$ is obtained. The targeted energy saving is 2,139,148 kWh, the budget limit is \$150,000. The payback period limit is 2 years. The weighting factors $\lambda_1 = 0.5$, $\lambda_2 = 0.5$. The maintenance actions are

Table 7.3. Performances of different groupings

Groupings	Cases	Energy savings (kWh)	Percentage saved (f_e)	NPV ($)	Payback ratio (f_r)	Payback period (years)	Maintenance cost ($)	Total investment ($)
Grouping I	Full M	3565246.65	166.67%	132726.88	261.69%	2.02	148060	198780
	No M	742134.67	34.69%	28851.48	56.88%	1.42	0	50720
Grouping II	Full M	3628951.41	169.64%	132983.3	260.48%	2.03	149073	200127
	No M	755576.22	35.32%	28920.06	56.65%	1.42	0	51054
Grouping III	Full M	3591316.04	167.89%	139893.52	277.21%	1.93	144460	194925
	No M	754750.77	35.28%	31044.26	61.52%	1.37	0	50465
Grouping IV	Full M	3565773.24	166.69%	133007.1	262.21%	2.02	147861	198586
	No M	742832.98	34.73	28945.88	57.06%	1.41	0	50725
Grouping V	Full M	3316338.75	155.03%	85321.66	167.3%	2.83	145860	196860
	No M	698450.1	32.65%	15805.12	30.99%	1.86	0	51000

scheduled to take place at the end of each year during the sustainability period. Therefore, the maintenance time schedule $Q = \{11, 23, ..., 119\}$, i.e., when $k \neq 11, 23, ..., 119$, $u_i(t_k) = 0$.

The performances of the five different groupings are given in Table 7.3. The percentage savings and payback ratios indicate the value of objective functions (7.14) under full maintenance and no maintenance policies. Thereafter, the distance of groupings D_p and distances of performances D_u are illustrated in Table 7.4, where D_p and D_u are computed according to (7.5) and (7.25). From 7.4, generally, $D_p \propto D_u$ when D_u is small.

From Table 7.3, it is very possible that two groupings result in significantly different performances. The differences among the groupings I-IV are relatively small. Considering grouping I as the baseline, grouping II manifests 1.8% more energy savings, and 0.2% more NPV; grouping III manifests 0.7% more savings and 5.4% more NPV; grouping IV manifests 0.012% more savings and 0.21% more NPV. From grouping V, 7% less savings and 35.7% less NPV are resulted. The difference between grouping I and V are much more significant than the differences between other pairs. From Table 7.4, the distances from grouping I to other groupings are much larger than the distances between other pairs: the distances are generally proportional to the differences of performances. This indicates the effectiveness of theorem 2. Furthermore, the relationship between performances and distances reveal a fact that the difference groupings can cause significant and reasonable differences in the optimization performances. It is important to compare the performances carefully.

Table 7.4. Distances between different groupings

Groupings	Distances	To I	To II	To III	To IV	To V
From I	D_p	N/A	0.0388	0.2025	0.007	1.2108
	D_u	N/A	3.4862	22.2062	1.0593	74.889
From II	D_p	0.0388	N/A	0.2169	0.0414	1.2012
	D_u	3.4862	N/A	19.4646	4.1411	73.1244
From III	D_p	0.2025	0.2169	N/A	0.1954	1.413
	D_u	22.2062	19.4646	N/A	24.9317	56.8762
From IV	D_p	0.007	0.0414	0.1954	N/A	1.2178
	D_u	1.0593	4.1411	24.9317	N/A	83.7064
From V	D_p	1.2108	1.2012	1.413	1.2178	N/A
	D_u	74.889	73.1244	56.8762	83.7064	N/A

7.4 CONCLUSION

This chapter aims at answering the following question: how does the grouping influence the output of a grouping based optimisation problem? The purpose of the study is to figure out a kind of groupings that allow the robustness of the outputs of maintenance plan optimisation in building retrofitting. According to the definitions, a grouping contributes a set of representative items, each corresponds to one homogeneous group, and the overall performances of the RMP can be obtained by the group population and the representative item attributes. Given the optimal control problem formulation of RMP, alternative groupings can result in the variation of representative item attributes. This results in a change in the performances of the grouping based control systems. In order to characterise such a change, a distance of performances is proposed based on the open loop performances under full maintenance and no maintenance strategies. Thereafter, a distance of two alternative groupings is further identified to characterise the similarity of the groupings. Taking advantage of the two distances, a theorem is proved that if two alternative groupings are similar according to a certain criterion, the two groupings result in very similar performances on the same RMP problem under equivalent maintenance plan. By computing the distances between two groupings, it is possible to verify the similarity of their performances. A case study illustrates the utilisation of the criterion.

CHAPTER 8 CONCLUSION AND FUTURE WORKS

The dissertation proposes a control system framework to facilitate the investment decision for building energy retrofitting and maintenance planning. The long-term energy and economy performances of a retrofitting project manifest significant dynamics due to the joint effects of the retrofitted item failures and maintenance actions. A basic form of the control system framework is proposed. Thereafter, this basic framework is improved by taking into account the effects of a series of different maintenance actions.

8.1 CONCLUSIONS

The established retrofitting plan optimisation model identifies and takes advantage of the system dynamics at the planning level. The planning level dynamics results from the impacts of the failures of retrofitted items and the corresponding maintenance. According to M&V principles, failed items contribute zero energy savings, as a result, the aggregate energy savings in a retrofitting project vary over time subject to the failures and maintenance of the retrofitted items. Due to the different specifications of the interventions, some retrofit options appear to be energy efficient at the initial stage but are actually expensive if taking into account the lost energy savings and maintenance costs. Therefore, the proposed retrofitting plan optimisation model employs the life cycle cost analysis to evaluate the long-term energy and economy performances of the interventions.

The planning level dynamics brings in the maintenance planning problem. According to the life cycle cost analysis for the interventions, the aggregate energy and economy performances of a retrofitting project can be further improved by optimising the maintenance plan. A grouping method is employed to establish the maintenance plan optimisation model, where retrofitted items are categorised into several groups that items from the same group are considered to be homogeneous ones. The population dynamics for each item group can be optimised to achieve desired performances over a specific time period. The maintenance intensities, i.e., the count of maintained items at a specific time instant, namely the maintenance instant, are selected to be the decision variables. Given that the maintenance intensities at latter maintenance instants depend on the effects of the maintenance intensities at the former maintenance instants, the maintenance plan optimisation problem is identified to be a dynamic programming problem. Thereafter, a control system modelling can be obtained for the planning level dynamics, which allows the implementation of control system approaches, e.g., the model predictive control (MPC). A subproblem of the maintenance planning, namely building retrofitting corrective maintenance planning, is employed to facilitate the derivation of the control system formulation. The population of the item groups are selected to be the state variables. The maintenance intensities subject to pre-decided maintenance time schedule are selected to be the control variables. In the case study, the optimal maintenance plan results in around 93% of the full maintenance savings and only consume a very limited maintenance budget, around 69% of the full maintenance strategy.

Thereafter, a series of studies have been conducted to extend the selective state variables and control inputs. The interacting energy and reliability effects are introduced to develop the corrective maintenance plan optimisation model into an optimal control problem with coupled state variables. Further energy savings and financial benefits can be lost if the interacting effects are omitted. In the investigated case study, it is possible to reach up to 8.9% of the energy saving and up to 9.6% of the IRR can be improved against the without interaction strategies. Furthermore, the performance deterioration can take place during operation before the malfunctions. Such deterioration is taken into account via a multi-state system approach. The effects of preventive maintenance can also be incorporated into the multi-state system dynamics. The preventive maintenance intensities are selected to be the control inputs apart from the corrective maintenance, subject to pre-decided preventive and corrective maintenance time schedules. The preventive maintenance can contribute further savings when there is performance deterioration. The maintenance time schedule optimisation can also be taken into account to extend the control variables. The collaborative optimisation of the maintenance intensities and instants manifest significant energy saving potential in comparison with the fixed time schedule subject to the budget limit. In the investigated case study, up to 20.8% of the IRR and up to 6.9% of the NPV can be improved against the fixed maintenance time schedule under the same budget limit with relaxed payback period limit. When tight payback period limit is applied, up to 3.36% of the energy savings and up to 23.09% of the IRR can be improved.

The grouping method is a necessary simplification to allow the selection of state variables and control inputs. The robustness of the grouping method thereby becomes a problem due to the possible opinions from decision makers on the way of grouping. In the last part of the dissertation, a mathematical description of the grouping is illustrated for the grouping based control system framework. Taking advantage of the open loop performances of a control system under full maintenance and no maintenance policy, a distance of performance is defined to evaluate the performances of alternative groupings. Thereafter, a distance of different groupings is defined within the scope of the retrofitting and maintenance planning problems in the building energy retrofitting context. The distance of grouping provides a criterion to evaluate the similarity of two alternative groups. Based on the two distances, a theorem is proved to characterise the relationship of groupings and performances for the maintenance planning problems. A theoretical characterisation of grouping robustness is given, and a case study is shown for the effectiveness of the characterisation.

8.2 FUTURE WORKS

A new perspective to facilitate the building energy efficiency at the planning level has been proposed in this dissertation. There are many promising research topics under the scope of retrofitting and maintenance planning. Firstly, there is huge potential to improve the population decay model. The adopted population decay models are mainly statistical laws, which are quite inaccurate. Furthermore, the parameter identifications are also necessary in practice. Secondly, the control system modelling requires further exploration. There are actually many possible plans to select the state variables and control inputs, each facilitate the implementation of our optimisation model in practice. The theoretical study are also required to guarantee the performances of the control system. Thereafter, the enormous methodologies from the control science can be employed to facilitate the building energy optimisation at planning level. Finally, the uncertainty factors imply a broad field to be incorporated into the planning level dynamical system. At the current stage, the uncertainty factors are addressed in a very general way. Actually, some of the uncertainty factors can be identified to be part of the decision variables, e.g., the emergency maintenance. Some can be address by feed-forward or robust control mechanism. There are many promising technologies to employ for the uncertainty factors.

In summary, the study in this dissertation calls for considerable future studies to bring systematic approaches from other fields to the building energy efficiency.

REFERENCES

[1] H. Khatib, "IEA world energy outlook 2011: a comment," *Energy Policy*, vol. 48, pp. 737–743, 2012.

[2] X. Xia, J. Zhang, and W. Cass, "Energy management of commercial buildings - a case study from a POET perspective of energy efficiency," *Journal of Energy in Southern Africa*, vol. 23, no. 1, pp. 23–31, 2012.

[3] S. M. Sichilalu and X. Xia, "Optimal energy control of grid tied pv–diesel–battery hybrid system powering heat pump water heater," *Solar Energy*, vol. 115, pp. 243–254, 2015.

[4] H. Tazvinga, B. Zhu, and X. Xia, "Energy dispatch strategy for a photovoltaic–wind–diesel–battery hybrid power system," *Solar Energy*, vol. 108, pp. 412–420, 2014.

[5] B. Nykvist and M. Nilsson, "Rapidly falling costs of battery packs for electric vehicles," *Nature Climate Change*, vol. 5, no. 4, pp. 329–332, 2015.

[6] O. Sezgen and J. G. Koomey, "Interactions between lighting and space conditioning energy use in us commercial buildings," *Energy*, vol. 25, no. 8, pp. 793–805, 2000.

[7] Y. Zhang and H. Altan, "A comparison of the occupant comfort in a conventional high-rise office block and a contemporary environmentally-concerned building," *Building and Environment*, vol. 46, no. 2, pp. 535–545, 2011.

[8] S. Mekhilef, A. Safari, W. Mustaffa, R. Saidur, R. Omar, and M. Younis, "Solar energy in

malaysia: current state and prospects," *Renewable and Sustainable Energy Reviews*, vol. 16, no. 1, pp. 386–396, 2012.

[9] T. S. Bisoniya, A. Kumar, and P. Baredar, "Experimental and analytical studies of earth–air heat exchanger (eahe) systems in india: a review," *Renewable and Sustainable Energy Reviews*, vol. 19, pp. 238–246, 2013.

[10] I. G. Capeluto, "Energy performance of the self-shading building envelope," *Energy and buildings*, vol. 35, no. 3, pp. 327–336, 2003.

[11] D. Tuhus-Dubrow and M. Krarti, "Genetic-algorithm based approach to optimize building envelope design for residential buildings," *Building and environment*, vol. 45, no. 7, pp. 1574–1581, 2010.

[12] S. B. Sadineni, S. Madala, and R. F. Boehm, "Passive building energy savings: A review of building envelope components," *Renewable and Sustainable Energy Reviews*, vol. 15, no. 8, pp. 3617–3631, 2011.

[13] B. Kyle, M. A. Lacasse, S. M. Cornick, D. Richard, K. Abdulghani, and T. Hilly, "A gis-based framework for the evaluation of building façade performance and maintenance prioritization," in *11th International Conference on Durability of Building Materials and Components, Istanbul, Turkey*, 11 May, 2008.

[14] B. Resch, G. Sagl, T. Törnros, A. Bachmaier, J.-B. Eggers, S. Herkel, S. Narmsara, and H. Gündra, "Gis-based planning and modeling for renewable energy: Challenges and future research avenues," *ISPRS International Journal of Geo-Information*, vol. 3, no. 2, pp. 662–692, 2014.

[15] P. Waide, S. Tanishima *et al.*, *Light's Labour's Lost: Policies for Energy-efficient Lighting*. OECD/IEA, Paris, 2006.

[16] T. Mahlia, M. Said, H. Masjuki, and M. Tamjis, "Cost-benefit analysis and emission reduction of lighting retrofits in residential sector," *Energy and Buildings*, vol. 37, no. 6, pp. 573–578,

2005.

[17] P. Rousseau and G. Greyvenstein, "Enhancing the impact of heat pump water heaters in the south african commercial sector," *Energy*, vol. 25, no. 1, pp. 51–70, 2000.

[18] J.-L. Lin and T.-J. Yeh, "Modeling, identification and control of air-conditioning systems," *International Journal of Refrigeration*, vol. 30, no. 2, pp. 209–220, 2007.

[19] Z. Ma and S. Wang, "Energy efficient control of variable speed pumps in complex building central air-conditioning systems," *Energy and Buildings*, vol. 41, no. 2, pp. 197–205, 2009.

[20] K. Zhao, X.-H. Liu, T. Zhang, and Y. Jiang, "Performance of temperature and humidity independent control air-conditioning system in an office building," *Energy and Buildings*, vol. 43, no. 8, pp. 1895–1903, 2011.

[21] A. Dubreuil, E. Assoumou, S. Bouckaert, S. Selosse, N. Maı *et al.*, "Water modeling in an energy optimization framework–the water-scarce middle east context," *Applied energy*, vol. 101, pp. 268–279, 2013.

[22] E. M. Wanjiru and X. Xia, "Energy-water optimization model incorporating rooftop water harvesting for lawn irrigation," *Applied Energy*, vol. 160, pp. 521–531, 2015.

[23] A. Von Meier, *Electric power systems: a conceptual introduction*. John Wiley & Sons, 2006.

[24] R. C. Dugan, M. F. McGranaghan, and H. W. Beaty, "Electrical power systems quality," *New York, NY: McGraw-Hill,| c1996*, vol. 1, 1996.

[25] A. van Deventer, "South African power system status overview," in *64th Association of Municipal Electricity Utilities (AMEU) Convention, Johannesburg, South Africa*, 05-08 October, 2014.

[26] K. M. Abo-Al-Ez, A. Elaiw, and X. Xia, "A dual-loop model predictive voltage control/sliding-mode current control for voltage source inverter operation in smart microgrids," *Electric Power*

Components and Systems, vol. 42, no. 3-4, pp. 348–360, 2014.

[27] Y. Liu, Q. Zhang, C. Wang, and N. Wang, “A control strategy for microgrid inverters based on adaptive three-order sliding mode and optimized droop controls,” *Electric Power Systems Research*, vol. 117, pp. 192–201, 2014.

[28] D. G. Wilson, R. D. Robinett, W. W. Weaver, R. H. Byrne, and J. Young, “Nonlinear power flow control design of high penetration renewable sources for ac inverter based microgrids,” in *2016 International Symposium on Power Electronics, Electrical Drives, Automation and Motion (SPEEDAM)*. IEEE, 2016, pp. 701–708.

[29] L. Mokgonyana, J. Zhang, L. Zhang, and X. Xia, “Coordinated two-stage volt/var management in distribution networks,” *Electric Power Systems Research*, vol. 141, pp. 157–164, 2016.

[30] C. K. Sao and P. W. Lehn, “Autonomous load sharing of voltage source converters,” *IEEE Transactions on Power Delivery*, vol. 20, no. 2, pp. 1009–1016, 2005.

[31] H. Nikkhajoei and R. H. Lasseter, “Distributed generation interface to the certs microgrid,” *IEEE Transactions on Power Delivery*, vol. 24, no. 3, pp. 1598–1608, 2009.

[32] X. Yu, A. M. Khambadkone, H. Wang, and S. T. S. Terence, “Control of parallel-connected power converters for low-voltage microgridąłpart i: A hybrid control architecture,” *IEEE Transactions on Power Electronics*, vol. 25, no. 12, pp. 2962–2970, 2010.

[33] A. Esmaeli, “Stability analysis and control of microgrids by sliding mode control,” *International Journal of Electrical Power & Energy Systems*, vol. 78, pp. 22–28, 2016.

[34] N. Wang, J. Zhang, and X. Xia, “Energy consumption of air conditioners at different temperature set points,” *Energy and Buildings*, vol. 65, pp. 412–418, 2013.

[35] Q. Catherine, J. Wheeler, R. Wilkinson, and G. de Jager, “Hot water usage profiling to improve geyser efficiency,” *Journal of Energy in Southern Africa*, vol. 23, no. 1, pp. 39–45, 2012.

[36] E. Arens, C. Federspiel, D. Wang, and C. Huizenga, "How ambient intelligence will improve habitability and energy efficiency in buildings," in *Ambient intelligence*. Springer, 2005, pp. 63–80.

[37] L. Portmess and S. Tower, "Data barns, ambient intelligence and cloud computing: the tacit epistemology and linguistic representation of big data," *Ethics and Information Technology*, vol. 17, no. 1, pp. 1–9, 2015.

[38] T. G. Stavropoulos, E. Kontopoulos, N. Bassiliades, J. Argyriou, A. Bikakis, D. Vrakas, and I. Vlahavas, "Rule-based approaches for energy savings in an ambient intelligence environment," *Pervasive and Mobile Computing*, vol. 19, pp. 1–23, 2015.

[39] T. G. Stavropoulos, G. Koutitas, D. Vrakas, E. Kontopoulos, and I. Vlahavas, "A smart university platform for building energy monitoring and savings," *Journal of Ambient Intelligence and Smart Environments*, vol. 8, no. 3, pp. 301–323, 2016.

[40] D. Setlhaolo, X. Xia, and J. Zhang, "Optimal scheduling of household appliances for demand response," *Electric Power Systems Research*, vol. 116, pp. 24–28, 2014.

[41] D. Setlhaolo and X. Xia, "Optimal scheduling of household appliances with a battery storage system and coordination," *Energy and Buildings*, vol. 94, pp. 61–70, 2015.

[42] ——, "Combined residential demand side management strategies with coordination and economic analysis," *International Journal of Electrical Power & Energy Systems*, vol. 79, pp. 150–160, 2016.

[43] H. Tazvinga, X. Xia, and J. Zhang, "Minimum cost solution of photovoltaic–diesel–battery hybrid power systems for remote consumers," *Solar Energy*, vol. 96, pp. 292–299, 2013.

[44] H. Tazvinga, B. Zhu, and X. Xia, "Optimal power flow management for distributed energy resources with batteries," *Energy Conversion and Management*, vol. 102, pp. 104–110, 2015.

[45] B. Zhu, H. Tazvinga, and X. Xia, "Switched model predictive control for energy dispatching of a photovoltaic-diesel-battery hybrid power system," *IEEE Transactions on Control Systems Technology*, vol. 23, no. 3, pp. 1229–1236, 2015.

[46] Z. Wu, H. Tazvinga, and X. Xia, "Demand side management of photovoltaic-battery hybrid system," *Applied Energy*, vol. 148, pp. 294–304, 2015.

[47] S. M. Sichilalu and X. Xia, "Optimal power dispatch of a grid tied-battery-photovoltaic system supplying heat pump water heaters," *Energy Conversion and Management*, vol. 102, pp. 81–91, 2015.

[48] S. Sichilalu, H. Tazvinga, and X. Xia, "Optimal control of a fuel cell/wind/pv/grid hybrid system with thermal heat pump load," *Solar Energy*, vol. 135, pp. 59–69, 2016.

[49] N. I. Nwulu and X. Xia, "Implementing a model predictive control strategy on the dynamic economic emission dispatch problem with game theory based demand response programs," *Energy*, vol. 91, pp. 404–419, 2015.

[50] N. Nwulu and X. Xia, "A combined dynamic economic emission dispatch and time of use demand response mathematical modelling framework," *Journal of Renewable and Sustainable Energy*, vol. 7, no. 4, p. 043134, 2015.

[51] S. Ntsaluba, B. Zhu, and X. Xia, "Optimal flow control of a forced circulation solar water heating system with energy storage units and connecting pipes," *Renewable Energy*, vol. 89, pp. 108–124, 2016.

[52] E. M. Malatji, J. Zhang, and X. Xia, "A multiple objective optimisation model for building energy efficiency investment decision," *Energy and Buildings*, vol. 61, pp. 81–87, 2013.

[53] B. Wang, X. Xia, and J. Zhang, "A multi-objective optimization model for the life-cycle cost analysis and retrofitting planning of buildings," *Energy and Buildings*, vol. 77, pp. 227–235, 2014.

[54] Z. Wu, B. Wang, and X. Xia, "Large-scale building energy efficiency retrofit: Concept, model and control," *Energy*, vol. 109, pp. 456–465, 2016.

[55] J. Zuo and Z.-Y. Zhao, "Green building research–current status and future agenda: A review," *Renewable and Sustainable Energy Reviews*, vol. 30, pp. 271–281, 2014.

[56] P. Wu, C. Mao, J. Wang, Y. Song, and X. Wang, "A decade review of the credits obtained by leed v2. 2 certified green building projects," *Building and Environment*, vol. 102, pp. 167–178, 2016.

[57] J. P. Praene, M. David, F. Sinama, D. Morau, and O. Marc, "Renewable energy: Progressing towards a net zero energy island, the case of reunion island," *Renewable and Sustainable Energy Reviews*, vol. 16, no. 1, pp. 426–442, 2012.

[58] X. Yuan, X. Wang, and J. Zuo, "Renewable energy in buildings in chinaąła review," *Renewable and Sustainable Energy Reviews*, vol. 24, pp. 1–8, 2013.

[59] D. H. Li, L. Yang, and J. C. Lam, "Zero energy buildings and sustainable development implications–a review," *Energy*, vol. 54, pp. 1–10, 2013.

[60] A. J. Marszal, P. Heiselberg, J. S. Bourrelle, E. Musall, K. Voss, I. Sartori, and A. Napolitano, "Zero energy building–a review of definitions and calculation methodologies," *Energy and buildings*, vol. 43, no. 4, pp. 971–979, 2011.

[61] B. Berggren, M. Hall, and M. Wall, "Lce analysis of buildings–taking the step towards net zero energy buildings," *Energy and Buildings*, vol. 62, pp. 381–391, 2013.

[62] M. Dabaieh, N. N. Makhlouf, and O. M. Hosny, "Roof top pv retrofitting: A rehabilitation assessment towards nearly zero energy buildings in remote off-grid vernacular settlements in egypt," *Solar Energy*, vol. 123, pp. 160–173, 2016.

[63] Z. Zhou, S. Zhang, C. Wang, J. Zuo, Q. He, and R. Rameezdeen, "Achieving energy efficient buildings via retrofitting of existing buildings: a case study," *Journal of Cleaner Production*,

vol. 112, pp. 3605–3615, 2016.

[64] M.-D. Yang, Y.-P. Chen, Y.-H. Lin, Y.-F. Ho, and J.-Y. Lin, "Multiobjective optimization using nondominated sorting genetic algorithm-ii for allocation of energy conservation and renewable energy facilities in a campus," *Energy and Buildings*, vol. 122, pp. 120–130, 2016.

[65] C. B. Webster and B. C. Dunn, "Creating a model of sustainability through the design, construction, and operations of a new high school," *College Publishing*, vol. 6, no. 3, pp. 1–20, 2011.

[66] C. Poon, A. T. Yu, A. Wong, and R. Yip, "Quantifying the impact of construction waste charging scheme on construction waste management in hong kong," *Journal of construction engineering and management*, vol. 139, no. 5, pp. 466–479, 2013.

[67] . Efficiency valuation organization (EVO), "International performance measurement and verification protocol: concepts and options for determining energy and water savings, vol. 1," National Renewable Energy Lab., Golden, CO (US), Tech. Rep., 2012.

[68] G. Thondhlana and H. Kua, "Promoting household energy conservation in low-income households through tailored interventions in grahamstown, south africa," *Journal of Cleaner Production*, 2016.

[69] S. Khashe, A. Heydarian, B. Becerik-Gerber, and W. Wood, "Exploring the effectiveness of social messages on promoting energy conservation behavior in buildings," *Building and Environment*, vol. 102, pp. 83–94, 2016.

[70] U. E. Ekpenyong, J. Zhang, and X. Xia, "How information propagation in social networks can improve energy savings based on time of use tariff," *Sustainable Cities and Society*, vol. 19, pp. 26–33, 2015.

[71] K. Li and B. Lin, "Impact of energy conservation policies on the green productivity in chinaąŕs manufacturing sector: Evidence from a three-stage dea model," *Applied Energy*, vol. 168, pp. 351–363, 2016.

[72] C. Wilson and M. R. Marselle, "Insights from psychology about the design and implementation of energy interventions using the behaviour change wheel," *Energy Research & Social Science*, vol. 19, pp. 177–191, 2016.

[73] Z. Ma, P. Cooper, D. Daly, and L. Ledo, "Existing building retrofits: Methodology and state-of-the-art," *Energy and buildings*, vol. 55, pp. 889–902, 2012.

[74] G. Bin and P. Parker, "Measuring buildings for sustainability: Comparing the initial and retrofit ecological footprint of a century home–the reep house," *Applied Energy*, vol. 93, pp. 24–32, 2012.

[75] D. Fiaschi, R. Bandinelli, and S. Conti, "A case study for energy issues of public buildings and utilities in a small municipality: Investigation of possible improvements and integration with renewables," *Applied Energy*, vol. 97, pp. 101–114, 2012.

[76] Y. Huang, J.-l. Niu, and T.-m. Chung, "Study on performance of energy-efficient retrofitting measures on commercial building external walls in cooling-dominant cities," *Applied energy*, vol. 103, pp. 97–108, 2013.

[77] F. Ascione, N. Bianco, C. De Stasio, G. M. Mauro, and G. P. Vanoli, "Multi-stage and multi-objective optimization for energy retrofitting a developed hospital reference building: A new approach to assess cost-optimality," *Applied Energy*, vol. 174, pp. 37–68, 2016.

[78] J. Lizana, Á. Barrios-Padura, M. Molina-Huelva, and R. Chacartegui, "Multi-criteria assessment for the effective decision management in residential energy retrofitting," *Energy and Buildings*, vol. 129, pp. 284–307, 2016.

[79] C. Diakaki, E. Grigoroudis, and D. Kolokotsa, "Towards a multi-objective optimization approach for improving energy efficiency in buildings," *Energy and Buildings*, vol. 40, no. 9, pp. 1747–1754, 2008.

[80] E. Asadi, M. G. da Silva, C. H. Antunes, and L. Dias, "Multi-objective optimization for building retrofit strategies: A model and an application," *Energy and Buildings*, vol. 44, pp. 81–87, 2012.

[81] D. S. Remer and A. P. Nieto, "A compendium and comparison of 25 project evaluation techniques. part 1: Net present value and rate of return methods," *International Journal of Production Economics*, vol. 42, no. 1, pp. 79–96, 1995.

[82] F. Kreith and D. Y. Goswami, *Energy Management and Conservation Handbook*. CRC Press, 2007.

[83] M. Krarti, *Energy audit of building systems: an engineering approach, second edition*. CRC Press, 2011.

[84] G. Verbeeck and H. Hens, "Energy savings in retrofitted dwellings: Economically viable," *Energy and Buildings*, vol. 37, no. 7, pp. 747–754, 2005.

[85] ——, "Life cycle inventory of buildings: a calculation method," *Building and Environment*, vol. 45, no. 4, pp. 1037–1041, 2010.

[86] ——, "Life cycle inventory of buildings: A contribution analysis," *Building and Environment*, vol. 45, no. 4, pp. 964–967, 2010.

[87] S. Petersen and S. Svendsen, "Method for component-based economical optimisation for use in design of new low-energy buildings," *Renewable Energy*, vol. 38, no. 1, pp. 173–180, 2012.

[88] Z. Gou, S. S.-Y. Lau, and F. Chen, "Subjective and objective evaluation of the thermal environment in a three-star green office building in china," *Indoor and Built Environment*, p. 1420326X11419311, 2011.

[89] Z. Gou and S. Siu-Yu Lau, "Post-occupancy evaluation of the thermal environment in a green building," *Facilities*, vol. 31, no. 7/8, pp. 357–371, 2013.

[90] W. L. Paul and P. A. Taylor, "A comparison of occupant comfort and satisfaction between a green building and a conventional building," *Building and Environment*, vol. 43, no. 11, pp. 1858–1870, 2008.

[91] J. S. Gero, N. D'Cruz, and A. D. Radford, "Energy in context: A multicriteria model for building design," *Building and Environment*, vol. 18, no. 3, pp. 99–107, 1983.

[92] F. Flourentzou and C.-A. Roulet, "Elaboration of retrofit scenarios," *Energy and Buildings*, vol. 34, no. 2, pp. 185–192, 2002.

[93] M. Jaggs and J. Palmer, "Energy performance indoor environmental quality retrofit: A european diagnosis and decision making method for building refurbishment," *Energy and Buildings*, vol. 31, no. 2, pp. 97–101, 2000.

[94] E. Rey, "Office building retrofitting strategies: Multicriteria approach of an architectural and technical issue," *Energy and Buildings*, vol. 36, no. 4, pp. 367–372, 2004.

[95] P. Blondeau, M. Spérandio, and F. Allard, "Multicriteria analysis of ventilation in summer period," *Building and Environment*, vol. 37, no. 2, pp. 165–176, 2002.

[96] Z. Chen, D. Clements-Croome, J. Hong, H. Li, and Q. Xu, "A multicriteria lifespan energy efficiency approach to intelligent building assessment," *Energy and Buildings*, vol. 38, no. 5, pp. 393–409, 2006.

[97] M. Santamouris, C. Pavlou, P. Doukas, G. Mihalakakou, A. Synnefa, A. Hatzibiros, and P. Patargias, "Investigating and analysing the energy and environmental performance of an experimental green roof system installed in a nursery school building in athens, greece," *Energy*, vol. 32, no. 9, pp. 1781–1788, 2007.

[98] D. B. Crawley, J. W. Hand, M. Kummert, and B. T. Griffith, "Contrasting the capabilities of building energy performance simulation programs," *Building and environment*, vol. 43, no. 4, pp. 661–673, 2008.

[99] D. J. Sailor, "A green roof model for building energy simulation programs," *Energy and buildings*, vol. 40, no. 8, pp. 1466–1478, 2008.

[100] S. Chidiac, E. Catania, E. Morofsky, and S. Foo, "Effectiveness of single and multiple energy retrofit measures on the energy consumption of office buildings," *Energy*, vol. 36, no. 8, pp. 5037–5052, 2011.

[101] A. L. Pisello, A. Petrozzi, V. L. Castaldo, and F. Cotana, "On an innovative integrated technique for energy refurbishment of historical buildings: thermal-energy, economic and environmental analysis of a case study," *Applied Energy*, vol. 162, pp. 1313–1322, 2016.

[102] T. Østergård, R. L. Jensen, and S. E. Maagaard, "Building simulations supporting decision making in early design–a review," *Renewable and Sustainable Energy Reviews*, vol. 61, pp. 187–201, 2016.

[103] S.-I. Gustafsson, "Sensitivity analysis of building energy retrofits," *Applied Energy*, vol. 61, no. 1, pp. 13–23, 1998.

[104] Y. Heo, "Bayesian calibration of building energy models for energy retrofit decision-making under uncertainty," 2011.

[105] C. C. Menassa, "Evaluating sustainable retrofits in existing buildings under uncertainty," *Energy and Buildings*, vol. 43, no. 12, pp. 3576–3583, 2011.

[106] X. Ye, X. Xia, and J. Zhang, "Optimal sampling plan for clean development mechanism energy efficiency lighting projects," *Applied Energy*, vol. 112, pp. 1006–1015, 2013.

[107] ——, "Optimal sampling plan for clean development mechanism lighting projects with lamp population decay," *Applied Energy*, vol. 136, pp. 1184–1192, 2014.

[108] X. Ye and X. Xia, "Optimal metering plan for measurement and verification on a lighting case study," *Energy*, vol. 95, pp. 580–592, 2016.

[109] H. Carstens, X. Xia, and X. Ye, "Improvements to longitudinal clean development mechanism sampling designs for lighting retrofit projects," *Applied Energy*, vol. 126, pp. 256–265, 2014.

[110] H. Carstens, X. Xia, and S. Yadavalli, "Low-cost energy meter calibration method for measurement and verification," *arXiv preprint arXiv:1610.04196*, 2016.

[111] R. Evins, "A review of computational optimisation methods applied to sustainable building design," *Renewable and Sustainable Energy Reviews*, vol. 22, pp. 230–245, 2013.

[112] K. Deb, *Multi-objective optimization using evolutionary algorithms*. John Wiley & Sons, 2001, vol. 16.

[113] Z. Wu, X. Xia, and B. Wang, "Improving building energy efficiency by multiobjective neighborhood field optimization," *Energy and Buildings*, vol. 87, pp. 45–56, 2015.

[114] X. Hu and R. Eberhart, "Solving constrained nonlinear optimization problems with particle swarm optimization," in *Proceedings of the sixth world multiconference on systemics, cybernetics and informatics*, vol. 5. Citeseer, 2002, pp. 203–206.

[115] Z. Wu and T. W. Chow, "Neighborhood field for cooperative optimization," *Soft Computing*, vol. 17, no. 5, pp. 819–834, 2013.

[116] ——, "Binary neighbourhood field optimisation for unit commitment problems," *IET Generation, Transmission & Distribution*, vol. 7, no. 3, pp. 298–308, 2013.

[117] B. Wang, Z. Wu, and X. Xia, "A multistate-based control system approach toward optimal maintenance planning," *IEEE Transactions on Control Systems Technology*, vol. 25, no. 1, pp. 374–381, 2017.

[118] C. Valdez-Flores and R. M. Feldman, "A survey of preventive maintenance models for stochastically deteriorating single-unit systems," *Naval Research Logistics (NRL)*, vol. 36, no. 4, pp. 419–446, 1989.

[119] X. Xia and J. Zhang, "Mathematical description for the measurement and verification of energy efficiency improvement," *Applied Energy*, vol. 111, pp. 247–256, 2013.

[120] A. Michaelowa and F. Jotzo, "Transaction costs, institutional rigidities and the size of the clean development mechanism," *Energy policy*, vol. 33, no. 4, pp. 511–523, 2005.

[121] UNFCCC, *Approved small scale methodology AMS II.J, Demand-side activities for efficient lighting technologies*. Technical Report, Version 04, 2010.

[122] M. O. of the Legislative Auditor, "Preventive maintenance for local government buildings: A best practices review," Tech. Rep., April 2000.

[123] H. Wang, "A survey of maintenance policies of deteriorating systems," *European Journal of Operational Research*, vol. 139, no. 3, pp. 469–489, 2002.

[124] A. Lisnianski, I. Frenkel, and Y. Ding, *Multi-state system reliability analysis and optimization for engineers and industrial managers*. Springer Science & Business Media, 2010.

[125] Y. Liu and H.-Z. Huang, "Optimal replacement policy for multi-state system under imperfect maintenance," *IEEE Transactions on Reliability*, vol. 59, no. 3, pp. 483–495, 2010.

[126] M. D. Le and C. M. Tan, "Optimal maintenance strategy of deteriorating system under imperfect maintenance and inspection using mixed inspectionscheduling," *Reliability Engineering & System Safety*, vol. 113, pp. 21–29, 2013.

[127] E.-K. Boukas and H. Yang, "Optimal control of manufacturing flow and preventive maintenance," *IEEE Transactions on Automatic Control*, vol. 41, no. 6, pp. 881–885, 1996.

[128] E. Boukas and Z. Liu, "Production and maintenance control for manufacturing systems," *IEEE Transactions on Automatic Control*, vol. 46, no. 9, pp. 1455–1460, 2001.

[129] S.-H. Sheu, C.-C. Chang, Y.-L. Chen, and Z. G. Zhang, "Optimal preventive maintenance and repair policies for multi-state systems," *Reliability Engineering & System Safety*, vol. 140, pp. 78–87, 2015.

[130] Y.-L. Chen, C.-C. Chang, and D.-F. Sheu, "Optimum random and age replacement policies for customer-demand multi-state system reliability under imperfect maintenance," *International Journal of Systems Science*, vol. 47, no. 5, pp. 1130–1141, 2016.

[131] J. Vesterstrom and R. Thomsen, "A comparative study of differential evolution, particle swarm optimization, and evolutionary algorithms on numerical benchmark problems," in *Evolutionary Computation, 2004. CEC2004. Congress on*, vol. 2. IEEE, 2004, pp. 1980–1987.

[132] S.-K. Wang, J.-P. Chiou, and C.-W. Liu, "Non-smooth/non-convex economic dispatch by a novel hybrid differential evolution algorithm," *IET Generation, Transmission & Distribution*, vol. 1, no. 5, pp. 793–803, 2007.

[133] S. Sayah and K. Zehar, "Modified differential evolution algorithm for optimal power flow with non-smooth cost functions," *Energy conversion and Management*, vol. 49, no. 11, pp. 3036–3042, 2008.

[134] X.-S. Yang, S. S. S. Hosseini, and A. H. Gandomi, "Firefly algorithm for solving non-convex economic dispatch problems with valve loading effect," *Applied soft computing*, vol. 12, no. 3, pp. 1180–1186, 2012.

[135] P. Civicioglu and E. Besdok, "A conceptual comparison of the cuckoo-search, particle swarm optimization, differential evolution and artificial bee colony algorithms," *Artificial intelligence review*, pp. 1–32, 2013.

[136] B. Mohanty, S. Panda, and P. Hota, "Controller parameters tuning of differential evolution algorithm and its application to load frequency control of multi-source power system," *International journal of electrical power & energy systems*, vol. 54, pp. 77–85, 2014.

[137] O. Kaynakli, "A review of the economical and optimum thermal insulation thickness for building applications," *Renewable and Sustainable Energy Reviews*, vol. 16, no. 1, pp. 415–425, 2012.

[138] Y. K. Juan, J. H. Kim, K. Roper, and D. Castro-Lacouture, "GA-based decision support system for housing condition assessment and refurbishment strategies," *Automation in Construction*,

vol. 18, no. 4, pp. 394–401, 2009.

[139] R. Storn and K. Price, "Differential evolution: A simple and efficient heuristic for global optimization over continuous spaces," *Journal of Global Optimization*, vol. 11, no. 4, pp. 341–359, 1997.

[140] P. O'Connor and A. Kleyner, *Practical Reliability Engineering*. Wiley, Chichester, UK, 2011.

[141] H. Ong, T. Mahlia, H. Masjuki, and D. Honnery, "Life cycle cost and sensitivity analysis of palm biodiesel production," *Fuel*, vol. 98, pp. 131–139, 2012.

[142] R. T. Marler and J. S. Arora, "The weighted sum method for multi-objective optimization: new insights," *Structural and Multidisciplinary Optimization*, vol. 41, no. 6, pp. 853–862, 2010.

[143] S. J. Qin and T. A. Badgwell, "A survey of industrial model predictive control technology," *Control Engineering Practice*, vol. 11, no. 7, pp. 733–764, 2003.

[144] W. Badenhorst, J. Zhang, and X. Xia, "Optimal hoist scheduling of a deep level mine twin rock winder system for demand side management," *Electric Power Systems Research*, vol. 81, no. 5, pp. 1088–1095, 2011.

[145] A. Elaiw, X. Xia, and A. Shehata, "Application of model predictive control to optimal dynamic dispatch of generation with emission limitations," *Electric Power Systems Research*, vol. 84, no. 1, pp. 31–44, 2012.

[146] A. Handbook, "ASHRAE handbook–Fundamentals," *Atlanta, GA*, 2009.

[147] R. Zmeureanu and C. Peragine, "Evaluation of interactions between lighting and hvac systems in a large commercial building," *Energy Conversion and Management*, vol. 40, no. 11, pp. 1229–1236, 1999.

[148] B.-L. Ahn, C.-Y. Jang, S.-B. Leigh, S. Yoo, and H. Jeong, "Effect of led lighting on the cooling and heating loads in office buildings," *Applied Energy*, vol. 113, pp. 1484–1489, 2014.

[149] M. S. Breuker and J. E. Braun, “Common faults and their impacts for rooftop air conditioners,” *HVAC&R Research*, vol. 4, no. 3, pp. 303–318, 1998.

[150] U. D. of Energy Efficiency and R. Energy, “Thermal management of white leds,” *Technical Report*, 2009.

[151] R.-Y. Kwak, A. Takakusagi, J.-Y. Sohn, S. Fujii, and B.-Y. Park, “Development of an optimal preventive maintenance model based on the reliability assessment for air-conditioning facilities in office buildings,” *Building and environment*, vol. 39, no. 10, pp. 1141–1156, 2004.

[152] J. Yan and D. Hua, “Energy consumption modeling for machine tools after preventive maintenance,” in *Industrial Engineering and Engineering Management (IEEM), 2010 IEEE International Conference on*. IEEE, 2010, pp. 2201–2205.

[153] M. B. Yildirim and F. G. Nezami, “Integrated maintenance and production planning with energy consumption and minimal repair,” *The International Journal of Advanced Manufacturing Technology*, pp. 1–12, 2014.

[154] Z. Li, Y. Soh, and C. Wen, *Switched and Impulsive Systems: Analysis, Design and Applications*. Springer Science & Business Media, 2005, vol. 313.

[155] B. Wang, Z. Wu, B. Zhu, and X. Xia, “Optimal control of maintenance instants and intensities in building energy efficiency retrofitting project,” in *The 54th IEEE Conference on Decision and Control (CDC 2015), Osaka, Japan*, 15-18 December, 2015.

[156] M. A. Mian, *Project Economics and Decision Analysis: Deterministic Models*. Pennwell Books, 2011, vol. 1.

[157] B. Wang and X. Xia, “Optimal maintenance planning for building energy efficiency retrofitting from optimization and control system perspectives,” *Energy and Buildings*, vol. 96, pp. 299–308, 2015.

[158] Navigant, “Evaluation of the IFC/GEF Poland efficient lighting project CFL subsidy program,” Navigant Consulting, Philadephia, PA, USA, Final report, Edition 2, 1999.

[159] A. Saltelli, K. Chan, E. M. Scott *et al.*, *Sensitivity analysis*. Wiley New York, 2000, vol. 1.

[160] Z. Qu, *Robust control of nonlinear uncertain systems*. John Wiley & Sons, Inc, New York, USA, 1998.

[161] M. Green and D. J. Limebeer, *Linear robust control*. Courier Corporation, New York, USA, 2012.

ADDENDUM A DIFFERENTIAL EVOLUTION ALGORITHM WITH BNFO

A.1 DE ALGORITHM BASED NUMERICAL SOLVER

Generally, the DE algorithm follows the basic procedure of an evolutionary algorithm, including three mathematical operations as the main steps: *Mutation*,*Crossover* and *Selection*. In common evolutionary algorithm, a set of candidate solutions, namely individuals, are adopted to represent the possible values of the decision variables, e.g., x_i^j in our model. These individuals are moved around in the search-space which is regulated by the boundary of the problem. With the iterative search, the DE algorithm can hopefully, although not guaranteed, discover a satisfactory solution for the problem.

The employed DE algorithm is improved by the binary neighborhood field optimisation method. The idea of the BNFO method comes from the biological world, where individuals often communicate with and learn from their neighbors within limited perceptual range. Similarly, the individuals in BNFO algorithm are mostly affected by the local environment rather than the global one, i.e., each individual is updated under the concept of 'learning from the neighbors' that is following superior neighbors and diverging from inferior neighbors. The utilisation of the attractive field of the superior neighbor and the repulsive field of the inferior neighbor in the BNFO method is able to deliver promising results efficiently within acceptable computational time, thereby reduces the computational cost [115].

The binary coding suggests that the individuals are coded as bit strings. In practice, the optimisation problem is discrete as x_i^j indicates the number of items, which are obviously integers. As a result, the individuals representing possible x_i^j are a collection of integers with number 0 as the lower bound. The upper bounds are regulated by constraint (2.8). These integers are translated into binary codes, which facilitate the diversity of the candidate solution population and the effectiveness of the *Mutation* and *Crossover* operations. The detailed procedure of implementing DE algorithm with the BNFO method is illustrated as following [116]:

Initialisation: randomise the initial np individuals, which are sampled uniformly in the search-space;
(i) *Localisation*: for each individual $x_{i,G}$ at the generation G, find the superior neighbor $xc_{i,G}$ and the inferior neighbor $xw_{i,G}$ in the search-space as

$$\begin{cases} xc_{i,G} = arg \min_{J(x_{k,G})<J(x_{i,G})} \|x_{k,G} - x_{i,G}\|, \\ xw_{i,G} = arg \min_{J(x_{k,G})>J(x_{i,G})} \|x_{k,G} - x_{i,G}\|, \end{cases} \tag{A.1}$$

where $J(x)$ denotes the minimisation problem, i.e., the weighted sum objective function in our models. $\|\cdot\|$ denotes the distance evaluation, which is Hamming distance in the present model. $xc_{i,G}$ is the nearest superior neighbor with a smaller function value than $J(x_{i,G})$ and $xw_{i,G}$ is the nearest inferior neighbor with a larger function value. If $x_{i,G}$ is in the best individual in the population, $xc_{i,G}$ is defined as $x_{i,G}$; if $x_{i,G}$ is in the worst individual in the population, $xw_{i,G}$ is defined as $x_{i,G}$.
(ii) *Mutation*: perturb each individual as

$$v_{i,G} = x_{i,G} \ominus [\alpha_{r1} \otimes (xc_{i,G} \ominus x_{i,G}) \oplus \alpha_{r2} \otimes (xc_{i,G} \ominus xw_{i,G})], \tag{A.2}$$

to obtain the mutation vector $v_{i,G}$. $\ominus$ denotes 'XOR' operator, $\otimes$ denotes 'AND' operator and $\oplus$ denotes 'OR' operator. α_{r1} and α_{r2} are random binary integer vectors generated by:

$$\begin{cases} \alpha_{r1} = rand_1 < \alpha, \\ \alpha_{r2} = rand_2 < \alpha, \end{cases} \tag{A.3}$$

where $rand_1$ and $rand_2$ are random vectors uniformly distributed in $[0,1]$ and α denotes the learning rate $\in (0,1)$.
(iii) *Crossover*: recombine the mutation vector with the target vector $x_{i,G}$:

$$u_{j,i,G} = \begin{cases} v_{j,i,G}, & if\ rand(0,1) \leq C_r\ or\ j = j_{rand}, \\ x_{j,i,G}, & otherwise, \end{cases} \tag{A.4}$$

with $j = 1,2,...,D$ denoting the dimension index. C_r denotes the crossover probability. $rand(0,1)$ represents a uniformly distributed random number over $[0,1]$. j_{rand} denotes the randomly selected component where the obtained mutant vector is accepted to generate the trail vector.
(iv) *Selection*: in the next generation, the individual $x_{i,G+1}$ will be updated as the better one between $x_{i,G}$ and $u_{i,G}$:

$$x_{i,G+1} = \begin{cases} u_{i,G}, & if\ J(u_{i,G}) < J(x_{i,G}), \\ x_{i,G}, & otherwise, \end{cases} \tag{A.5}$$

(v) Go back to step (i) in case the stopping criteria are not satisfied, otherwise stop the algorithm and let $x = x_{\bar{i},\bar{G}}$ be the obtained optimal solution, where $x_{\bar{i},\bar{G}}$ denotes the individual with the lowest function value, i.e., $J(x_{\bar{i},\bar{G}}) \leq J(x_{i,G}|\forall i, \forall G)$.

Remark 1 *Existing studies reveals that the improved DE algorithm with the BNFO method manifests better performances on a series of benchmark numerical problems than many conventional stochastic optimisation approaches. Thorough investigations and discussions can be found in Wu's relevant studies [116, 115].*

The pseudocode of the above algorithm is illustrated in Algorithm 1.

A.2 PSEUDOCODE

Algorithm 1 Pseudocode of DE algorithm with BNFO method

Definition:

np: the population size;

d: dimension of the problem;

X: the decision matrix with the size of $np*d$;

J: the function value vector with the size of $np*1$;

Mg: the maximum number of generations for stopping criterion.

BEGIN
Set mutation probability C_r and learning rate α;
Create a random, binary coded initial population $\{x_{i,1}|i = 1, 2, ..., np\}$;
Let $x_{best} = x_{1,1}$;
while $G = 1$ *to* Mg **do**
    while $i = 1$ *to* np **do**
        Locate $x_{i,G}$ in X and obtain its superior neighbor $xc_{i,G}$ and inferior neighbor $xw_{i,G}$;
        $\alpha_{r1} = rand < \alpha$; $\alpha_{r2} = rand < \alpha$;
        $v_1 = \alpha_{r1}$ & $xor(x_{i,G}, xc_{i,G})$;
        $v_2 = \alpha_{r2}$ & $xor(xw_{i,G}, xc_{i,G})$;
        $v_{i,G} = xor(x_{i,G},\ v_1|v_2)$;
        Repair $v_{i,G}$ if it violates the upperbound or lowerbound;
        Generate $j_{rand} = randint(1, d)$;
        while $j = 1$ *to* d **do**
            if $j = j_{rand}$ or $rand(0,1) < CR$ **then**
                $u_{j,i,G} = v_{j,i,G}$;
            else
                $u_{j,i,G} = x_{j,i,G}$;
            end if
        end while
        if $J(u_{i,G}) \leq J(x_{i,G})$ **then**
            $x_{i,G+1} = u_{i,G}$;
            if $J(x_{i,G+1}) < J(x_{best})$ **then** $x_{best} = x_{i,G+1}$;
            end if
        else
            $x_{i,G+1} = x_{i,G}$;
        end if
    end while
end while
Return x_{best};
END